A network of flow speed sensors estimating fish activity for assisting in feeding decisions in cage aquaculture

著者	Bautista Solpico Dominic
year	2022-09-26
その他のタイトル	水産養殖における給餌支援を目的とした養殖魚活動量推定センサネットワーク
学位授与年度	令和4年度
学位授与番号	17104甲生工第447号
URL	http://doi.org/10.18997/00009082

Doctoral Dissertation

A network of flow speed sensors estimating fish activity for assisting in feeding decisions in cage aquaculture

水産養殖における給餌支援を目的とした養殖魚活動量推定センサネットワーク

SOLPICO DOMINIC BAUTISTA
Department of Life Science and Systems Engineering
Graduate School of Life Science and Systems Engineering
Kyushu Institute of Technology

26th of September, 2022

A Doctoral Dissertation

submitted to Graduate School of Life Science and Systems Engineering

Kyushu Institute of Technology

in partial fulfillment of the requirements for the degree of

Ph. D. in ENGINEERING

SOLPICO DOMINIC BAUTISTA

Thesis Committee:

Professor Kazuo Ishii	(Supervisor)
Professor Hiroaki Wagatsuma	(Co-supervisor)
Professor Keisuke Watanabe	(Co-supervisor)
Associate Professor Hiroyuki Miyamoto	(Co-Supervisor)

In memory of my two grandfathers – Benjamin Alfonso Bautista, who inspired me to pursue excellence for the betterment of my countrymen, and Benito Gendrano Solpico, who was one of the first to spark my interest in Japan.

Abstract

With the expansion of aquaculture production to meet the growing demand for food fish worldwide, there is an increasing need for its sustainable management not only to mitigate any threat to the aquatic environment but also to produce more high-quality fish that meet the market standards for seafood. Digital transformation (DX) holds an important role in achieving this need, enabling fish farmers make better decisions in using their resources as well as in reducing their costs of production through knowledge transfer and data. One such decision-making where DX can assist is in feeding, which generally has the largest share in production costs.

Conventionally, farmers control the feeding from judging the fishes' behavior. They learn this practice through their subjective experiences, leading to substantial differences in results between expert and novice farmers. The latter tends to feed the fishes inefficiently, producing uneaten feeds, which do not only increase financial burden in culture operations but also contribute to the pollution of the aquatic environment, which affect the growth and quality of the fish stocks and ultimately the sustainability of their operations. Applying DX to estimate the fish behavior therefore becomes important.

While several intelligent feeding control methods using various technologies have been developed for applying such DX, many of are either easily affected by changes or noise from external sources or are technically difficult to implement in larger scales. An alternative approach is by measurement of outward flow from the cage, which has been observed to be fish induced. If we assume that fishes tend to swim upward when they sense feeds coming from the surface and swim back down when satiated, and that

they tend to move in circles, fish activity at different depths can be visualized with this measurement to help farmers make feeding decisions.

An off-grid modular sensor network was thus designed and developed to collect flow speed measurements and underwater video recordings from at least two depths and from multiple sides of a fish cage. This was realized by organizing sensors into sensor modules, which are connected to each other and are organized into sensor units. The sensor units were designed wirelessly relay data from all modules to a hub unit. Flow sensors were modified to measure flow speeds underwater. The network's operation was also designed to be scheduled to manage its offshore power supply to enable long-term observation by the system.

To demonstrate its functionality, the sensor network was deployed in fish cages and collected data, especially during feeding. The flow measurements and underwater videos were analyzed together to estimate the fish activity. Although there were various patterns, it could be observed that surface flow increased significantly at the beginning of feeding and declined toward the end. Vigorous surface activity was observed at most cages, validating the observed flow speeds. Offset between speeds at opposite sides was also observed, suggesting cancellation of global currents. In some experiments, increase of flow below the surface was also observed at the beginning and towards the end of feeding, indicating fishes to climbing and descending.

There are many factors that contribute to the speed of flow coming out of the cage. However, the fishes' locomotion and depth distribution have a large contribution to the changes in flow speed. These parameters depend on their hunger level and on the availability of feeds in water, as fishes may tend to swim up fast when they sense feed in water and swim less vigorously when they start to become full. A simplified model

of the fish activity as a response to feeding was developed for simulation. Its output could be compared with the collected flow data for the farmers to use in improving their feeding decisions. Some observed flow patterns such as the decline of surface flow and the increase of flow at lower depths could be used for deciding on when to stop feeding. With these insights, a DX system was envisioned to collect flow speed and other measurements from multiple fish cages, assisting fish farmers in feeding.

This research contributes to the development of DX application in cage aquaculture by introducing a flexible self-correcting system that could help farmers visualize underwater fish activity to help them improve their feeding decisions.

Keywords: Cage aquaculture; Feeding behavior; Sensor network; Flow speed; Fish activity

Table of Contents

List of Figures

List of Tables

Nomenclature

Symbol	Quantity [unit]
a	Constant coefficient for fish aversion to swim to surface [unitless]
b	Constant coefficient for fish attraction to feeds at surface [unitless]
c_f	Constant amount of feed eaten by fish at time t [kg]
e_f	Instantaneous amount of feed eaten by a single fish [kg]
E_{SN}	Daily sensor network energy consumption [J/day]
f_0	Amount of feed dispensed on water [kg]
F	Amount of
h_{ca}	Height of fish cage above sea level [m]
h_C	Fish cage depth/height of surface from cage bottom [m]
h_f	Fish height from the bottom of the fish cage [m]
h_n	Depth of sensor module n below sea level [m]
I_m	Sensor module current draw [A]
I_t	Top module current draw [A]
I_U	Sensor unit current draw [A]
I_H	Hub unit computer current draw [A]
k_1	Feed dispersion and sinkage constant coefficient [unitless]
k_2	Constant coefficient for fish's eagerness to eat [unitless]
L	Length of each sensor module frame [m]
l_n	Position of sensor module n from the top of the module frame [m]
m	Moving average interval size (number of data points)
n	Number of fishes in a single cage
N_m	Number of sensor modules
N_U	Number of sensor units
P_U	Sensor unit power consumption [W]
P_H	Hub unit computer power consumption [W]
P_{SN}	Sensor network power consumption [W]
P_{SP}	Required solar panel power output
S	Fish satiation level [unitless, 0-1 (0: hungry; 1: full)]
t	Time [s]
t_{MA}	Moving average interval time [s]
t_s	Flow sensor sampling time [s]
t_{SN}	Daily sensor network operation duration [s/day]
$\bar{t}_{Smin}$	Daily average of minimum monthly total sunshine duration [s/day]
u	Flow speed [cm/s]
$\hat{u}_t$	Moving average flow speed [cm/s]
V_U	Sensor unit supply voltage [V]
V_H	Hub unit computer supply voltage [V]
v_f	Fish circling speed [m/s]
τ_1	Time constant for the change in the fish's satiation [unitless]
τ_2	Time constant for the change in the fish's height [unitless]

Chapter 1
Introduction

Chapter 1. Introduction

1.1. The state of aquaculture worldwide

In the last few decades, aquaculture has become one of the important industries for achieving sustainable food production. It is seen as a key contributor to the meeting the United Nations' Sustainability Development Goals (SDGs) 2 and 14, which are attaining zero hunger and sustainable use of marine resources. It is thus considered a key component in building the Blue Economy.

For the last 70 years, capture fishing has been the larger contributor to global fish production. But despite the growing demand for aquatic foods, its production has levelled off in the past two decades, as shown in Figure 1-1. This could be attributed to the decline of fish populations due to overfishing, pollution, and poor management among others. Fish stocks within biologically sustainable levels has decreased from 90% to 65.8% from 1990 to 2017, which resulted to reduced catches [1].

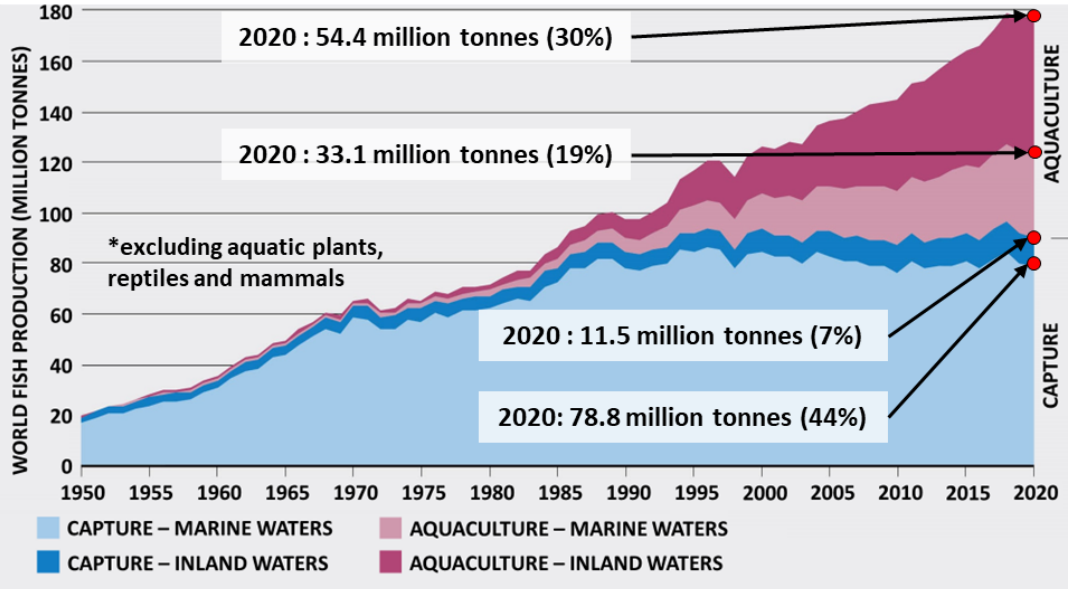

Figure 1-1 Global fisheries and aquaculture production (1950-2020) [1]

Aquaculture production, on the other hand, has been expanding since the late 1980s, meeting the growing demand for aquatic food as capture fisheries production remains

stable. From a four percent share in 1950, aquaculture production doubled every 20 years, accounting for 49% in the total fish production worldwide at 87.5 million tonnes in 2020 [1]. Of this amount, inland and marine aquaculture productions accounted for 62% and 38%, respectively. Over 20 million people were engaged in aquaculture in 2020, with most coming from Asia. It is then no surprise that the top five aquaculture producers of aquatic animals (finfishes, crustaceans, and mollusks) in the years 2005-2020 are China, India, Indonesia, Vietnam, and Bangladesh. For the first time in 2020, the contribution of aquaculture to aquatic foods available for human consumption became greater than that of capture fisheries, estimated at 56%, as seen in Figure 1-2. This estimate is expected to rise to 59% in 10 years [1].

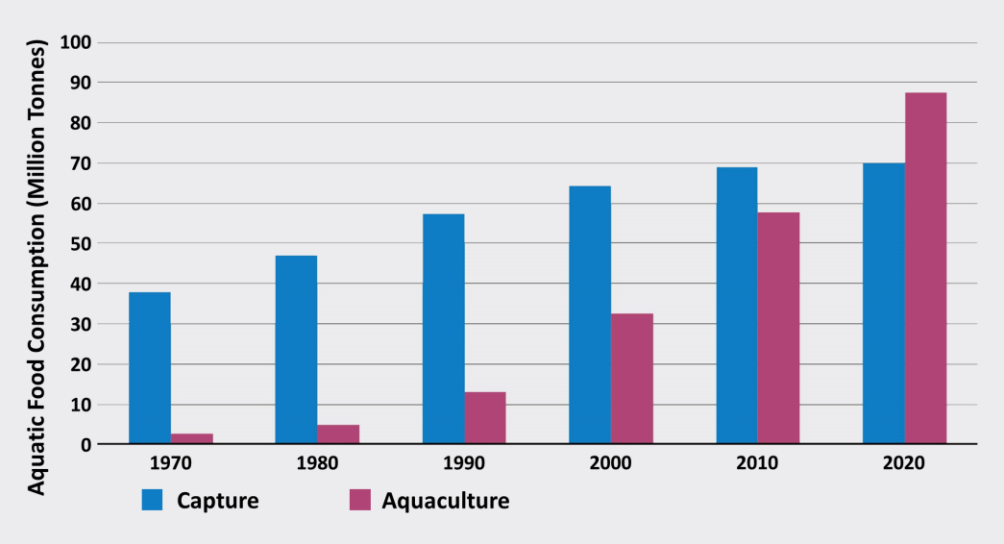

Figure 1-2 Relative contribution of aquaculture and capture fisheries to aquatic foods available for human consumption [1]

This chapter also explores the state of aquaculture production in two countries – the Philippines and Japan. The Philippines is the home country of the author of this dissertation, while Japan is the country where this research was made. Both countries are archipelagic and lie in the Western Pacific Ocean. Surrounded by seas and oceans, fish and other aquatic products are major sources of food in both countries, making

aquaculture an important industry in both. And yet, their aquacultures are very much different, as influenced by different geography, climate, culture, and economy among others.

1.1.1. Aquaculture in the Philippines

Aquaculture is a major source of aquatic food in the Philippines. The country ranks 11th in the largest aquaculture producers of aquatic animals in the world, with a production volume of around 854,000 tonnes in 2020. As an archipelagic country with a 36,289 km coastline, 246,063 ha of swamplands, 200,000 ha of lakes, 31,000 ha of rivers, 19,000 ha of reservoirs, and 253,323 ha of man-made fishponds, the Philippines is rich in aquatic resources suitable for fish culture. Fish production in the country is classified into three sub-sectors – commercial and municipal capture fisheries, and aquaculture. Aquaculture production contributes the smallest share, accounting to 29.14% of the country's production of aquatic animals in 2020. Of the two million registered fisherfolk engaged in fish production, 233,725 or 11% engage in aquaculture [2].

Most aquaculture operations are done in brackish water and freshwater environments, producing 346,566 and 284,916 tonnes in 2020, respectively. Most fishes in these environments are raised in fishponds. Others are raised in fish cages and in fish pens, as shown in Figure 1-3. Marine aquaculture, excluding shellfish and seaweed, produced 150,507 tonnes in the same year. Fishes in this environment are grown in cages and pens, with more in the former. Aquaculture is also practiced in small reservoirs and rice paddies, although they only yield 114.38 and 5.20 tonnes, respectively. Milkfish (*Chanos chanos*) is the fish species cultured the most in the country, accounting for around 48.5% of the total production. This is followed by

tilapia (*Oreochromis niloticus* and *mossambicus*) and shrimps/prawns (mainly giant tiger prawn *Penaeus monodon*), accounting for 30.9% and 8.2%, respectively. Other species including mudcrabs, bivalves, carps, groupers, and siganids comprise 12.4% of total aquaculture production [2].

Figure 1-3 A fish farmer from the Philippines feeding tilapia in a bamboo cage

Aquaculture in the Philippines encounter various challenges that have either been brought by human activities, including aquaculture itself, or by the effects of climate change [3]. Documented occurrences of algal blooms and fish kills in freshwater or brackish water farms have been attributed to decline in water quality due to large concentrations of organic matter in water [4]. This was mostly caused by increased aquaculture activities – overfeeding, overstocking, and occupation of fish farm structures exceeding the coverage limits imposed by law. Higher water temperatures attributed to climate change pose a threat to the egg survival of milkfish and Asian seabass as well as to the survival of rabbitfish larvae [5]. The Philippines also stands in the path of many typhoons, as it is situated along typhoon belt. Destructive typhoons of increasing frequency, which are also attributed to climate change, have been

bringing extensive damages to aquaculture farms, causing farmers to incur losses, and hindering their economic growth.

1.1.2. Aquaculture in the Japan

Fish production in Japan is classified into marine fisheries (subdivided into coastal, offshore, and pelagic/distant), marine aquaculture, and inland water fisheries and aquaculture. Marine aquaculture accounts for 96.7% of the country's aquaculture production, with a volume of around 915,000 tonnes in 2019. Inland aquaculture on the other hand contributes 3.3% at a volume of around 31,000 tonnes in the same year [6]. Despite the rapid decrease in production by fisheries, production volume by aquaculture has not changed substantially throughout the years, as shown in Figure 1-4 [7]. Out of the 202,430 jobs employed in the fisheries and aquaculture sector in 2018, the number of workers engaged in aquaculture was less than 50,000 [8].

Among the cultured species, yellowtail (*Seriola quinqueradiata*) is the most raised fish in marine environments, accounting for around 64% of the marine finfish aquaculture production in 2019 at around 136,000 tonnes. It is the first marine fish to be cultured in Japan in 1927 [9]. It is followed by red sea bream (*Pargus major*), coho salmon (*Oncorhynchus kisutch*), and Pacific bluefin tuna (*Thunnus orientalis*) at around 23%, 4% and 4% of the production, respectively. After 32 years, Japanese scientists were able to complete a full life cycle of cultured bluefin tuna in 2002 [10]. Their research was a milestone in achieving sustainable aquaculture of one of the most popular fishes in the country. Figure 1-5 shows newly harvested bluefin tunas. In freshwater environments, eel (*Anguilla japonica*) is the most raised, accounting for around 51% of the freshwater fish production in 2019 at around 17,000 tonnes. It is followed by ayu (*Plecoglossus altivelis*), rainbow trout (*Oncorhynchus mykiss*), carp

(*Cyprinus rubrofuscus*), and other trout species, accounting for around 15%, 15%, 9% and 9% of the production [7] [11].

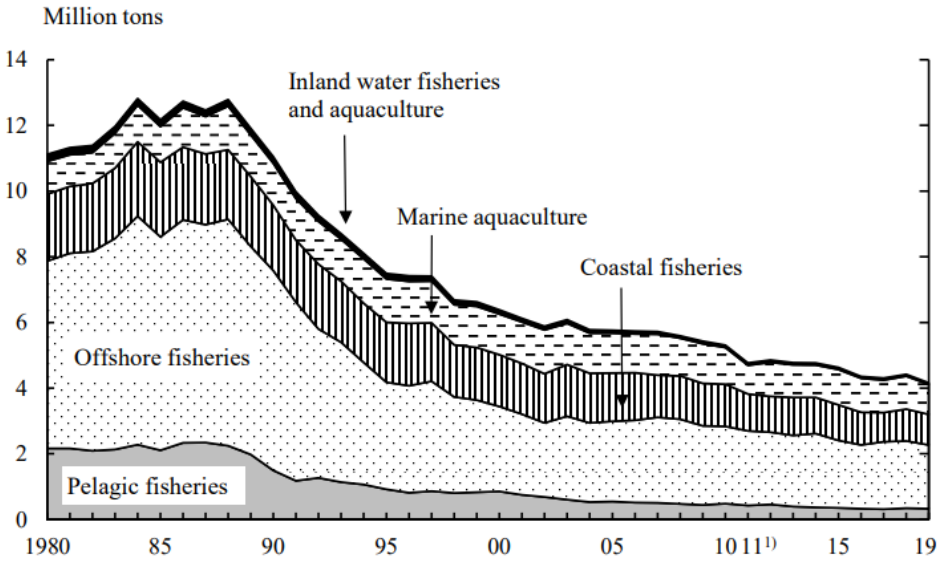

1) Excluding figures lost in Iwate, Miyagi and Fukushima prefectures because of the Great East Japan Earthquake.
Source: Ministry of Agriculture, Forestry and Fisheries.

Figure 1-4 Fish production in Japan by type of fishery (1980-2019) [12]

Figure 1-5 Fish farmers in Japan weighing harvested bluefin tuna

One of the main problems of the aquaculture in Japan is the decreasing number of workers engaged in the industry. This is related to the general problem of country about its population, with the increasing proportion of elderly persons and declining

birth rates [12]. Another problem in the sector is the decline in local catch for raw feed. Catch of sardines (*Sardinops melanostictus*), which was considered an important raw aquaculture feed, gradually declined to a very small amount from the late 1980s [13]. Catch of mackerel (*Scomber japonicus*) has also been decreasing in the recent years [6]. Both have been attributed to changes in marine environment and to more intensive operations by foreign fishing boats in waters surrounding the country [7].

1.2. Research problems

Although aquaculture has become an emerging industry, several problems arise with regards to its sustainability, as shown in Figure 1-6. While some of these are brought by natural phenomena, most result from poor aquaculture management practices. Unsustainable management of fish farms not only affect their surrounding aquatic environment but also the health of the cultured fishes, thus affecting their production [14].

The expansion of the aquaculture production results to increase in demand for feeding materials. Ingredients such as fish meal and fish oil come from wild catches. With the production of capture fisheries already plateauing, aquaculture adds more pressure to the wild fisheries stocks and results to rise in their prices [15]. Some parts of the industry also still rely on seedstocks captured from the wild [15] [10]. This maintains the pressure on wild fisheries stocks. Aquaculture operations would also produce wastes from uneaten feeds and fish excrements. These wastes decompose in the water, reducing the quality of water in the cage [16] [17]. As a result, cultured fishes would become stressed and grow slower or may even die in large numbers, leading to production losses. This is further discussed in section 1.4.

Fishes stocked in cages at high density are prone to diseases and parasites, which may also be transmitted to other species in the surrounding environment [18]. To prevent their spread, farmers would apply various drugs and chemicals, such as antibiotics, pesticides, and disinfectants [16]. Others such as hormones would also be used to improve their growth performance. If not administered properly, these substances would find their way to the environments surrounding the cages, which may harm wild populations [14].

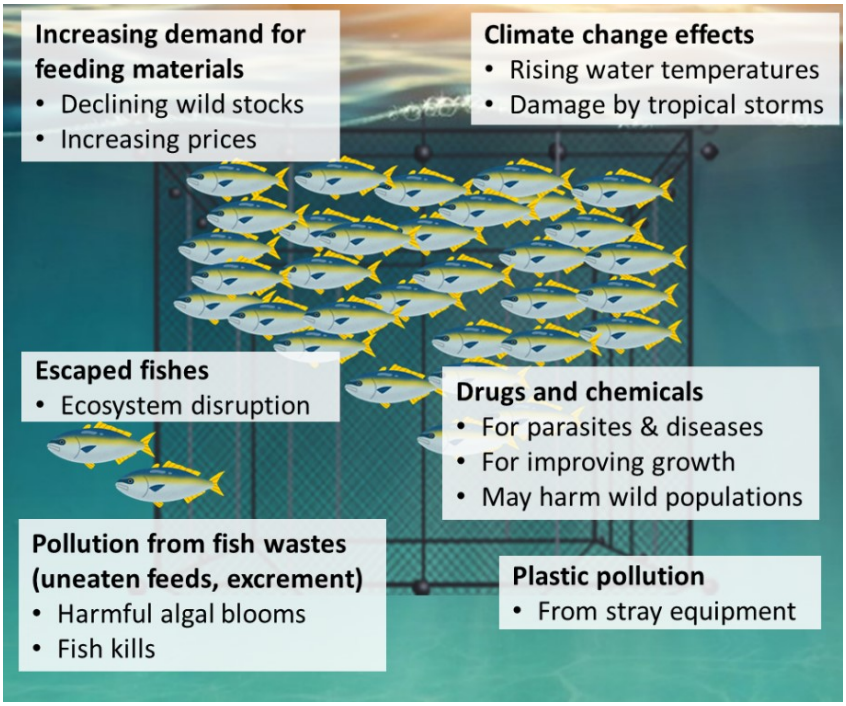

Figure 1-6 Environmental and economic problems in aquaculture

Climate change is also seen to exacerbate problems brought by aquaculture. Resulting rising water temperatures are credited for the increasing frequency of harmful algal blooms, such as red tides. These blooms, which are also worsened by the effects of aquaculture wastes, are threat to the fishes either by asphyxiation or poisoning [19]. In addition, increasingly destructive typhoons worsened by climate change could cause damage to fish cages. Farmed fishes escaping from these cages could threaten local species by predation, competition, and spreading of diseases and parasites [20]. Typhoons also lead to stray plastic equipment from cages that could harm not only local wildlife but also farmed species by entanglement and ingestion among others [21].

These are some of the notable problems faced by the aquaculture industry. If not addressed properly, these issues could cause the industry to collapse and undo its contribution to meeting the growing demand for seafood worldwide. Therefore, various research efforts have been made on the different aspects of aquaculture

towards sustainable growth. Most research works are being done in the fields of biology to improve culture management and optimize fish welfare, with research in other fields assisting to achieve this goal. Main topics include fish growth performance, reproduction and breeding, and regulation of aquatic environment [22] [23]. Engineering topics mostly tackle the development of intelligent monitoring and control systems as well as of optimal design of cages [24] [25].

1.3. Digital transformation (DX) in aquaculture

Digital transformation (DX), defined as the adoption of disruptive digital technologies to increase productivity, value creation and social welfare, has been embraced by an increasing number of industries, governments, and various organizations around the world [26]. The increasing affordability and ubiquity of sensors, embedded systems, and mobile devices and the expanding network connectivity have paved the way to the emergence of the Internet of Things (IoT), big data analytics, cloud computing, and artificial intelligence. With the incentives in using these technologies increasing throughout the years, especially with the recent COVID-19 pandemic, more of the said groups begin to make DX an integral part of their organizational structures, participating in Industry 4.0.

In adopting digitization, many of them, especially industry associations, do not only aim to implement innovative business models and increase income generation, productivity and added value to the economy. They also aim to bring social transformations by fostering innovative and collaborative cultures and improve accessibility and quality of digital services to the general population. In businesses, DX adds another way of creating new value for customers and new markets while maintaining the traditional business operations.

In the aquaculture industry, DX has been seen as a tool for remedying the environmental challenges faced by the industry and as an enabler of predictability, efficiency, and productivity [27]. With work in this industry considered as hazardous, introduction of DX is also seen to bring positive effects on the health and security of personnel. It is estimated that applying DX in aquaculture operations by reducing operation costs and personnel, as well as increasing feeding efficiency [28]. By

applying DX, long-term monitoring of fish cages can be done to collect considerable amounts of data on the fish biomass and health, environment, feeding, etc.

Information from this data augments the knowledge of expert farmers, which would not only help them improve their feeding decisions, but also those of less experienced farmers. This in turn enables them to optimize their use of resources, such as feed and fuel, not only reducing their production and maintenance costs but also improve fish feed conversion ratio (FCR) and health, minimizing stressors, and preventing fish kills. DX not only leads to the increase in their income amount but ultimately, produce more high-quality fishes for the seafood market and reduce the pollution in the aquatic environment, moving the aquaculture towards becoming a sustainable industry. Figure 1-7 maps the contribution of DX towards sustainable aquaculture.

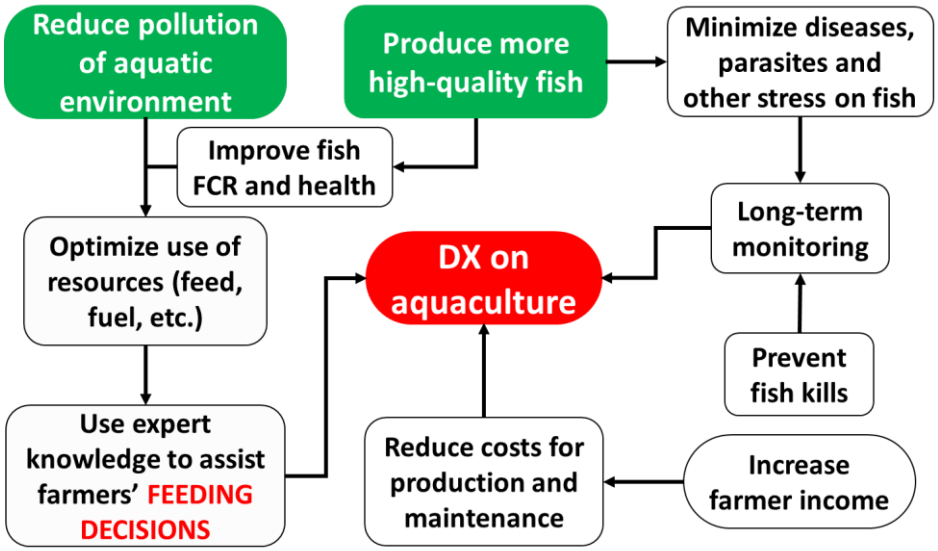

Figure 1-7 The impact of applying DX to achieving sustainable aquaculture

1.4. Optimization of fish feeding

One crucial issue in aquaculture is the need for efficient decision making in fish feeding. In many aquaculture operations, feeds make up a large portion of the production costs, since growing fishes require feeding them and takes a few months to many years to achieve the desired fish weight, depending on the fish species. Although the proportion to the overall production costs in different countries vary due to differences in intensity and feeding practices, feeding costs account for as high as 92.5%. Figure 1-8a shows the relative proportion of aquaculture costs by item in all farm categories (intensive, semi-intensive and traditional) in six countries – Bangladesh, China, Philippines, Thailand, Vietnam, and India, having an average relative proportion of 58% for feeding [29]. In Japan, the proportion of feeding costs for yellowtail and red sea bream, two major aquaculture species in the country, make up 67% and 64% of the production costs, respectively (Figure 1-8b).

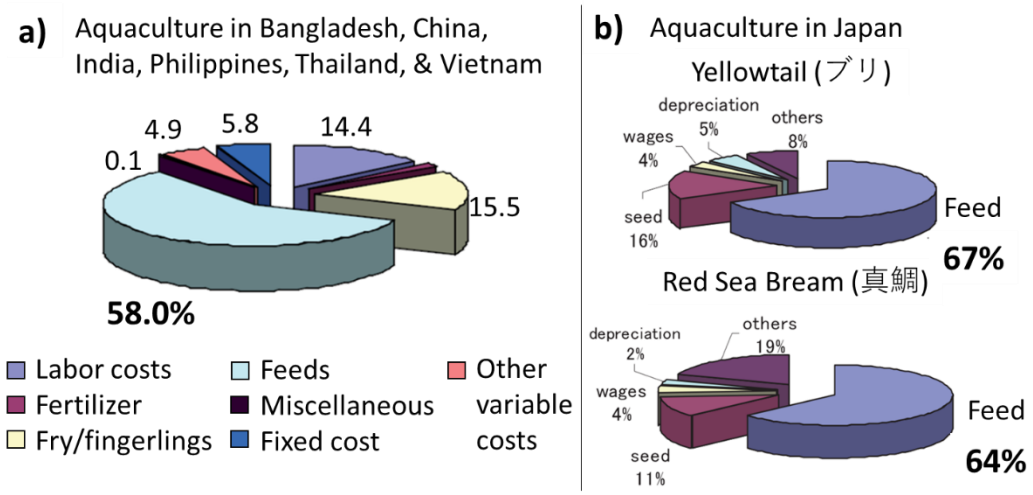

Figure 1-8 Share of production costs in six Asian countries [29] and in Japan [13]

As mentioned in section 1.2, the expansion of aquaculture operations increases the demand for feeding materials. Fish meal, fish oil, and raw feed, important ingredients for feeds, are sourced from wild caught fishes. With the increasing pressures in wild

fish stocks, the increasing demand drive the rising prices in these ingredients, adding economic burden on aquaculture operations [13] [15]. Figure 1-9 shows increase in prices of raw feed and imported fish meal in Japan from 2005 to 2021. Plant-based ingredients such as soybean, wheat gluten, and corn meals are cheaper alternatives to fish-based ingredients but have nutritional drawbacks for cultured fishes [30]. Their prices also have been increasing in the recent years. Other sources such as animal by-products, microalgae, and insect larva (e.g., black soldier fly) also have potential as alternatives but these also may have some nutritional drawbacks and still need to be developed for large scale commercialization [31] [32]. Therefore, to maximize the return of investment from the large costs incurred from feeds, farmers need to make sure every gram of feed gets eaten, not wasted to the surrounding environment. In other words, feeding needs to be optimized.

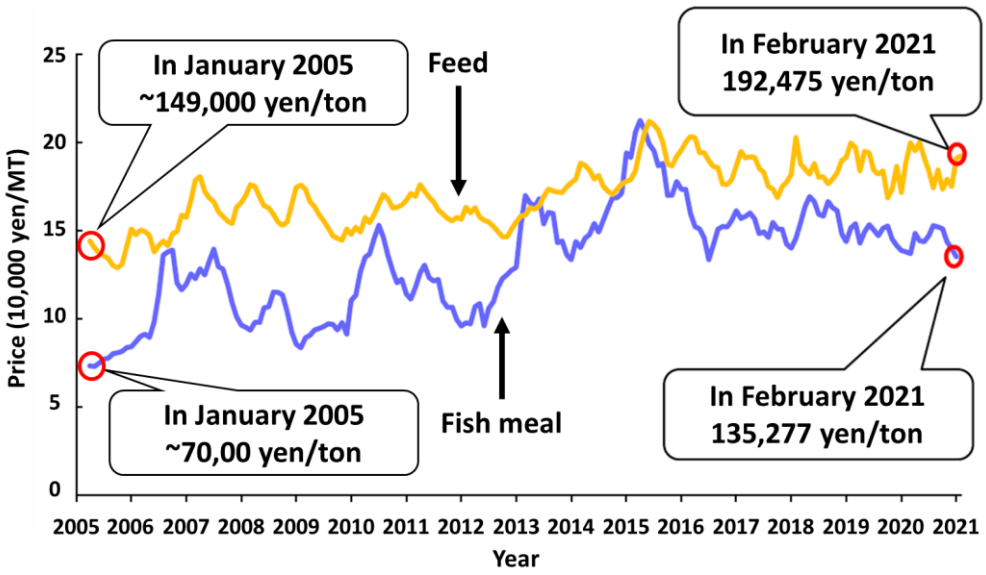

Figure 1-9 Price of feed and imported fish meal in Japan (2005-2021) [6]

The conventional farmers' practice of fish feeding is deciding the timing and the amount based on their visual judgement of fishes' appetite through their behavior as seen from the surface. At the start, a farmer would usually throw a few feeds on the

water gradually to lure the fishes to the surface. He would then check how many fishes are swimming actively at the surface and how much turbulence they are making at the surface (Figure 1-10). Upon assessing that many fishes are ready to eat, he would start giving them feeds continuously, either with hand or a feed ejecting machine. He would constantly look out for changes in the intensity of the turbulence, how it weakens over time. He would finally stop giving the feeds when he sees that they are no longer grabbing food at the surface, as indicated by almost calm water.

Figure 1-10 Intense surface turbulence made by fishes while feeding

Efficient feeding has usually been achieved with decisions made by expert farmers who, through years of acquiring much skill and experience, could assess of the fishes' behavior and their appetite with high accuracy, and effectively control the feeding. This reduces the fishes' feed conversion ratio (FCR) or the ratio between the amount of feed given to a population and its weight gain thus improving fish welfare and reducing costs [33]. However, this practice of feeding remains to be an "art," where prediction of the appetite relies on the farmer's intuition of the fishes' behavior. The decision-making process is subjective, where the basis of each one's judgement is based on his own experiences of feeding. Therefore, information of when to stop

giving feeds cannot be quantified by a unified standard [23] [33]. As a result, in the difference in quality of the harvest of expert and novice farmers are substantial. Fishes grown by the experts are consistent in size and shape and are heavy for their age. Those raised by novices, on the other hand, vary in shapes and size, indicating unequal distribution of feeding among the population. Novice farmers also have the tendency to feed the fishes inefficiently, either by underfeeding or by overfeeding, which could have serious effects on the aquaculture operations, as shown in Figure 1-11.

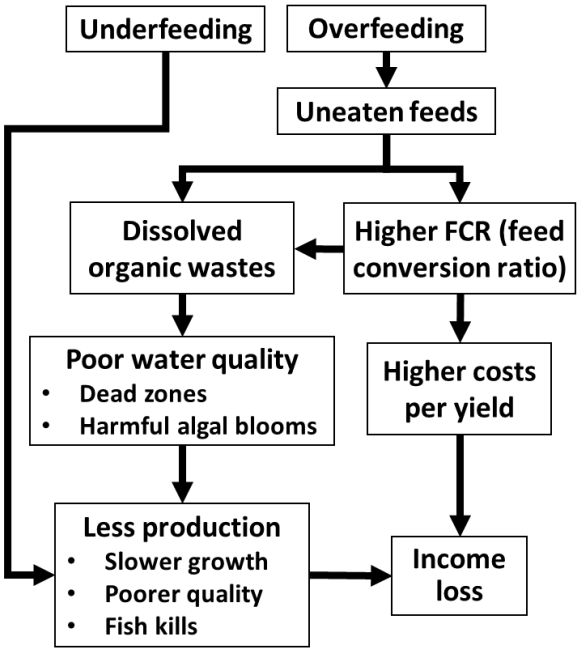

Figure 1-11 Effects of inefficient feeding of cultured fishes

Poorly timed and estimated feeding leads to poor cost-efficiency in raising fishes [34]. Underfeeding results to the slower growth and poorer quality of fishes. On the other hand, overfeeding results to uneaten feeds. Some researchers estimated that 8.26% of the supplied feed get lost to the environment in a sea bream farm although it could be more in other cases [35]. This increases the FCR of the fishes i.e., excess feeds do not contribute to their nourishment and further growth. Therefore, costs expended on the uneaten feeds do not get into increase in their quality and

consequently value. This, in turn, reduces the potential income that farmers can earn from them.

In addition, these feeds either sink to the bottom of the sea, river, lake, or pond, or become suspended in the water. Either way, these wastes decompose in water with the help of bacteria, producing organic compounds such ammonia, nitrite, nitrate, and phosphate, reducing the water quality [16]. Ammonia and nitrite are toxic to fishes and can disrupt normal functioning of their internal organs [36] [37]. These can also make them more vulnerable to diseases. When in large concentrations, nitrate and phosphorous cause eutrophication in the surrounding aquatic environment, accelerating growth of algal blooms [16] [17]. Decay of algal blooms as well as feeds consume dissolved oxygen (DO) and can deplete the supply for the fishes. The stress caused by this depletion result to less food intake, higher FCR, slower growth rates, and poorer health of fishes, reducing the quality of harvest [22] [38]. At worst, massive fish kills can occur in the cages, wiping entire populations [4].

In the end, not only inefficient feeding could limit the profitability of the farm operation, but it could also cause fish farmers could even lose their investments as a result. Therefore, DX may prove useful to fish farmers in estimating fish activity so they can improve their feeding practices and optimize their use of feeds. Not only this enables them to increase their harvest of high-quality fishes and minimize economic losses but also reduce the pollution in the aquatic environment.

1.5. Literature review

1.5.1. DX applications in aquaculture

Although the application of digital technologies in fisheries and aquaculture began sometime in the 1990s, the practice of DX in the industry have only become prevalent for around the past 15 years [24] [39] [40]. Many research works focus on monitoring the environment or the fish activity and welfare and on the controlling of feeding. The following are a few research works applying DX in aquaculture.

Garcia et al. proposed a sensor-based system to control feeding in fish cages [41]. As shown in Figure 1-12, a management system would collect various measurements from arrays of sensors in the cage and use data fusion to predict the suitable feeding decision. So far, they demonstrated their system through simulation using real-world measurements. Their placement of sensors also seemed limited, having each sensor array only at one side.

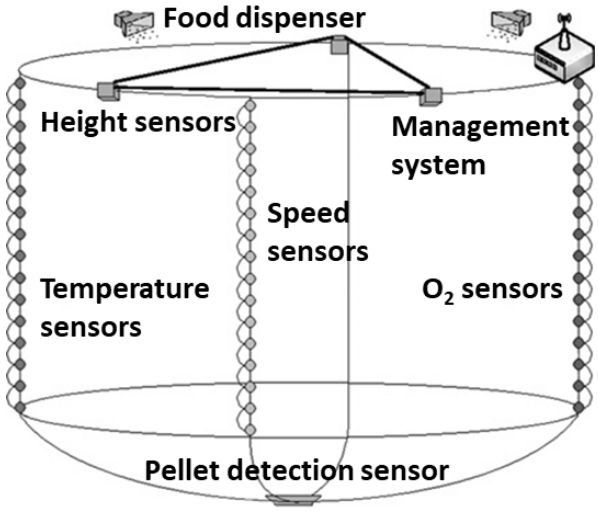

Figure 1-12 sensor network made of different sensors placed at multiple depths [41]

Føre et al. developed a real-time monitoring system for Atlantic salmon in sea cages using acoustic telemetry [42] [43]. As shown in Figure 1-13, they used two acoustic receivers at two depths to track fishes tagged with depth or activity sensors and

wirelessly transmit the data to a monitoring system in the feeding barge. While their system could track the fishes in real time, tagging a small sample may not represent the feeding behavior of a large feeding population. On the other hand, equipping more fishes with telemetry tags could cause interferences in data transmission, causing large data losses while monitoring.

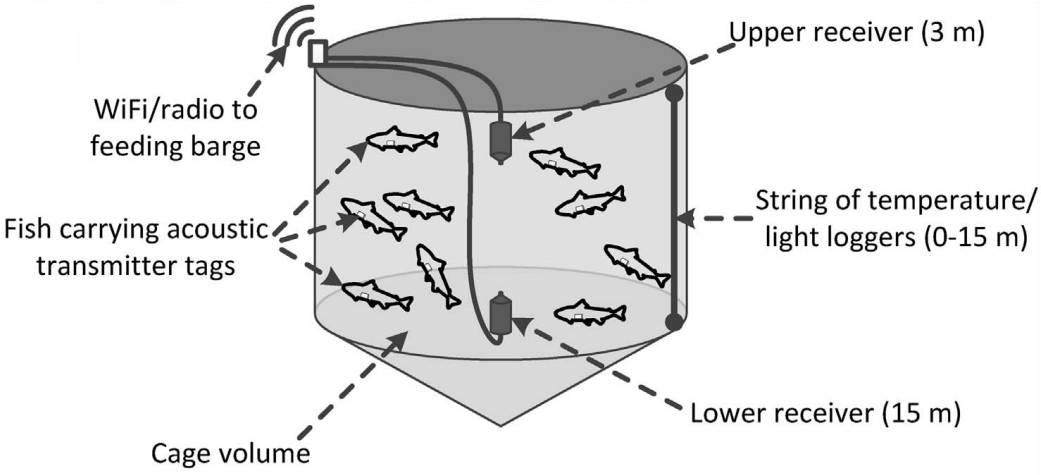

Figure 1-13 Acoustic-telemetry-based fish behavior monitoring system [43]

Skøien et al. measured the attitude and direction of a feed spreader in a fish cage by using an attitude and heading reference system reading rotation data from a rotary encoder attached to the spreader pipe. At the same time, they characterized the spatial distribution of pellets from the feed spreader by imaging the surface with an unmanned aerial vehicle (UAV). They could use this system to assist fish farmers evaluate the performance of various feed spreaders and help feeding equipment producers make better designs [44].

Eichhorn, Karimanzira et al. developed a modular unmanned underwater vehicle (AUV) system that could carry various sensors for real-time monitoring of water quality in the surrounding environment of aqua farms [45] [46]. They conceptualized the AUV navigating through fish cages while avoid obstacles, collecting measurements at different depths near each cage before docking near a station to

upload data (Figure 1-14). They also deployed this system and measured nitrate discharge at different depths near aqua farms.

Kim et al. developed a control system for submerging and surfacing a fish cage in the sea to make it withstand adverse weather conditions [47]. The system incorporates wind speed and wave height sensors and uses the data they collect to determine the weather conditions. After deciding, it automatically controls motors to pump air into or out of ballast tanks at the bottom of the cage to make it sink or float.

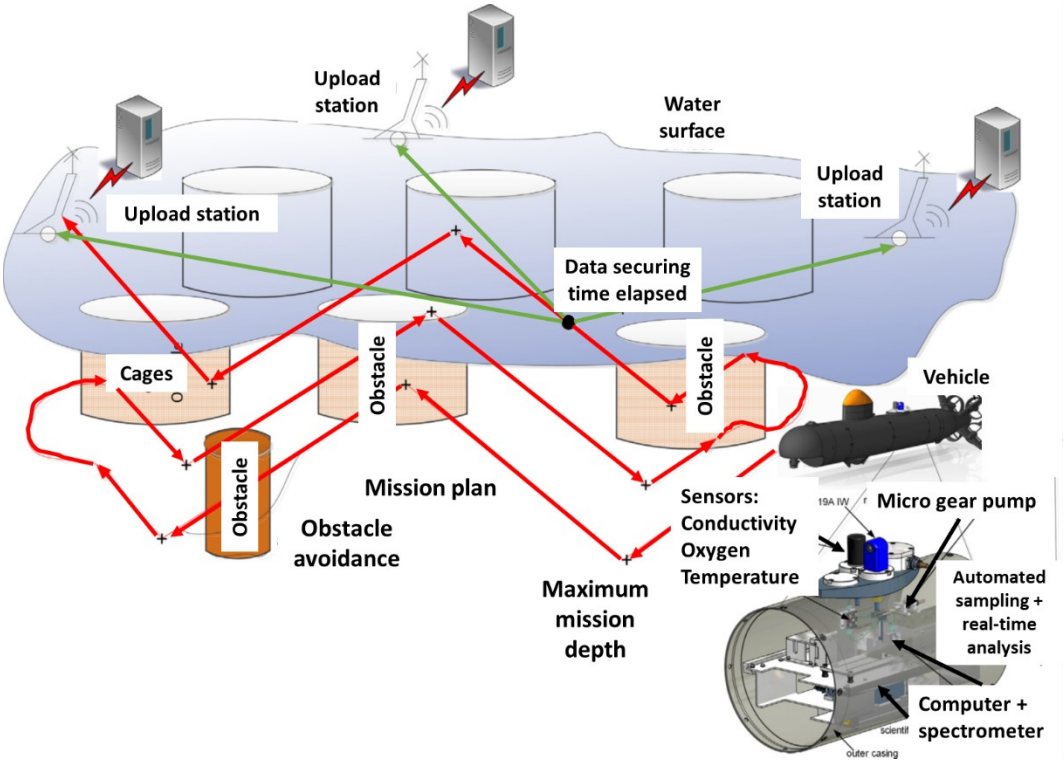

Figure 1-14 AUV water quality measurement collection mission plan [45]

1.5.2. Fish activity estimation

Especially with the recent advancements in artificial intelligence, intelligent feeding control has become one of main topics of current research efforts in aquaculture. Researchers have developed various methods to recognize and analyze fish feeding in water [33] [48]. Applications vary from tracking fish movement to detecting feeds in water. Some of these methods feed the information collected into

machine learning models to generate feeding decisions [34] [49] [50]. Different information technologies developed fall into three broad categories: computer vision (CV), acoustic technologies, and sensors-based technologies.

Recognizing fish activity with computer vision is the most widely used technology in aquaculture in recent years, as optical sensors and machine vision systems are becoming more power and sensitive, while becoming less expensive throughout the years [51]. Researchers take various approaches to recognizing fish activities from images.

Zhou et al. developed two automatic feeding decision systems based on near-infrared (NIR) imaging. The first system calculates the snatching intensity of the fishes in a tank from the texture features of the near-infrared images as well as their flocking behavior from their distances from each other, as shown in Figure 1-15 [49]. They feed these calculations to an adaptive network-based fuzzy inference system (ANFIS) to make a feeding decision. The second system used the images to train a convolutional neural network that classifies the feeding into four intensity levels – none, weak, medium, and strong [50].

The method developed by Zhao et al. extracts foreground feature points from a RGB images of tilapia feeding in a tank using optical flow and obtains the school's dispersion degree and the interactive force using covariance and social force models, respectively (Figure 1-16) [52]. It also estimated the water flow fields from the reflective areas extracted of the image and calculated their kinetic energy. The appetite is estimated from the combination of the three obtained values.

Using the property of NIR to be absorbed by water, Pautsina et al. tracked the 3D position of the fishes through imaging the fish tank surface illuminated by NIR [53].

From the image intensities, they obtain the fishes' 3D coordinates as well as their relative speeds. In another research, Saberioon and Cisar developed a system for tracking multiple fishes in a fish tank using a structured light sensor [54]. They combined sensor's RGB camera and NIR camera to obtain the fishes' position in 2D space and their depth to ultimately track them in 3D space. Other researchers detect uneaten feeds from underwater images to indirectly estimate fish feeding activity [48].

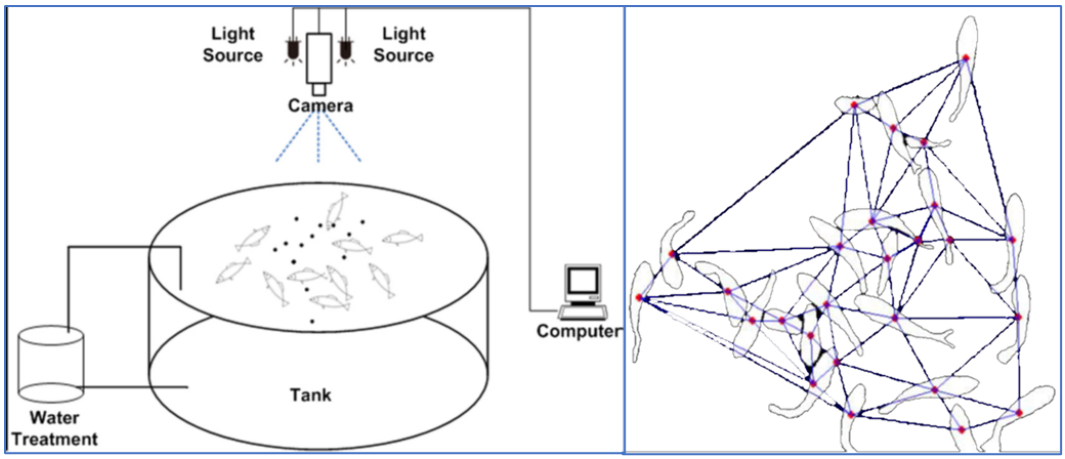

Figure 1-15 Calculating flocking behavior from image of fishes in a fish tank [49]

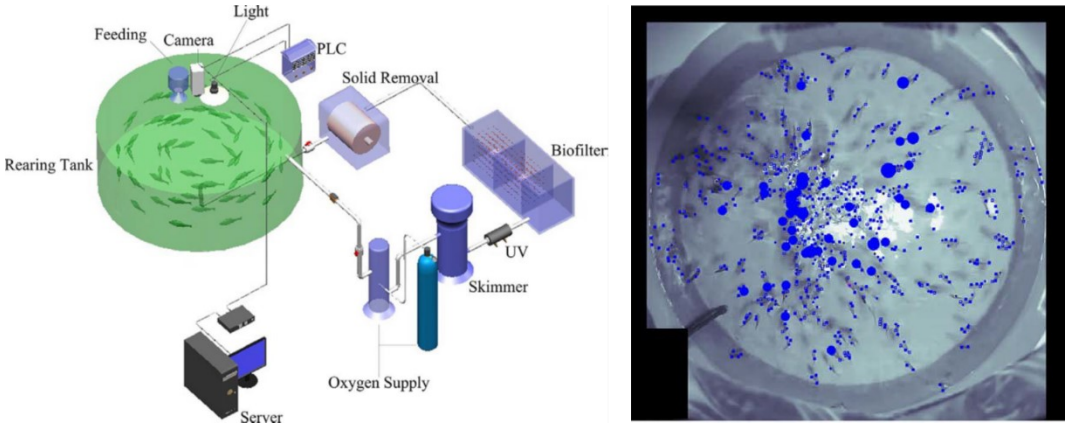

Figure 1-16 Measuring dispersion and interactive forces from a fish tank image [52]

Although CV is a prevalent technology for fish activity estimation, a significant issue in its use is the complexity of the aquaculture environments causing various degradation to images [55]. Experiments most of the research works cited were made in indoor fish tanks where environment was controlled. While some methods use near

infrared to adapt to low lighting and turbid water, their resolution and accuracy need to be improved.

Acoustic technologies overcome the problems of degradation brought by varying illumination and water turbidity conditions affecting the performance of CV, as sound propagates in water with much less attenuation. Acoustics-based activity recognition can be classified into imaging and non-imaging methods. Imaging uses sonar to generate images of fishes underwater. Tao et al. used a moving vertical and fixed horizontal echo sounders to observe spatial distribution and swimming speeds of fishes in a dam [56]. By attaching the sounders to a boat and to a ship lock, they found out that the fishes there follow a diel vertical migration pattern. Rakowitz et al. observed fishes entering and escaping a trawl by imaging with a multibeam acoustic camera [57]. They attached the camera to the trawl, extracted eight numeric track features from the imaged fishes and identified their behavior from eleven avoidance behavior categories. Zhang et al. used the same device to measure the length and observe the swimming patterns of Chinese sturgeons in a cage [58]. They placed the camera in one corner, pointed to the opposite corner. While acoustic imaging is intuitive and easy to use, imaging equipment is relatively expensive.

Non-imaging acoustics are also applied in various ways. Mallekh et al. measured the intensity of feeding sounds of turbots in a fish farm using a hydrophone and evaluated the feeding intensity from the signal variance [59]. They also characterized the feeding characteristics of brown trout and rainbow trout using this method [60]. Polonschii et al. used an 3D array of ultrasound transducers to track the 3D position of sturgeons in a fish tank, as shown in Figure 1-17 [61]. Using their system, they observed normal and abnormal fish behavior at different conditions with parameters

adjusted to outside normal levels. Each kind of method also face specific problems. Detecting feeding sounds with hydrophones may be affected by ambient noise from aquaculture equipment and weather. Using too many transducers in a culture environment may cause interference with each other, possibly leading to data losses.

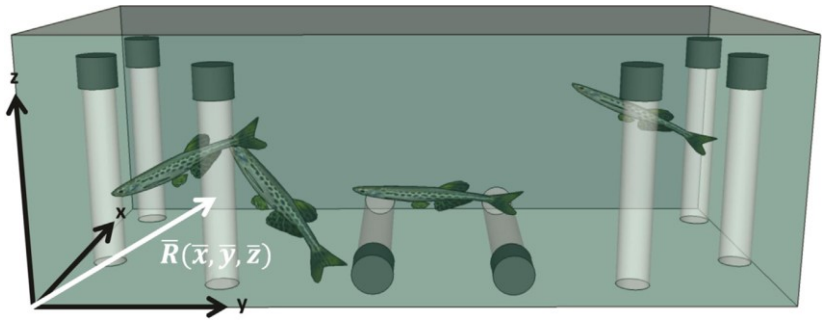

Figure 1-17 3D ultrasound transducers placed in a fish tank to track sturgeons [61]

While various sensor-based activity recognition technologies are applied, those widely used usually fall into two groups – sensor tagging (inertia, depth, muscle activity, etc.) and water quality sensing (DO, temperature, pH, etc.). With tagging, data from sensors attached to fishes are usually logged internally or are transmitted in real time using acoustic or radio telemetry. Noda et al. attached inertial measurement unit (IMU) loggers on yellowtails to reconstruct their dynamic accelerations and angular velocities [62]. Together with a high-speed camera, they used the data to characterize the fishes' fast-start behaviors (for feeding or escaping). Cubitt et al. attached electromyogram (EMG) transmitters on rainbow trout fishes to measure their muscle activity in real-time [63]. Using support vector machines (SVM), they were able to classify the fishes' hunger states with high success. As already mentioned, Føre et al. tagged fishes with depth sensors or accelerometers with acoustic telemetry for real-time activity monitoring [42] [43].

While sensor tagging can measure fish activity with high accuracy, this method is invasive, which may affect the welfare of the fish. In addition, data from a small

sample group may not accurately represent the activity of a large fish population. However, tagging a larger sample becomes logistical more difficult and may cause technical problems such as transmission interference and data losses.

On the other hand, measuring water quality using sensors for parameters such as dissolved oxygen and temperature are non-invasive methods for estimating fish activity. Soto-Zarazúa et al. implemented a fuzzy-logic-based system to control the feeding of tilapia by measuring the DO and temperature in the fish tank [64]. They get the fishes' feeding demand as affected by their feeding rhythms. Wu et. al developed an ANFIS fuzzy-logic controller that uses DO measurements to make feeding decisions for silver perches in fish tanks [34]. They used changes in DO not only as an indicator of fish appetite but also as a transient effect of the fishes' flocking and struggling behavior. Zhao et al. also developed an ANFIS controller that uses DO and temperature for feeding grass carps in ponds [65]. They obtained the percent values of feeding, which are indicators for the fish feeding activity. Although not a water quality sensor, Chang et al., developed an intelligent feeding controller that uses infrared a photoelectric sensor to observe the gathering behavior of eels [66]. While these methods generate feeding decisions with high success rates, effectively reducing feed wastes, their measurements are susceptible to changes in the external environment.

1.6. Flow measurement in aquaculture

Offshore cage aquaculture environments, whether freshwater or marine, are complex, with many sources of noise and environmental changes that can affect the measurements made in water. We therefore need a flexible self-correcting system for estimating fish activity underwater in cage aquaculture to assist farmers in making feeding decisions. In addition, it must be able to make long-term observations to help farmers throughout the growth cycle of the fishes.

A measurement that has been barely explored for estimating fish activity is of the water flow generated by fish movements. Most studies on fish-induced flow in aquaculture focused on its interaction with the effect of sea currents on net structures as well as on the water exchange for oxygen resupply [67]. Chacon-Torres et al. evaluated the effects of fish movements on the water exchange in small cages containing rainbow trout and observed faster dye dispersion at increased fish activity [68]. Findings from dye experiments and current measurements by Gansel et al. suggested that the circular motion of large group of fishes pushes water out of the cage, creating vertical water exchange [69]. Tang et al. also made similar observations through numerical simulations, with higher fish densities reducing drag force on the net cage [70].

While Zhao et al. estimated the change in water flow magnitude to assess fish appetite, measurement was still based on CV as it extracted the reflective areas from the images taken by cameras [52]. Garcia et al. proposed the use of fish speed sensor that senses streams produced by fish movement to assess feeding behavior but did not elaborate on the sensor details as they only simulated their system using real-world measurements [41]. In addition, their system is not self-correcting since they proposed

a sensor array placed only on one side of the cage, having to rely on external current sensors for calibration.

For designing a system that estimates the fish activity through the measurement of induced flow, we make some assumptions about the fish behavior inside and the flow around the cage, as shown in Figure 1-17. When held at high density, a shoal of fishes can adopt a polarized schooling as a response of each fish to minimize the risk of collision with others [71]. Therefore, we can first assume that fishes swim in a circular pattern within a highly stocked cage. Outside feeding times, we assume that the fishes tend to stay at the bottom of the cage. They only swim to the surface when they detect feeds in water and when they are hungry. Given these conditions, they swim actively at the surface. They swim back to lower depths when they become satisfied.

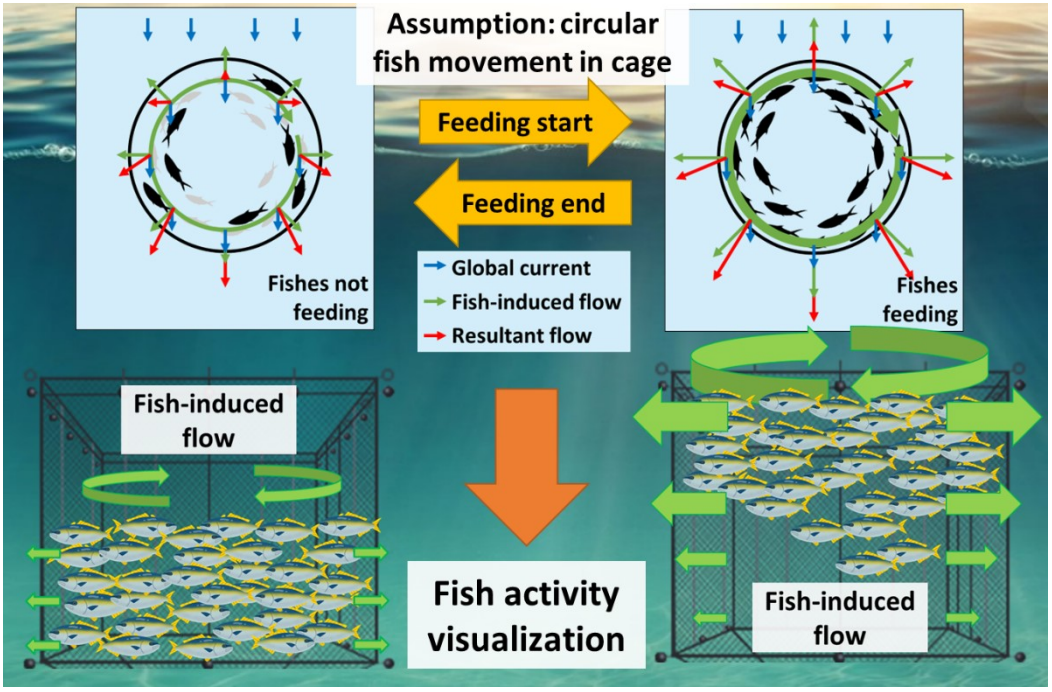

Figure 1-18 Concept of fish-induced flow by outside of and during feeding

We also assume that the circular motion of a school of fishes generates water flow moving radially out of the fish cage. We also assume that the instantaneous flow speed is uniform in all directions. This speed is mainly dependent on the fish school's

swimming speed and on its depth distribution. This means that flow speeds at different depths may vary. Global current mainly caused by the tide and winds can be assumed to flow uniformly through a fish cage in a single direction. Fish-induced flow at a given point can either be reduced, increased, or cancelled by the global current, depending on the velocities of both. With these assumptions, we may be able to help farmers, especially the less-skilled ones, better visualize the underwater fish activity by measuring the flow at different depths from different directions. This visualization could also help them gain better understanding of the fishes' feeding behavior and of the decision-making process of expert fish farmers and optimize their feeding.

1.7. Objectives

We therefore propose in this thesis a system that estimates the fish activity through flow measurements for assisting in making feeding decisions in cage aquaculture. The objectives of this research are enumerated below:

1. To introduce DX in fish cages by developing a sensor network. To meet this objective, we first need to construct a modular network that can collect sensor data – flow speeds and video recording of fish activity, at different depths from multiple sides of a fish cage. By doing this, we can realize observation of fish activity in cages of various configurations that can adapt to the changes in the environment. Second, we need to realize an offshore system to enable the sensor network to make long-term observations of the fish activity. This is an important aspect of introducing DX as estimation of fish behavior for making good feeding decisions is essential throughout the fishes' growth cycle.
2. To clarify the properties of fish activity in feeding. To achieve this, we must first observe the fish activity by recording flow speeds and videos in fish cages, especially during feeding. We then need to compare the collected flow speeds data with the recorded fish activity videos. By doing this, we can get a better understanding of their relationship as we find features in the flow data that correspond to the changes in the fishes' movement and distribution throughout the cage.
3. To propose a DX system for cage aquaculture, as shown in Figure 1-18. This needs to be done to set the direction of this research in the future. We can move towards the realization of DX in estimating fish behavior and in optimizing the use of resources in feeding cultured fishes.

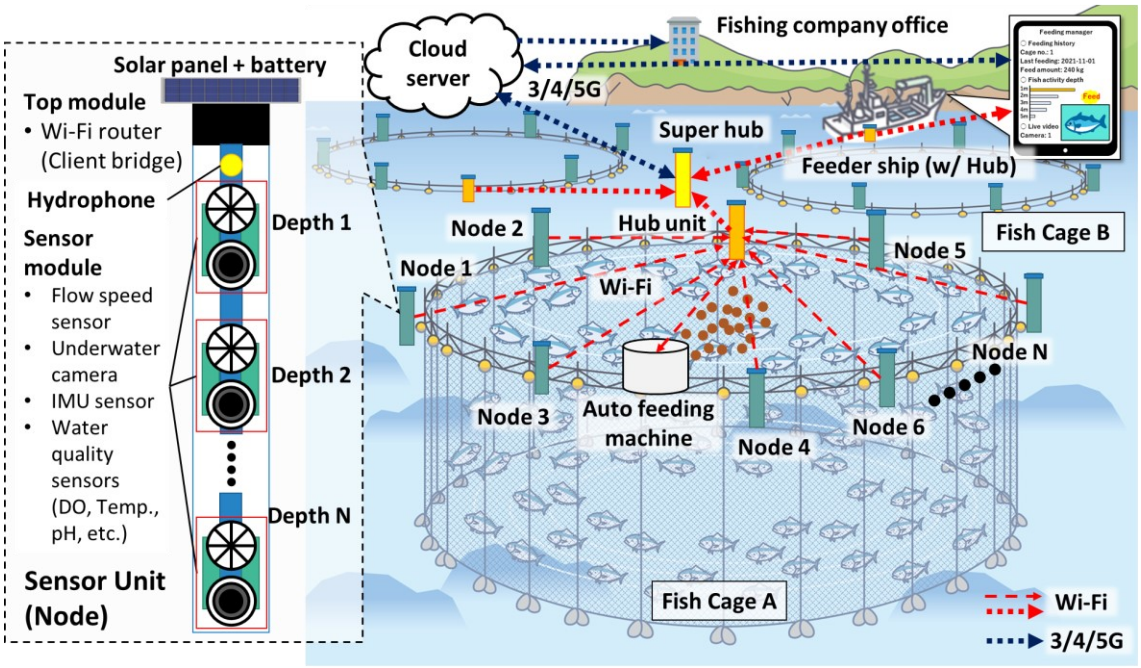

Figure 1-19 The envisioned sensor system deployed in fish farms

Chapter 2
Flow speed sensor network

Chapter 2. Flow speed sensor network

2.1. Modular sensor network design and development

2.1.1. System design requirements

Flow speed is the primary measurement of this system, as proposed. This is usually measured in meters per second or centimeters per second, as specified in commercial current meters. Since it was anticipated that fish-induced flow speeds would not exceed those of ocean currents, it was decided to use the latter unit for measurement. In addition to flow, video recordings of fish activity can validate the measured flow speeds.

While flow measurement is not affected by noise or by changes in ambient light or in the condition of water, is important to note that the flow measured at a single point could come not only that created by the fishes but also from currents outside the cage caused by various sources such as winds or tides. These external currents generally flow through cages in any single direction. Isolating the fish-induced flow could be done by measuring at different points of the cage, especially at opposing sides. Figure 2-1 shows the concept of cancelling the effects of external currents from the sensor measurements.

Fish cages, whether square or circular, come in varied sizes – area and depth. Measuring flow at deeper and wider cages requires positioning more sensors between the surface and the bottom at more than one point on one side. In addition, fish farm operators might have specific requirements on the position of measurements. A modular design for the network could address these issues by as allowing flexibility with the positioning of the sensors as well with the number of sensors to be installed at target depths and directions.

Cabling between sensors therefore needs to be minimized as installation of sensors in a fish cage is complex, especially without equipment, since space for movement is limited.

This is also needed to keep them as light as possible. This can be accomplished between sensors within a column in the cage by connecting them in a daisy-chain. Sensor arrays at different points in the cage are then connected wirelessly above surface, with their data being relayed to a central computer.

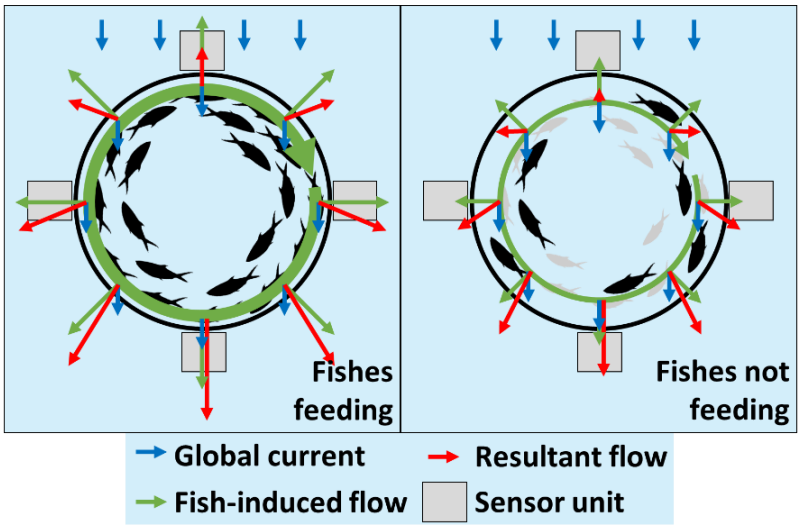

Figure 2-1 Sensor network design based on the concept of fish-induced flow from cage

Cages could be too far from cellular networks, so immediate access by the sensors to the cloud from the cage might not be possible. To address this, the central computer needs enough data storage that can temporarily hold three to seven days' worth of flow speeds and videos. The capacity could depend on the frequency of feeding, with some farmers feeding their fishes once in at least two days.

2.1.2. Sensor network structure

In essence, the sensor network is implemented as a combination of star and daisy-chain networks. A sensor module serves as the basic unit of the sensor network, measuring flow and recording video at a given point in the fish cage. Multiple modules connect to each other in a daisy chain arrangement and form a sensor unit, collecting data at multiple depths from one side of the cage. Each sensor unit contains a top module to which the

daisy chain of sensors connects. The top module wirelessly connects the sensor modules to a hub unit, which collects the data from all sensor units and controls the operation of the sensor modules. The sensor network's structure is illustrated in Figure 2-2.

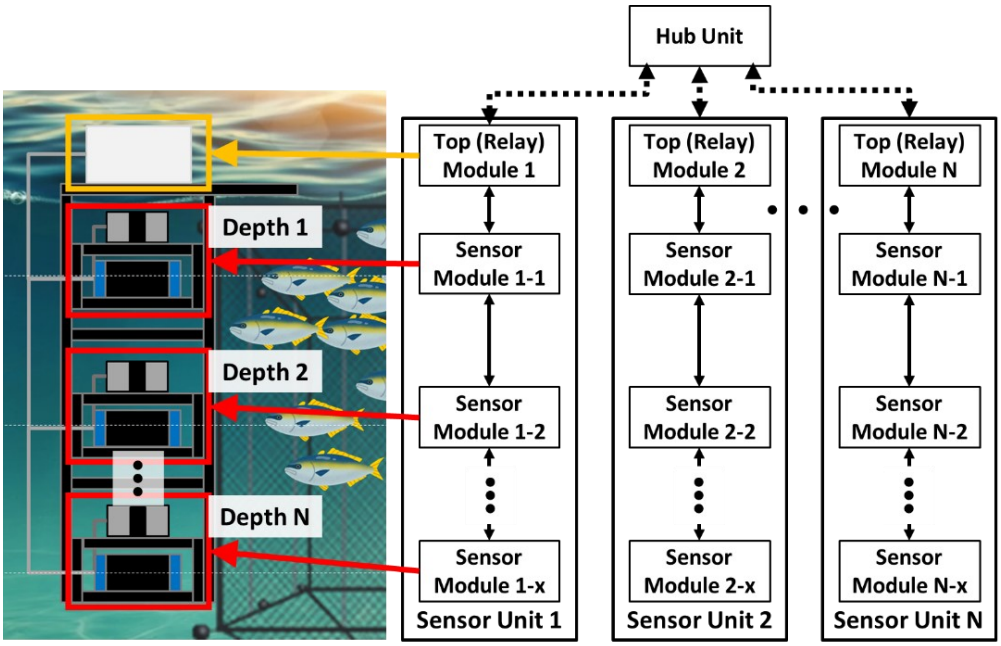

Figure 2-2 Network structure of the modular sensor system

Multiple sensor units can be installed at any position in one cage. However, the sensor network can function most effectively if at least one unit is positioned on each of at least two opposing sides so that sensors on either side could measure the flow caused by external currents, cancelling their effects. Ideally, each sensor unit can consist of as many sensor modules as possible. However, the number of installable modules per unit is limited by the voltage supplied to the top module as well as the voltage drop from the top module to the nth sensor module, which depends on the resistance of the power cables. The network bandwidth is also a limiting factor as the hub unit router, having a given bandwidth, becomes a bottleneck for all the data coming from the sensors. The number of sensor modules is therefore limited to avoid any data loss.

2.1.3. Sensor modules

To measure flow and record fish activity videos, each sensor module uses an underwater flow sensor and a network camera (Figure 2-3). A modified propeller-type flow sensor is mounted on the module frame to measure flow underwater. Development of this sensor is be discussed in the next subsection.

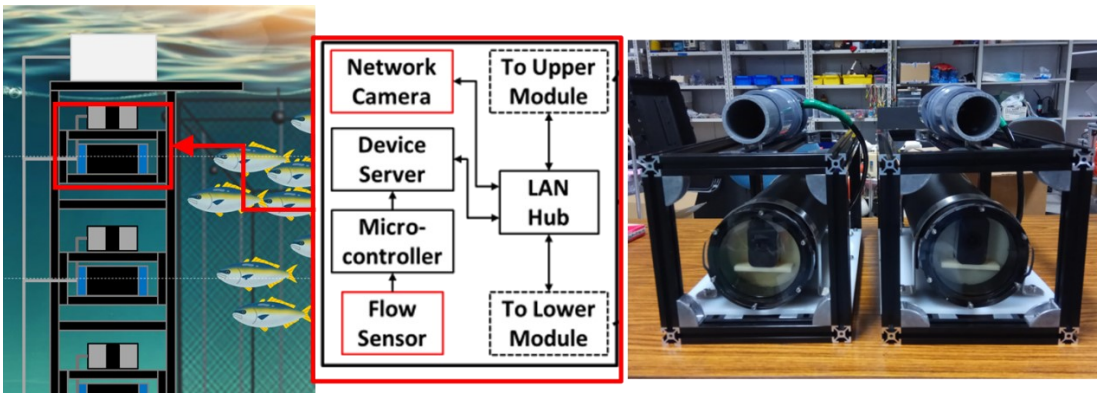

Figure 2-3 Sensor modules and their main components

The microcontroller reading the signals from the flow sensor outputs measurements by serial to a device server, which is connected to a LAN hub to transmit the data to the hub unit computer by TCP/IP. To access the flow server, the hub unit connects to the device server by Telnet. Another port of the LAN hub is designated for the network camera. Two other ports are for the LAN ports of the upper and lower sensor modules, so that sensor modules can form an Ethernet daisy chain. Isolated DC/DC converters are used so that the power supplied to the top module is converted to smaller voltages to properly operate the sensor microcontroller, the device server, and the LAN hub.

The network camera runs on Power over Ethernet (PoE) – power line runs through the Ethernet cable for communications. Since it is the only PoE device in the module, it connects to a PoE injector, whose data line is connected to the LAN hub and power line to the supply. Depending on the standard, voltage supplied to PoE devices is in the range

of 48-57 V. Since voltages at the power supply are usually lower than the said range, each sensor module houses an isolated step-up DC/DC converter for the network camera to operate.

Static IP addresses were assigned to each IP device of the sensor module for easier identification and access of the sensors. Both the device server and network camera of each module are assigned with addresses having the same end digit at the fourth dot decimal and designated tens digits to distinguish the kind of device. For example, the camera of a sensor module is assigned with 192.168.100.1X while the device server is assigned with 192.168.100.2X. This organization, however, will have to be changed when expanding the number of modules of the sensor network as it only assumes 9 modules in the system.

All module electronics other than the flow sensor are housed inside a watertight enclosure. Together with the other sensor electronics except for the current sensors, the network camera is enclosed inside a cylindrical watertight enclosure, with one side attached with a transparent cap for the camera and the other for the watertight connectors that connect the module to others. The connector side has three connectors. One is for the flow sensor, which leads straight to the microcontroller's pins. The other two connect to the sensor module or top module above and to the sensor module below (unless it is the bottom sensor). Both connect to the power converters and to the LAN hub ports. An aluminum mounting frame is made for each sensor module to fix the position of the electronics enclosure inside and of the flow sensor on top.

Underwater cables for Ethernet and power were also constructed to connect all the sensor modules to each other and form a daisy chain with the top module. Although a sensor unit can theoretically be comprised of as many sensor modules as desired, the

actual number is limited by the voltage supplied and by the resistance of each cable. High resistance in cables due to length and wire gauge causes voltage to drop at the module connector. The sensor modules at the farthest end will not work if the dropped voltage is less than the minimum operating voltage for the component devices. More sensor modules could be added by using cables with lower wire gauges i.e., wires with larger diameter. While shortening the cable can also reduce the voltage drop, this limits the separation between the sensor modules. The trade-off between the two should be balanced.

Each sensor module is mounted on a modular four-legged stainless-steel frame that can be attached to other frames to form a sensor unit (Figure 2-4). Each frame has a mounting plate that can be shifted along the legs. This allows the sensor module to be fixed at any desired position within the frame length. Some of these frames have a mounting plate for the top module and for the arms that are attached to the fish cage. These modular frames were fabricated by Belltechne Co., Ltd., an engineering company that we collaborated with in doing this research.

To determine each sensor module's position in the frame, we first decide the target depths from the surface for measurement. While we can set an arbitrary depth for the first module, it is advised to set a consistent separation between the modules. We also measure the height of the cage frame from the water surface. The position of the top sensor module from the top of the sensor module frame l is calculated by the equation,

$$l_1 = h_1 - h_{ca} \tag{1}$$

where h_1 is the target depth of the top sensor module below sea level and h_{ca} is the height of the cage frame above sea level. It should not exceed the length of the frame L. The length of the subsequent sensor modules l_n from each frame is calculated by the equation,

$$l_n = (h_n - h_{n-1}) - (L - l_{n-1}) \tag{2}$$

where h_n and h_{n-1} are the depths of sensor modules and l_{n-1} is the position of the sensor module above.

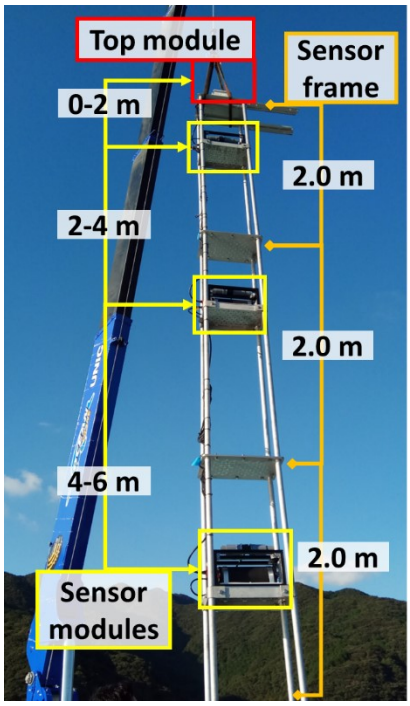

Figure 2-4 Sensor and top modules mounted on modular frames and assembled into a sensor unit (with depth ranges for each sensor module)

2.1.4. Flow sensor development

For the flow sensor to be used, one of its requirements is to be low cost since the system requires multiple sensors measuring at different depths and sides of the cage. Upon survey, many commercial current sensors do not meet this requirement. Some of them also have a proprietary interfacing that makes it difficult if not impossible to customize and interface them in another system. It was therefore decided to customize low-cost sensors to measure flow underwater.

The sensor selected for customization was a propeller-type flow sensors originally intended for measuring water flow through water pipes. It operates on the principle of Hall-effect, producing voltage when two opposing magnetic blades of the propeller's four blades are in proximity to the Hall sensor. One pass by the magnetic blade on the sensor

generates a pulse, thus making the number of pulses generated at a given time proportional to the propeller's rotation speed and to the speed of water flow through the sensor (Figure 2-5).

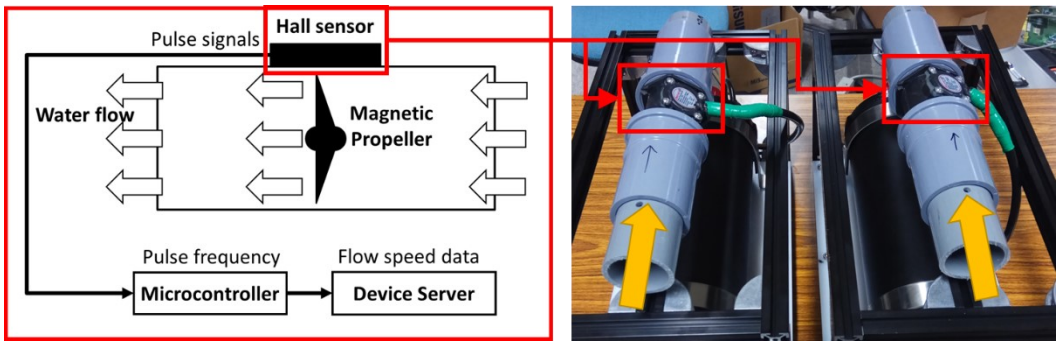

Figure 2-5 Propeller flow sensor design

For a selected flow sensor sampling interval, a microcontroller board detects the falling edge of the pulses sent by the Hall sensor on its interrupt pin and increments its pulse counter for every pulse. At the end of the sampling time, it then obtains the average frequency of the propeller rotation and then converts it into flow speed by multiplying to a calibration coefficient. After printing the calculated output, the microcontroller resets the pulse counter to zero before measuring the flow speed for the next sampling time.

To obtain the calibration coefficient, the flow sensor was cross-calibrated with a digital clamp-on type flow sensor (Keyence FD-Q32C). Both sensors were connected to an elevated water source where flow was partially controlled by a valve, as flow rate and speed were dependent on the height, and subsequently the volume, of the water in the container (Figure 2-6). Propeller sensor and digital sensor readings were collected at different flow rates by turning the valve. By the law of conservation of mass (through the continuity equation), the flow speeds at the propeller sensor were calculated from the area of its passageway and from the flow rate readings at the digital sensor. The frequency

readings and the calculated flow speeds were then correlated to get the calibration coefficient of the propeller flow sensor.

To determine the sampling interval to be used by the sensor modules, we selected three candidate values for calibration: 1 s, 5 s, and 10 s. Figure 2-7 shows the results of calibration values for the three candidate times. It was decided to use set the flow sensor's sampling time to five seconds as it produced better calibration results compared to when using one or ten seconds. This sampling time would be used in the following fish cage experiments. In retrospect, however, setting the sampling time to one second would have been better after finding out from experimental data that flow speeds could change significantly in less than five seconds. This should be considered for the next fish cage experiments provided that the propeller flow sensors will still be used.

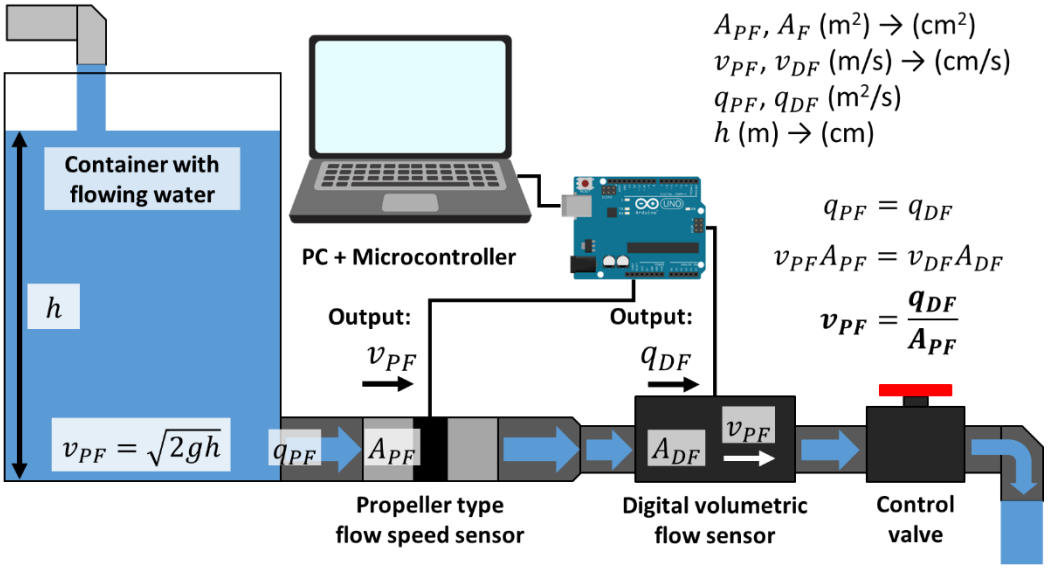

Figure 2-6 Flow sensor calibration experiment setup

Because these sensors were not originally designed to operate underwater, modifications were made on them. We replaced their wires with waterproof cables with connectors compatible with the sensor module connectors. To waterproof the Hall-effect sensors, we sealed the housing with epoxy to prevent any leak inside. We then sealed the

remaining exposed parts of the cable with butyl rubber to complete the waterproofing. We also added extra PVC pipe connectors on the ends of the sensor so that they could be mounted on the sensor module frames.

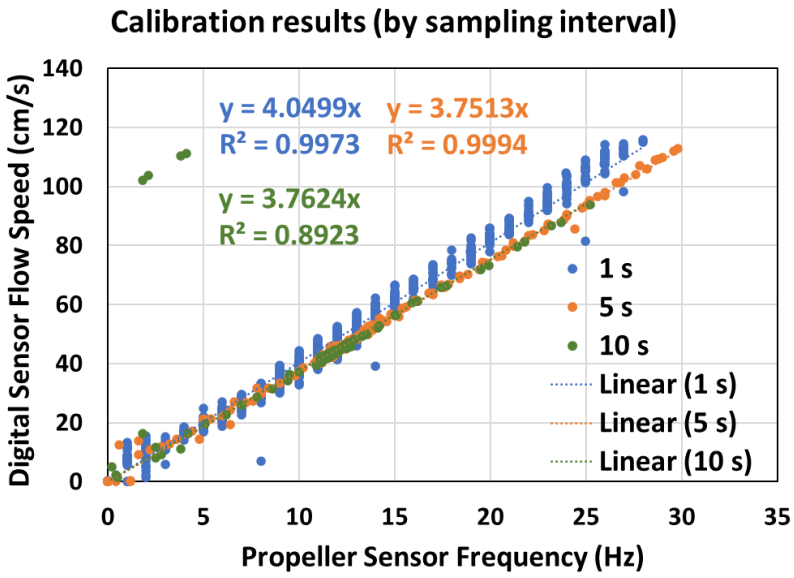

Figure 2-7 Comparison of propeller flow sensor calibration coefficients at three sampling intervals: 1 s, 5 s, and 10 s

2.1.5. Top modules

The top module is responsible for connecting the sensor modules wirelessly to the hub unit. As shown in Figure 2-8, it basically consists of a Wi-Fi router configured as a bridge to the router of the hub unit, so it does not broadcast its own network but serves as an extension of the hub router. Its LAN port is connected to the Ethernet component of the underwater cable connecting to the topmost module of the sensor module daisy chain. Through this configuration, the top modules connect all sensor modules to one network even when they are physically separated from each other, enabling them to transmit their data to the hub computer.

The top module receives power from an external source. The sensor units are separated from the power supply, therefore requiring cables to power them. As a result, voltage

drops across the length of the cable. To make sure module regulates this with an isolated DC/DC converter before supplying it to the sensor modules to maintain their stable operation. Supplied voltage is also converted to power the module router. All electric and electronic components of the module are placed in a waterproof enclosure. They are wired to an underwater cable connecting to the top sensor module's underwater connector. Plastic roofing was made for each box to block exposure to sunlight and prevent further heating to the electronics. The box's prefabricated screw holes are screwed to the top frame of the sensor unit.

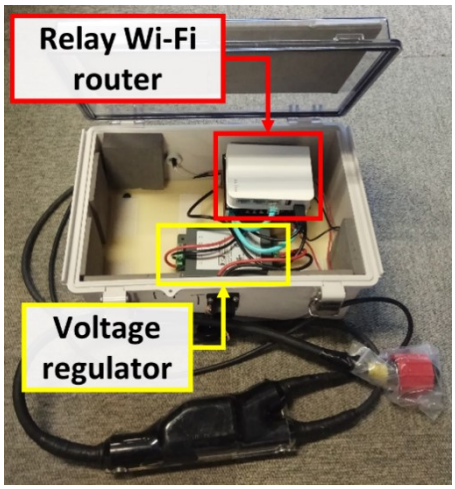

Figure 2-8 An open top module with a Wi-Fi router and voltage regulator inside

2.1.6. Hub unit module

The hub unit is basically any computer connected to a regular Wi-Fi router. A terminal emulator software is used to access the sensor modules by Telnet and log the data with timestamps into a file, while a video management software is used to record videos from the cameras. While one day's worth of flow speed data from one sensor module takes up only around 1 MB of storage, videos recorded by the module's camera for the same duration consumes an estimated 30 GB of storage. Depending on the number of sensor modules constructed and on number of recording hours per day, it is advised for the hub

unit computer to have a large data storage. For eight sensor modules tasked to collect data for 24 hours a day, it should have at least 500 GB available storage as backup for two days.

Since it communicates wirelessly with the sensor units, it can be placed in a separate enclosure, possibly with the power supply (see next section 2.2). Alternatively, one of the top modules can be configured into a hub unit module, which basically assumes the function of a hub unit, as shown in Figure 2-9. The modules of one sensor unit connect directly to the LAN port of the hub unit router which replaces the bridge router. The hub computer can either be inside the top module box. For this case, a single-board computer (SBC) is used to run the programs for collecting all sensor data.

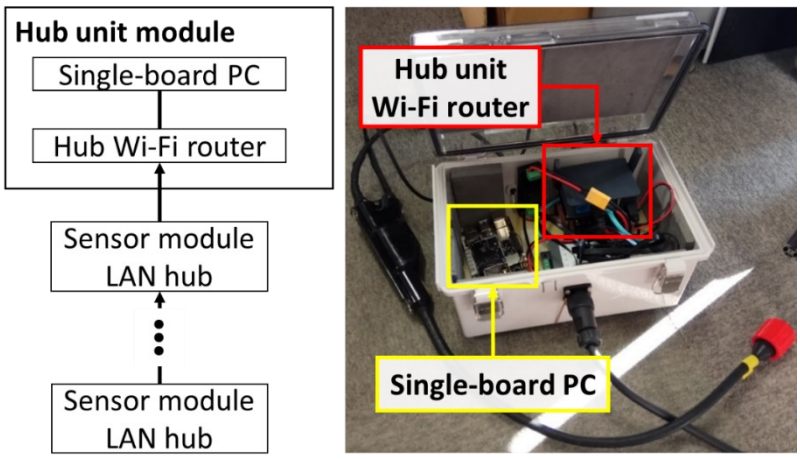

Figure 2-9 A hub unit module with its components

To automate data collection, the data recording programs used are configured to automatically start recording. After startup, the hub SBC automatically initializes the terminal emulator to execute scripts for connecting to and logging received data from each flow speed sensor at the preset schedules. It also initializes the video management software to start recording videos at the same time. It is configured to end both programs automatically by shutting down at the end of the recording periods to prevent data loss or errors in the operating system.

2.2. Offshore system for long-term observation

2.2.1. System design requirements

Improving the estimation of fish activity requires observation of fishes throughout their life cycle, from transferring from hatcheries to harvesting. This means collecting data on the fish activities for longer periods of time, with minimal human interference (apart from the fish farmers). Data collection is not only made during the feeding time but also at different times of the day, throughout the different seasons of the year. This allows observation of daily patterns in fish behavior and their changes as the season changes, which may indicate changes in fish appetite. Doing so requires not only sufficient daily power but also automation of recording.

In most instances, there is no access to grid power at fish cages since they are positioned hundreds of meters from the shore. Tethering power from shore not only incurs losses in power transmission but also poses several risks such as electrocution and collision with fishing boats among others. An off-grid power system therefore needs to be installed in the fish cage. This system consists of an energy storage with a capacity to power the sensor network for more than two hours, and an energy harvesting system to recharge the batteries and extend the network operation. Among the various methods existing, solar energy harvesting is used for the system, as solar panels and controllers are the most widely available energy harvesting devices in the market and are the easiest to install in fish cages.

Designing the sensor network's power system requires determining the daily schedule for data collection and consequently the daily duration of operation. Ideally, the sensor network collects data continuously every day. However, power supply may be limited due to physical constraints in the fish cage. It is therefore advised to allot separate window

periods of interest for the sensor network's operation throughout the day. The most important operation window is for the regular feeding routine, which is usually done during daytime. This may last from five minutes to more than one hour, depending on population size in the cage, on the fish farmer's feeding practices and on the feeding rate. About three to five hours may be allotted for data collection, depending on the farmer's daily schedule. In addition, collecting data outside the feeding schedule could provide additional insight on the fish activity at different times of the day, which could be affected by sunlight and temperature. One to two hours of observation each at daytime and at dusk could be allotted depending on the user's preference.

The time for manually operating the system on-site is limited, depending on the farmer as well as on the weather among others. For this reason, the sensor network needs to operate automatically. The power supply units need to have a system to switch on and off automatically according to the designated schedule. In response to switching on, the hub unit should also automatically start its data collection programs according to schedule. Its clock should therefore be synchronized with the actual time so that it adds an accurate timestamp to the collected data. Automatic operation requires the sensor units to be within the hub unit's wireless range. Because Wi-Fi has a limited range of less than 20 meters, the hub unit also needs to be placed in the cage. This is where the hub unit module design becomes useful.

2.2.2. System power management

The power supply units developed is photovoltaic system, basically consisting of solar panels, batteries, and solar charge controllers. Since the network components are designed to be powered by direct current electricity, inverters are not used. To determine the

capacity of power supply, we first measure the power consumption of a sensor unit P_U with n sensor modules. This is calculated by the equation,

$$P_U = VI_U = V(N_m I_m + I_t) \tag{3}$$

where V is the power supply voltage and I_U is the measured current draw by the sensor unit. I_m, and I_t are the current draws of a single sensor module and the top module, respectively. The power consumption of the sensor network P_{SN} consisting of N sensor units is given by the equation

$$P_{SN} = N_U P_U + P_H = N_U P_U + V_H I_H \tag{4}$$

where P_H is the power consumption of the hub unit computer while V_H and I_H are its supplied voltage and current draw, respectively. The current draw by the entire sensor unit is usually measured to get the power. Therefore, the total daily energy requirement E_{SN} of the sensor network with N sensor units is given by the equation,

$$E_{SN} = P_{SN} t_{SN} \tag{5}$$

where t_{SN} is the total daily duration of the sensor network's operation. The unit used for $E_{SN}\ is$ seconds/day This serves as the minimum energy capacity of the battery to power the system.

Once the daily energy requirement of the sensor network is obtained, we then calculate the total output power required from solar panel to replenish the recharge the power supply batteries every day. One of the most important factors to be considered for calculation is the location since the amount of solar energy received depends on the climate of the location. While orientation affects the yield of the panels, we assume them to be lying flat on the cage platform. We calculate the required daily panel output power P_S by using the equation,

$$P_{SP} = E_{SN}(\bar{t}_{Smin})^{-1} \tag{6}$$

where $\bar{t}_{Smin}$ is the daily average of minimum monthly total sunshine duration, with the unit of seconds/day. The sunshine duration is defined as the as the sum of the time for which the direct solar irradiance exceeds 120 W m^{-2} [72]. This value depends on the location. Since it only takes account for the global solar radiation, the energy output of a solar panel of a given rating could be more than the calculated value due to diffused light. The minimum monthly sunshine duration is used for calculating its output power to ensure that the energy supplied by the panels to the batteries is sufficient for the sensor network to operate even in the cold months when the amount of sunshine is minimal.

Depending on each sensor unit's energy requirement and on the installation setup, the calculated battery capacity and solar panel output power is evenly distributed among the sensor units as multiple power supply units. This means that one power supply unit may be used to power one or more sensor units, as shown in Figure 2-10. Upon determining the distribution of power supply, the number of units as well as the battery and panel specifications is decided.

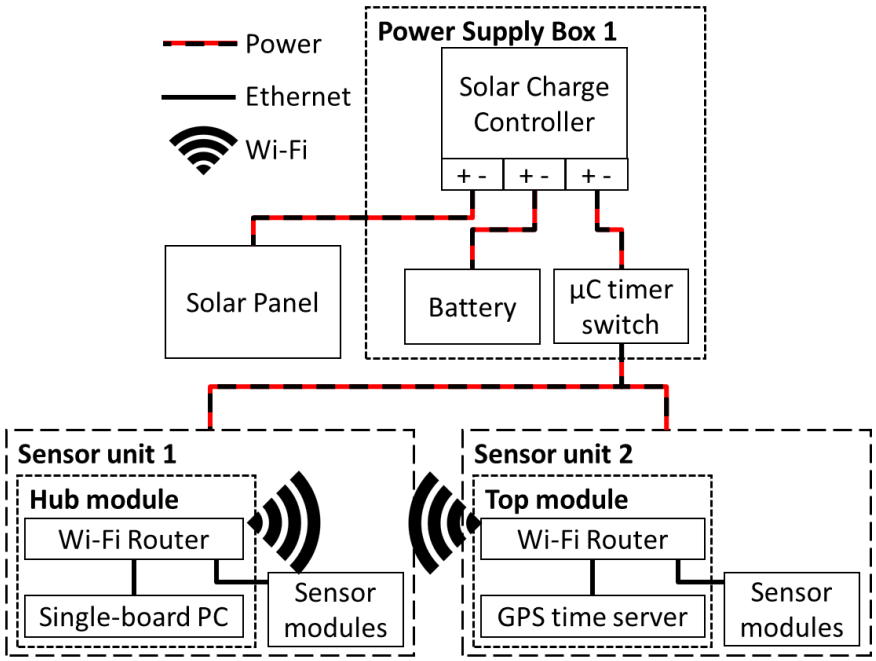

Figure 2-10 A design of the offshore power system for two sensor units (one with hub)

Automation of operation is implemented in the electrical and software levels. At the electrical level, the power supply unit switches on and off according to schedule using a microcontroller switch, as seen in Figure 2-11. A microcontroller board, which is continuously powered by the solar charge controller's USB port, sends signals to a relay circuit board, switching on and off the solar controller's output, which gets split into two power lines for two sensor units. The microcontroller is programmed to switch the power on ten minutes before the start of scheduled data collection and switch it off five minutes after the end of collection. This is done to give time for the devices to initialize and shut down properly. The switching schedules are hard coded in the microcontroller, which has a real-time clock to keep track of the time as accurately as possible. In response to the power supply switching on, automation at the software level begins as the sensor network devices initialize to prepare for the data collection schedule, as discussed in section 2.1.6.

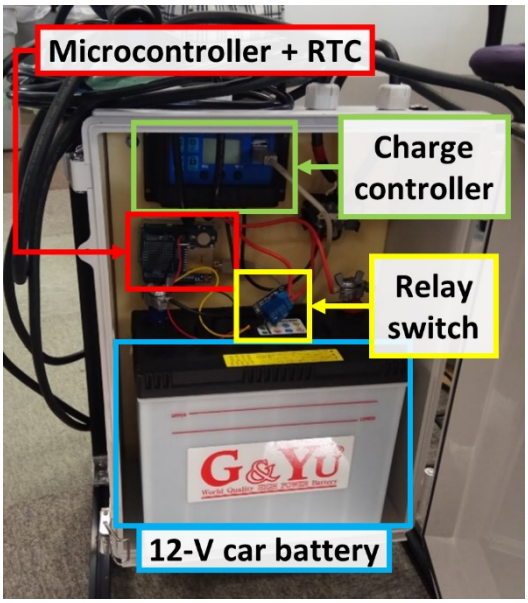

Figure 2-11 The microcontroller switch inside the power supply unit

For execution of data collection at the correct time and for accurate timestamping of data, the hub unit computer clock needs to be in sync with standard time. To keep track of the actual time even when without power, computers usually have a CMOS battery to

maintain their real-time clocks. However, some SBCs do not have such and rather rely on time servers for synchronization. Otherwise, they either retrieve the last time before shutdown or reset to Unix time, which is usually 00:00:00 UTC on 1 January 1970. Without any internet connection in fish cages, their clocks become lagged from the actual time. For such computers, a GPS time server can be installed in one of the sensor units (Figure 2-12), initializing after switching on. The hub unit can wirelessly communicate with this device and synchronize its time since both connect to the same network.

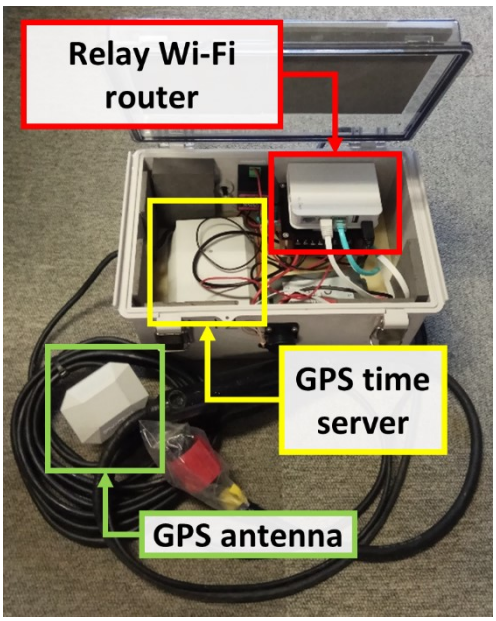

Figure 2-12 A GPS time server installed in one of the sensor unit top modules

2.3. Summary

A modular sensor network is designed and developed to observe flow and fish activity at different depths and from more than one side of a fish cage. Sensor modules, measuring flow speeds and recording videos at different depths, connect to each other and to a top module to form a sensor unit. The sensor module's flow speed sensor was developed by modifying a propeller-type flow sensor for water pipes, calibrated to measure flow speeds. The sensor unit's top module relays all sensor data to a hub unit and regulates the voltage it receives from the source to ensure stable operation. The hub unit receives data from all sensor modules and stores them in its computer. It can be alternately configured as a hub unit module by combined with one of the top modules. Its data collection programs are configured to automatically collect data after initialization.

An offshore system is also developed for long-term observations by the sensor network by designing power supply units for the sensor units and by automating the sensor network operation. The power supply units consist of photovoltaic systems, whose battery capacity and panel output power are determined by determining the daily energy consumption of the network, which is obtained from its power consumption and its operating schedule. They are programmed to switch power according to the determined schedule. The hub unit module automatically starts recording data from sensors modules after booting. To collect data at the correct time and with correct time stamping, the hub may be synchronized with a GPS time server.

Chapter 3
Fish activity estimation

Chapter 3. Fish activity estimation

3.1. Overview

Clarification of the properties of the fish activity during feeding and of its relationship with the fish-induced flow requires its observation through the recording of flow speeds from and videos in the fish cage, and comparison of the collected data. Three fish cage experiments were performed throughout this research to achieve these objectives. In addition, the functionality a system component was demonstrated for every experiment, starting from the developed sensors to the modular sensor network performing long-term observations.

3.2. Flow sensor functionality experiment

3.2.1. Setup

The first fish cage experiment primarily aimed to detect fish-induced flow using the modified propeller flow speed sensors and to observe fish activity especially during feeding. This initial experiment was performed on March 18, 2021, at a fish farm owned by Hyōshoku Co., Ltd., located in Usuki City in Oita Prefecture. Measurements were collected at two 10 m x 10 m square cages with depths of 7.5 meters while feeding operations were done by the farmer. These cages contained around 3500 yellowtail amberjacks (*Seriola aureovittata*), locally known as Hiramasa. The fishes had been raised for a year, each with an average weight of 3 kilograms. They were fed with moist feed, which is a combination of raw fish and powdered meal (fish, soybean etc.). Feeds were given using a feed ejecting machine installed in the feeding boat, as shown in Figure 3-1. Although the amount of feed provided to each cage was not recorded, it is safe to say that the feed amount given to each cage was within the scale of hundred kilograms. Feeding in the first cage lasted around 80 minutes while feeding in the second lasted around 70 minutes. Feeds were dispensed to the cages gradually for around 10 minutes to lure the fishes to the surface before continuously dispensing the feeds. Dispensing of feeds were stopped either when the ration for each cage was fully given or when the fish farmer assessed that the fishes became satiated. Table 1 summarizes the experiment details.

At this stage, the sensor network and its components had not been developed yet. The sensors collected flow speed data from the cage as a suite of dataloggers, serving as prototypes of the sensor unit. Calculated measurements from the sensor's microcontroller were written to the CSV file stored in an SD card, appended with timestamping from datalogger's real-time clock. A Bluetooth module was used to remotely trigger the data

collection by the sensor. Sensor electronics and batteries apart from the were placed in a waterproof enclosure. Two flow speed loggers were constructed for this experiment and were mounted on a custom frame to measure at two different depths (Figure 3-2). Together with each flow logger is a GoPro camera for recording the fish activity underwater.

Figure 3-1 Feeding machine giving feeds to fishes in the cage

Fish cage no.	Cage 1	Cage 2
Location	Usuki City, Ōita Prefecture (大分県臼杵市)	
Dimensions	10 m (length) x 10 m (width) x 7.5 m (depth)	
Sensor depths	0.4 and 3.4 m	
Fish; average weight	Yellowtail amberjack/ヒラマサ (*Seriola aureovittata*); 3 kg	
Est. population	3500	
Age	1 year old	
Feed type	Moist feed	
Feeding duration	~80 minutes	~70 minutes
Feed amount	unrecorded	
Feeding method	Machine	

Table 1 Cage and feeding parameters of the initial fish cage experiment

For each measurement, the sensor suite was mounted on the center of one side of the cage adjacent to the side where the feeding boat was docked at. To maintain the positioning of sensors, the senor frame was made as rigid as possible by attaching a

supporting bracket to its center was and binding its arms to the cage frame. The sensors were positioned 0.7 and 3.7 m from the top of the frame, as shown in Figure 3-3. But because the cage frame was elevated at 0.3 m above water, the sensors were positioned at depths of 0.4 m and 3.4 m, respectively. The sensors were powered on, closed, and triggered to record data before submerging them for measurement. Data files were retrieved from the sensor suite after it was retrieved and returned to shore. The flow speed measurements with timestamps were extracted from the CSV files and were processed for analysis.

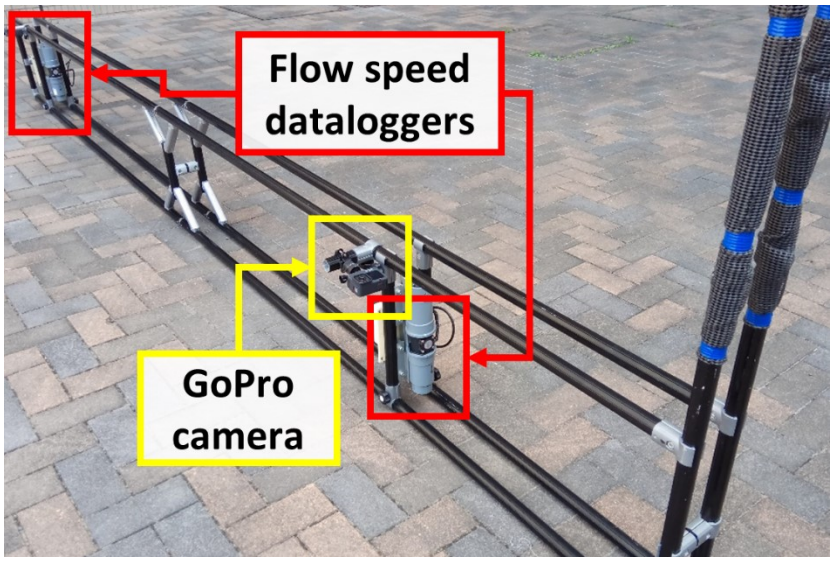

Figure 3-2 Prototype flow sensor logger suite used in the first experiment

In analyzing the data, it was expected there would be fluctuations in the readings. The trends were therefore obtained by calculating their centered moving averages. This type of calculation was used to prevent the trend from lagging from the data points. Generally, each centered moving average $\hat{u}_t$ at time t using odd or even m data points is calculated by the respective equations,

$$\hat{u}_t = \frac{1}{m}\left(\sum_{i=-k}^{k} u_{t+t_s i}\right) \text{ or } \hat{u}_t = \frac{1}{2m}\left(\sum_{i=-k}^{k-1} u_{t+t_s i} + \sum_{i=-k+1}^{k} u_{t+t_s i}\right) \quad (7)$$

where u_t is the measured flow speed at time t, t_s is the sampling time, and $k = \frac{m-1}{2}$ or $k = \frac{m}{2}$, respectively. Throughout all experiments, the m used throughout all the experiments is six data points, therefore calculating each moving average within a 30-second span of data. These were plotted together with the raw data. Noted observations were marked on the data plot according to the time they were recorded.

The changes in measurements were also analyzed with the video recordings of fish activity at the time of the noted observations. Since the cameras used were not automatically synchronized with the sensor loggers, the timestamps of the videos were manually adjusted during post-processing comparing the noted observations with the events in the camera. For the video recordings, only the first half of the feeding at the first cage had underwater recordings since the camera batteries were exhausted and no extra batteries were prepared. For the second cage, a camcorder was used to record observations from the surface instead. It was noted in both measurements that the spikes at the beginning and the end of the data series indicated the time the sensors were deployed and recovered.

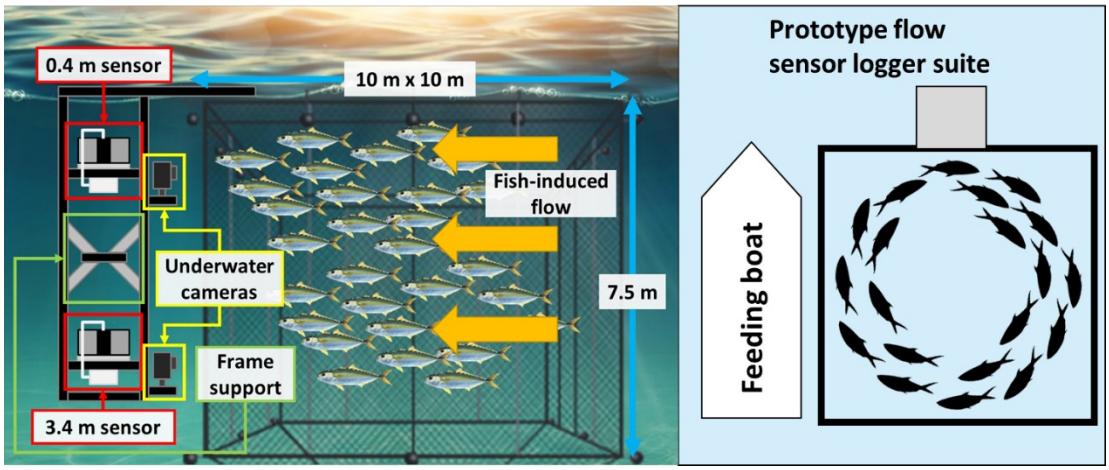

Figure 3-3 Initial fish cage experiment setup using the prototype sensor suite

3.2.2. Results

Figure 3-4 shows the measurements in the first cage. In the first fish cage, feed was started to be given in small amounts at around 11:34, seven minutes after the deployment of sensor, to attract the fishes to the surface. Before feeding began, video recordings showed no presence of fish at the surface (0.4 m). They were seen shoaling below, as seen from the second camera, as seen in Figure 3-4a. Throughout the gradual feeding, flow speed at the surface was close to zero, while speed at the lower depth (3.4 m) was slightly higher, by around 4 cm/s or less. At the start, surface flow did not increase right immediately. Fishes started schooling and few started swimming to the surface only at around 11:36, as seen in Figure 3-4b. The number of fish swimming to the surface continued increasing before the feeds started floating away from the cage, blurring the surface camera at around 11:42. Despite this observation, readings did not indicate significant increase in flow.

Surface flow rose to around 12 cm/s at 11:43. It exceeded the flow speed below, which did not change significantly. At around this time, the fisherman also started dispensing feed to the cage continuously. It was also around this time that the fishes at 3.4 meters depth became significantly less visible. This could be attributed to the decrease in illumination due to the increased fish activity at the surface blocking more amount of light, as well as to dispersion of light from splashing. It was also observed from the surface that the feeds landed closer to the side opposite of the sensor suite. Fishes gathered closer to that side, therefore making them less visible from the camera. At around 11:47, vigorous fish feeding was observed from the surface. This was also observed from the turbulence at the surface, as captured by the underwater camera, as shown in Figure 3-4c. The fishes at surface appeared to swim faster of the although this was difficult to confirm

due to their distance from the camera and from the blurred water. They also appeared to swim slightly faster than the fishes at 3 meters below. For around seven minutes, surface flow speed was maintained at an average of 8 cm/s. This slightly decreased afterwards.

From this point throughout the rest of the feeding, surface measurements were generally uniform, with peak values ranging within 4-10 cm/s. Flow at 3.4 m was also uniform, not exceeding 4 cm/s. Apparent swimming speeds of fishes at the two depths remained constant towards the end of the underwater videos, with fishes at the surface swimming slightly faster than those below. The visibility of fishes at both depths would vary, increasing and decreasing back-and-forth. These patterns could be attributed to the low feeding activity on that day, as noted by the farmer. Such observation could have been based on the previous observations of more vigorous swimming and splashing at the surface of the same cage at the start of feeding. The underwater cameras stopped recording at 12:09 (surface) and 12:04 (3.4 m depth), about halfway of the feeding. This was due to insufficient battery power, as they were previously used in a trial measurement in another fish cage.

Flow speed reading was at 4.51 cm/s when the fisherman stopped dispensing feeds at 12:56. It was noted that fishes were still swimming around the surface at that time. One minute later, measurements dropped to almost 0 cm/s, the same time it was noted that fishes were no longer visible from the surface, indicating that they swam back to the deeper part of the fish cage.

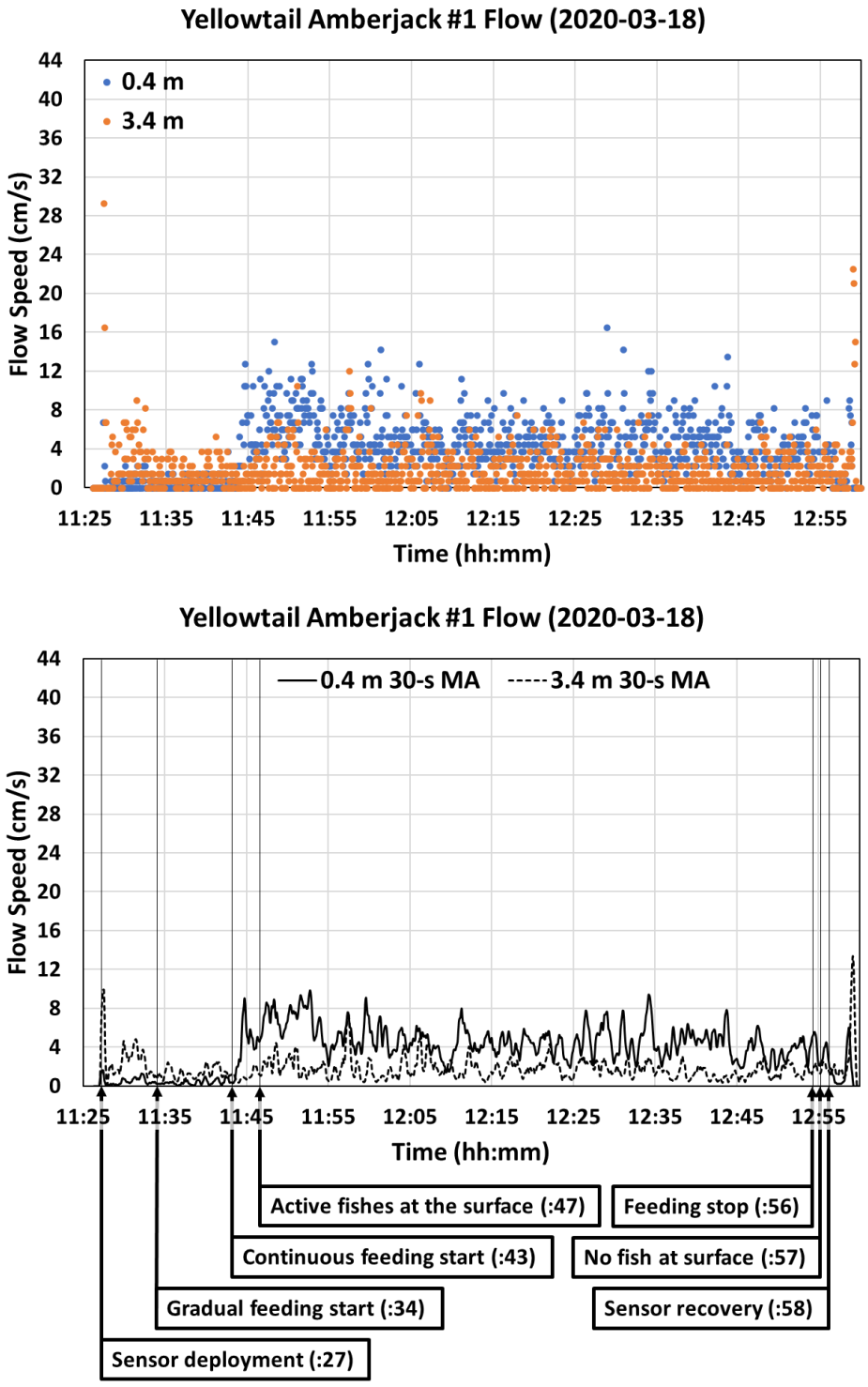

Figure 3-4 Flow speeds and their 30-second moving averages at the first fish cage

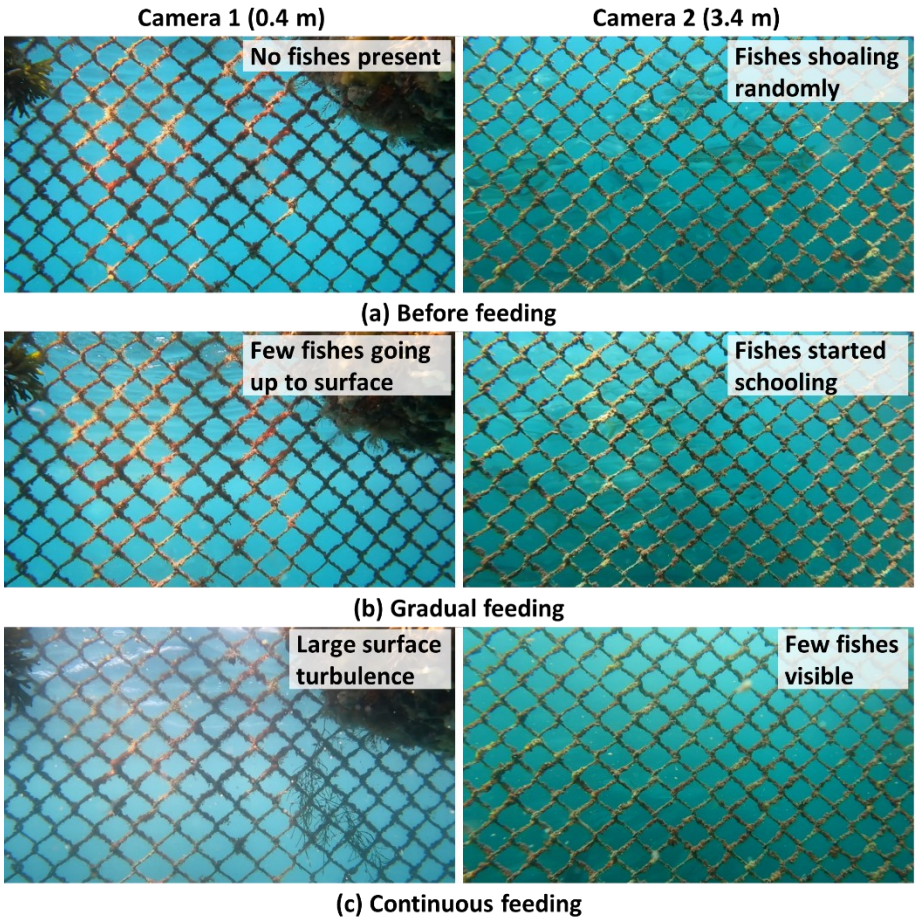

Figure 3-5 Snapshots of video recordings at the first fish cage

In the second cage, only a video recording above surface was taken for comparison with flow speed measurements. The time gradual feeding started was not noted properly, as the sensor suite was being mounted on the cage at around the same time. It could have begun sometime after 13:03, when the sensor suite was deployed, as indicated by the sensor readings.

Figure 3-6 shows the measurements in the second cage. At the start of the video at around 13:10, few fishes were swimming up during gradual feeding. Measurements at both depths remained low, up to 2.51 cm/s. At 13:17, while there was no increase in flow speed yet, feeds started to disperse from the cage, as observed in the video. Flow readings started increasing at 13:19, with some readings reaching over 4 cm/s. This corresponded

to more fishes started swimming at the surface as observed from increased splashing, as seen in Figure 3-7. The fisherman switched the feeding machine to dispense feeds continuously at 13:20. The fishes were observed to be actively swimming at the surface one minute later, corresponding with the flow speed exceeding 8 cm/s.

In the next 15 minutes, surface flow speed reached an average of around 10 cm/s, reaching as high as 15.79 at around 13:32. During this period, fishes were swimming actively at the surface. Splashes at the surface would also disappear occasionally, corresponding to brief drops in flow speed. Towards 13:35, fish activity gradually decreased, with less fishes causing smaller splashes.

From then towards 13:51, surface flow gradually increased, reaching speeds as high as 20 cm/s. Fish activity also increased. Although the intensity of splashes did not change much, more fishes were observed swimming around at the surface. Swirling water surface became more observable at around 13:45, indicating more fishes swimming around. The intensity of fish activity then decreased at 13:52 for around two minutes, which corresponded with the drop of flow speed to 4 cm/s. Fish activity increased again in the next six minutes before decreasing again at 14:00. This corresponded again with the flow readings averaging at around 11 cm/s before dropping again to 4 cm/s.

Flow speed increased from then to around 14:12, reaching speeds close to 20 cm/s again. Video also showed steady increase in fish activity from 14:00, as seen from the swirling of water surface and increased splashing. From 14:12, flow speed gradually declined to around 6 cm/s. Although there were still many fishes swimming at the surface, they appeared to be swimming more slowly and making less splashes compared to previous observations, as seen in Figure 3-8. Feeding was ended at 14:20, at which measurement was at around 4 cm/s. Reading eventually dropped to almost zero after

around one minute, just a few moments away from sensor recovery. At around this time, surface of the cage became calm.

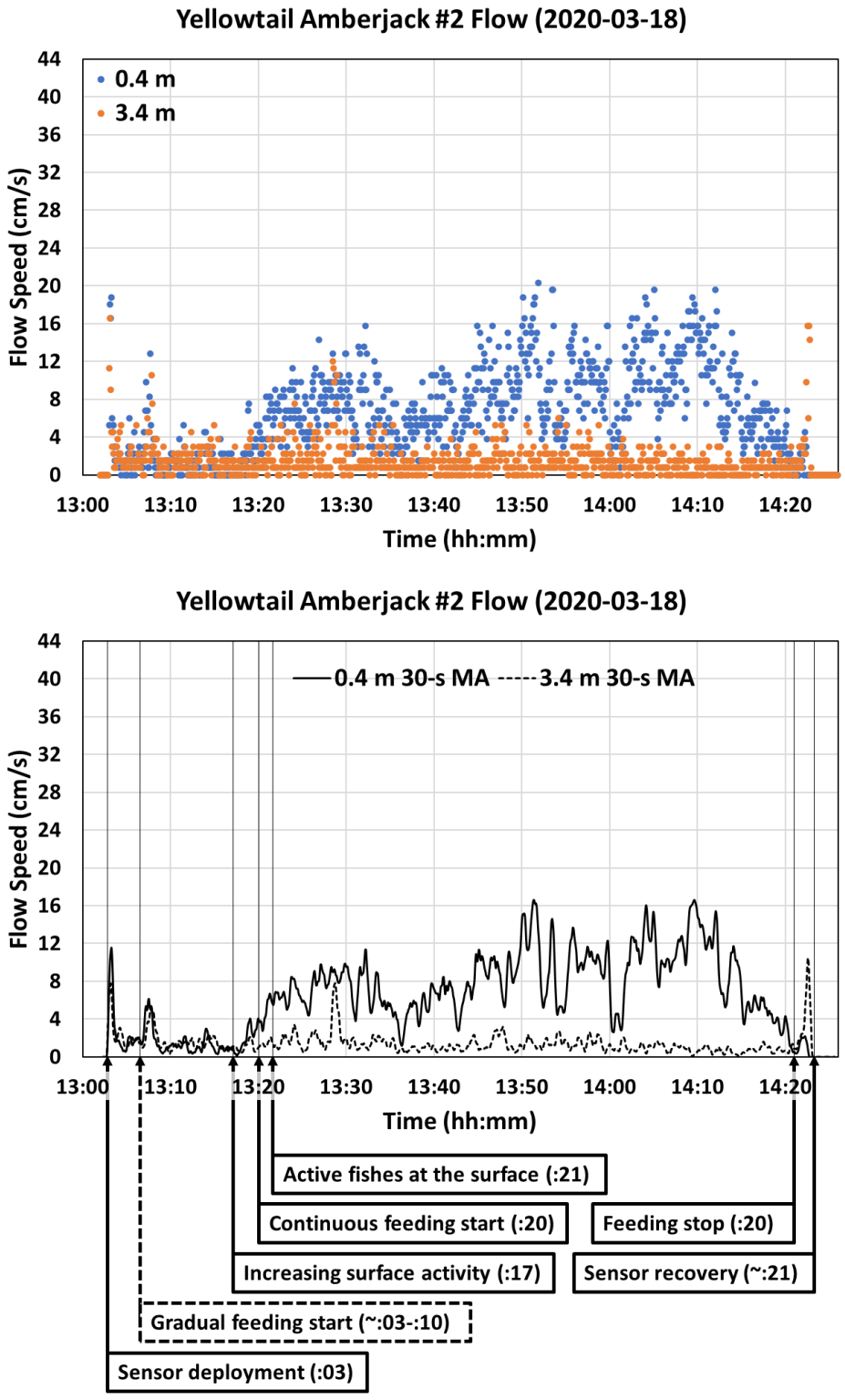

Figure 3-6 Flow speeds and their 30-second moving averages at the second fish cage.

Figure 3-7 Fishes actively splashing as continuous feeding started

Figure 3-8 Low splashing intensity at surface towards the end of feeding

The flow speed at 3.4 m was consistently low throughout the feeding, although it would sometimes exceed 4 cm/s. There was a drastic increase in readings that occurred once at around 13:28, reaching 12 cm/s. Although the brief decrease in fish activity indicated fishes going down, the spike could also be attributed to waves causing the fish cage to oscillate more, affecting the sensor measurements.

A similar observation on the feeding operations at both fish cages was that flow speed measurements were at around 4 cm/s when feeding was stopped by the fisherman. Both gradually dropped to almost zero after around one minute. Although flow speeds were

different at the start of the continuous feeding in the two cages, it was clear that increase in fish activity at the surface i.e., more fishes swimming and splashing at the surface, is followed by increase in flow speed. It was observed from this experiment that changes in flow speed, especially at the surface, correspond to changes in fish behavior as observed by the farmer. This also showed that the developed propeller flow speed sensors were able to detect flow induced by fishes, particularly at the surface, and could be used for collecting measurements at different depths.

3.3. Sensor network functionality experiment

3.3.1. Setup

The objective of the second fish cage experiment is to be able to collect flow speed measurements and underwater videos of the fish activity at different depths from more than one side of a fish cage using the modular sensor network. A two-day experiment was performed in November 2021 at a fish farm owned by Tokumaru Co., Ltd. in the town of Shin-Kamigotō in Nagasaki Prefecture. Three 11.7 m x 11.7 m square fish cages with depth of 7.5 m were selected for collecting sensor data during feeding routines. Each cage contained half year-old Japanese amberjacks or yellowtails (*Seriola quinqueradiata*), locally known as Buri. The first two cages contained around 11,000 and 8,000 fishes that were caught from the wild as fry (locally known as mojako), while the third cage contained 8,000 fishes that were transferred from an artificial hatchery. In this experiment, the average weight of each fish was not obtained from the farmers. Details of the experiment is summarized in Table 2.

Cage no.	1 (Day 1)	2 (Day 1)	3 (Day 2)
Location	Shin-Kamigotō Town, Nagasaki Prefecture (長崎県新上五島町)		
Dimensions	11.7 m (length) x 11.7 m (width) x 5 m (depth)		
No. of sensor units	1	1	2 (1 per side)
Sensor depths	0.5 and 2.5 m	0.5, 2.5 and 4.5 m	0.5 and 2.5 m
Fish	Yellowtail/Japanese Amberjack/ブリ (*Seriola quinqueradiata*)		
Population	~11,000	~8,000	
Age	~0.5 years		
Fish seed	Wild fry (mojako)		Lab hatchling
Feed type	Extruded pellet (EP)		
Feeding duration	~9 min.	~7 min.	~9 min.
Feed amount	240 kg	230 kg	240 kg
Feeding method	Machine		Manual

Table 2 Details of the second fish cage experiment

These fishes were fed with extruded pellets (EP), a combination of fish and powdered meal molded into pellets. Feeding in the first two cages was performed on the first day at around 8:00 AM. Like the first experiment, fishes were fed using a feed ejecting machine mounted on the feeding boat. The farmer would also stop the machine based on his assessment of their feeding behavior. Feeding was done for around nine minutes in the first cage, giving the fishes a total of 240 kg of feeds. On the other hand, the farmer decided to stop the feeding in the second cage after seven minutes, giving only a total of approximately 230 kg of feeds.

Feeding in the third cage on the second day was performed at around 9:55 AM. Unlike on the first day, feeds were given to the fishes manually. The farmer would place all 12 20 kg bags of feed on the platform in the middle of the cage and pour the feeds on the water at the south side of the cage, one bag at a time. At the start, he would pour them slowly until he assessed that most of the fishes were swimming actively at the surface. He would then pour the feeds continuously until all bags were emptied or until he would find the fishes no longer swimming vigorously to feed. All bags of feed were used up on that day, amounting to a total of 240 kg of feeds.

For this experiment, we decided to construct four top modules and eight sensor modules. With these, one sensor unit can be installed at each side of a square cage, and each can at least have two sensor modules. We designed these modules to be powered by 12-V sources as this is the most common voltage used for batteries. Throughout all the possible sensor unit combinations, a maximum of five underwater cables was needed and therefore constructed to connect all sensor modules to each other. Based on the experience from the previous experiment, each cable was made with a length of around three meters. However, these cables were made using large-gauged wire for the power line, therefore

having higher resistance per length. From a 12-V supply, the resulting dropped voltage at a fourth module was too large that it could not power that module sufficiently for proper operation. This limited the sensor unit to carry three sensor modules.

Given the number of constructed modules, multiple sensor units with more than two sensor modules could not be installed in all the cages in the same day. To resolve this, we decided to deploy the sensor network with different configurations on separate days. This explains why feeding on the third cage was done on the second day. This also allowed us to meet the different objectives of the experiment at different cages and gain more insights from them.

For the first two cages, we mounted one sensor unit on one side of each cage adjacent to where the feeding boat was docking (Figure 3-9a). The sensor units were supposed to be mounted on the center of cage frame. However, the unit in the first cage was placed one meter off the center to avoid the floating buoys that could have blocked the flow path and the view of the fish activity. This was done on the day before the experiments were performed. We decided to use three sensor modules for each unit and collect data at depths of 0.5, 2.5 and 4.5 meters, as shown in Figure 10. We first connected three modular steel mounting frames to each other. One these frames was made for attaching the top module to and for mounting on the fish cage frame. To make sure that the sensor modules would be positioned at the target depths, we measured the height of the fish cage frame from the water surface and adjusted the position of the sensor modules in the steel mounting frames by using that height.

Once the sensor modules and the top module were fixed on the frame as desired, cables were connected to the modules and were tied to the frame to prevent them from dangling and causing any untoward incident while performing the experiments. The unconnected

ports at the bottom sensor modules were sealed by covering them with plastic caps filled silicone grease. Connections of all modules were tested before mounting the sensor units on the cages. Each sensor unit was then carried to the side the cage with the help of the crane of the feeding boat and was then fixed to the cage frame once submerged (Figure 11).

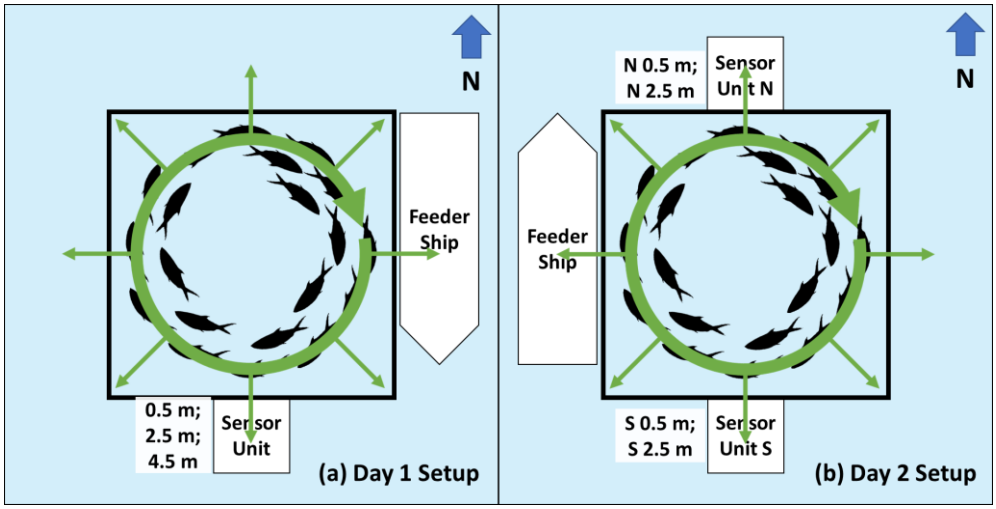

Figure 3-9 Top view of the experiment setups for both days

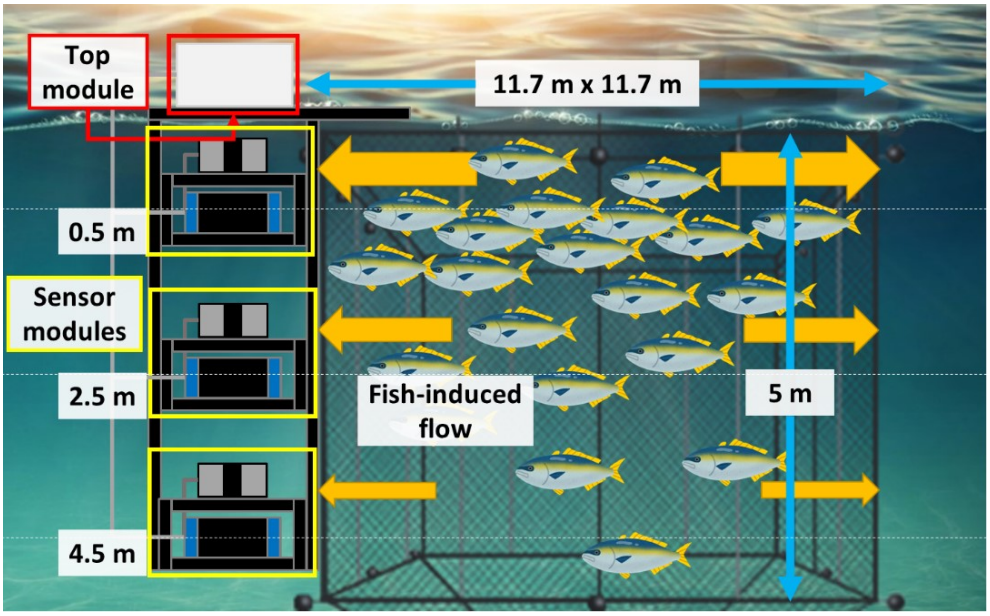

Figure 3-10 Side view of experiment setup for the first two cages on the first day

At this point of the research, the power system for long-term observations by the sensor units had not been developed yet. Each sensor unit was powered by three small $LiFePO_4$

batteries with a total energy capacity of 132 Wh. With this capacity, a sensor unit with three sensor modules could operate for four hours, which was considered sufficient for the experiment at the two cages, which lasted for less than one hour in total. These batteries were placed inside each top module. Since long-term observations were not performed in this experiment, we used a laptop computer connected to the hub unit router and collected sensor data from the feeding boat. We used a portable power supply to power these devices.

Figure 3-11 Installation of a sensor unit in one of the cages for the experiment

On the day of the experiment, we started collecting data from each cage by switching on the sensor unit and then manually initiating the programs used for recording the flow sensor data and the camera videos. We collected data from five minutes before the farmer started giving feeds to the fish until five minutes after he stopped the feeding. We did this to observe the state of the fishes and of the fish cage outside feeding activities. This was also done to observe changes in flow speeds as fishes started swimming towards the surface as feeding started and back to the bottom of the fish cage after they finished

feeding. In addition to the collecting data from the sensor modules, action cameras were used to record videos of the fish activity at the surface from the feeding boat.

To prepare for the experiment on the next day, the sensor units were then retrieved and brought back to shore for adjustments and repair. We decided to use four sensor units with two sensor modules each in the third fish cage. Since it was the only cage where the sensor units would be deployed on that day, we originally thought of placing one sensor unit on the center of each side, measuring at two depths (Figure 3-9b). However, the farmer said that they should not be installed on the east and west sides (docking sides for the boat) to avoid the risk of damaging the sensors and the boat by collision. Therefore, we decided to install two units on the center of the north and south sides, which were adjacent to the boat's docking sides. Since the third cage was the same with the two previous cages, the sensor modules were still fixed at 0.5 and 2.5 meters below surface, as shown in Figure 3-12. Remaining battery charge after the previous measurements was sufficient for the third cage, so they did not need to be recharged onshore.

On the day of the experiment, we performed the same procedure for collecting the data from all sensor modules. In this cage, two action cameras were used to record videos of the feeding operation from the feeding boat and from the feeding platform. In addition to noting observations from the feeding operation, these videos were used for estimating the accumulated amount of feed given to the fishes at a given time by noting the time each bag of feed (12 bags, 20 kg each) was used up. The data from the sensor modules were then retrieved from the hub unit computer after the experiment.

While the underwater cameras were properly synchronized with the hub unit computer, the action cameras were out of sync by a few minutes, which was still a crucial difference. To adjust the timestamp of the latter's videos as accurately as possible, noted events on

the water surface, such as splashes and waves, were compared with those in the videos recorded at 0.5 meters underwater. We used the timestamps from the underwater videos to estimate the time these events occurred in the videos from the action cameras and adjusted the latter's timestamps accordingly. A video processing software was used to add the timestamp to the recorded videos from all cameras used in the experiment.

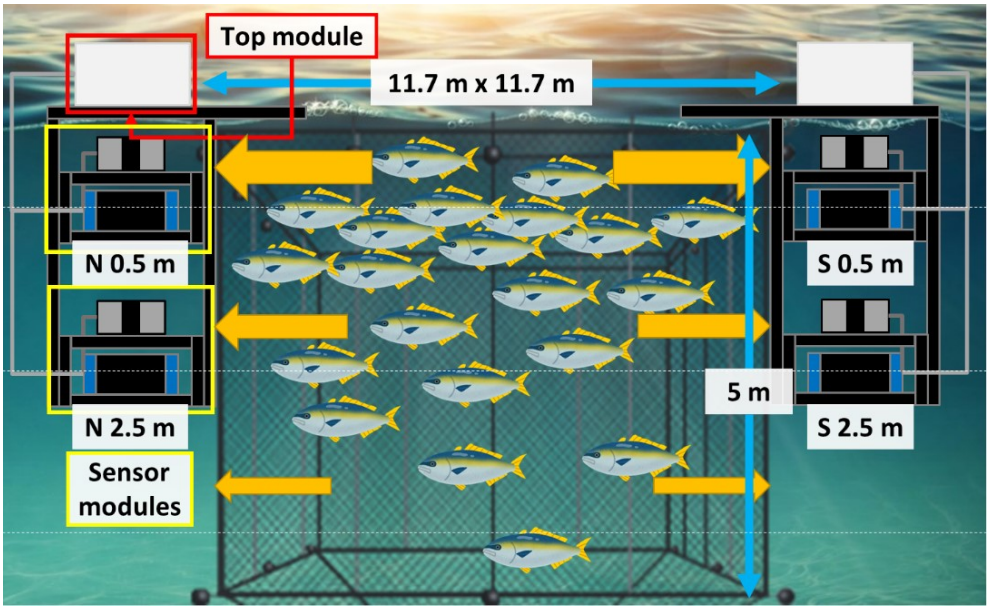

Figure 3-12 Day 2 experiment setup for the third cage

Like in the first experiment, we extracted the measurements with their respective timestamps from the CSV log files. We then calculated the moving averages from the raw data to obtain the trend and plotted both together and marked in the plot the noted observations from the feeding operations. For the experiment in the third cage, we used the synchronized action camera videos to obtain the times the farmer finished pouring each bag of feed. Since we knew the weight of each bag, we then plotted the accumulated weight of feeds given together with the flow sensor measurements. We then analyzed the relationship between the changes in flow speeds with the fish activity observations from the videos.

3.3.2. Results

Although three sensor modules were used in the first cage, only the modules from 0.5 and 2.5 meters were able to collect data, as shown in Figure 3-13. It was suspected that the sensor module at 4.5 meters had loose internal connections and was therefore unable to send data to the hub unit. The farmer immediately dispensed feeds continuously at the start of feeding in this cage.

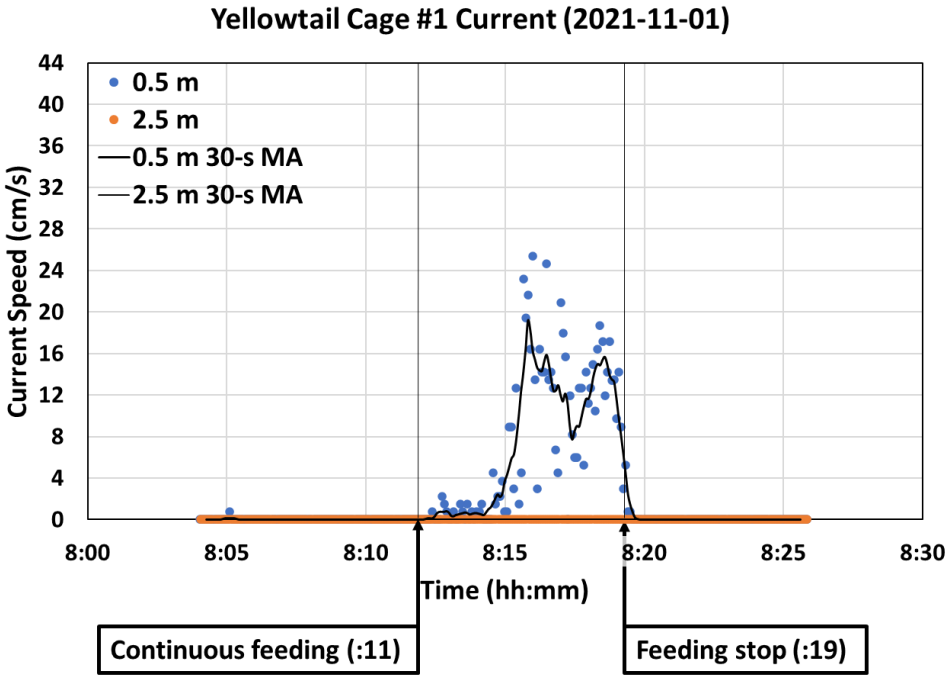

Figure 3-13 Flow measurement results from the first cage

Before feeding started, almost all measurements at both 0.5 and 2.5 m were at 0 cm/s and no fishes were observed from both underwater cameras. This meant that the fishes were swimming at the bottom of the cage. Large splashes were immediately observed from the action cameras in the first four minutes of feeding. At the same time, underwater cameras showed the fishes swimming to the surface very fast. Their vigorous movements after a few seconds caused so much water turbulence that their activity was hardly visible throughout the feeding. Despite these observations, surface sensor readings in the first

four minutes remained very small, at around 2 cm/s. This could be attributed to the non-alignment of the sensors to the center of the feeding activity, as observed from the action camera (Figure 3-14a). Fish activity was concentrated at the center of the cage while the sensor unit was a meter off the center. Most of the water flow at the surface must have been blocked by the flow sensor's mounting pipes, resulting to smaller readings.

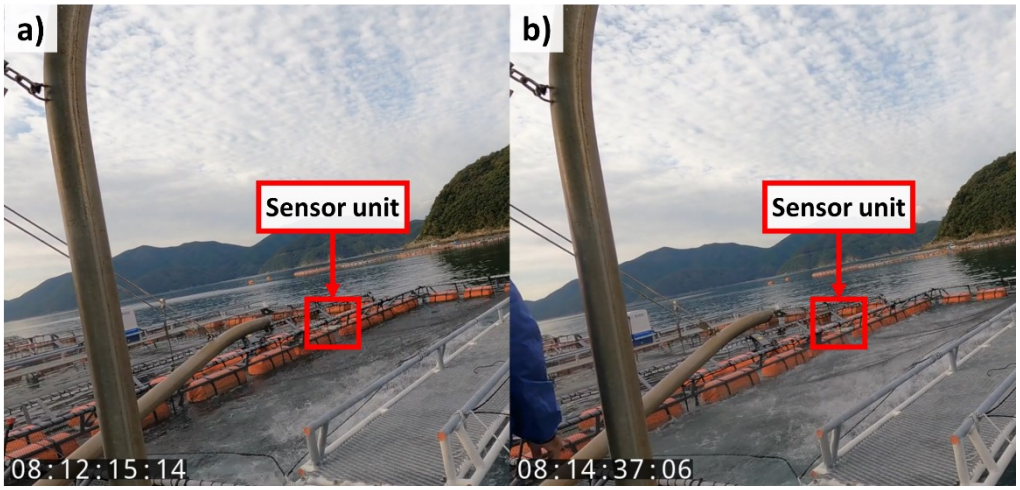

Figure 3-14 Less splashing in front of sensor unit; more splashing

The surface sensor started picking substantial readings at 8:14. A rising trend was observed for around 1.5 minutes, peaking at 25.4 cm/s. As seen from the splashes, fishes started moving towards the side opposite to the boat and closer to the sensor unit (Figure 3-14b). The trend started decreasing at 8:16. Action camera video showed splashing at the surface gradually decreasing from then on. Video at 0.5 m also showed the view gradually becoming clearer. Flow speed rose again briefly at 8:18 before it started declining from peak. Feeding was finally stopped around a minute after the decline. Then flow speed finally dropped to 0 cm/s after a few seconds. Flow speed measurements at 2.5 meters throughout the feeding were 0 cm/s even when fishes could be seen from the camera. It could possibly be attributed to the center of fish activity at that depth not

aligned with the flow sensor or to the fishes there swimming slower than those at the surface, among others.

In the second cage, measurements from all three depths were collected, as shown in Figure 3-15. At the start of recording, underwater cameras at all depths showed fishes circling the cage. Most fishes were swimming at 4.5 m while few fishes could be seen from the 0.5 m camera. Readings from 0.5 meters were detected before feeding, peaking at around 11 cm/s. Although few fishes could be seen there, small particles were observed moving toward the camera, indicating water flow. Three minutes before feeding started, readings briefly dropped close to 0 cm/s. After then, they shortly peaked to around 10 cm/s and dropped to zero for over a minute. At this time, the action camera captured a surf heading towards the cage, causing a small turbulence.

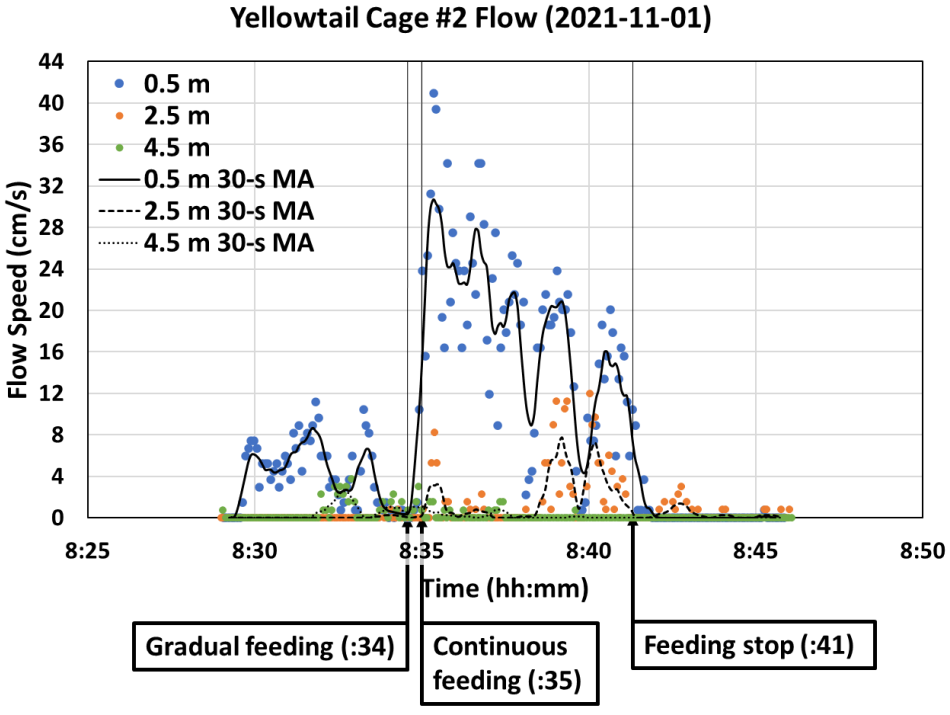

Figure 3-15 Flow measurement results from the second cage

As feeding continued from that point, flow speed gradually declined. It would still a reach series of peaks, although each succeeding peak was smaller than the previous.

Splashing observed from action camera gradually decreased while view from the underwater camera gradually cleared. Fishes could be seen swimming close to the surface but fishes reaching it gradually became fewer as time passed by. They were still swimming actively although slightly less than when feeding started (Figure 3-16a). Measurement reached the last peak at 20 cm/s before starting to decline and was at around 10 cm/s when the feeding machine was stopped. Fishes started going down although some fishes could still be seen from the 0.5 m camera. Flow speed dropped to 0 cm/s after 30 seconds and few fishes remained, eventually disappearing after around two minutes.

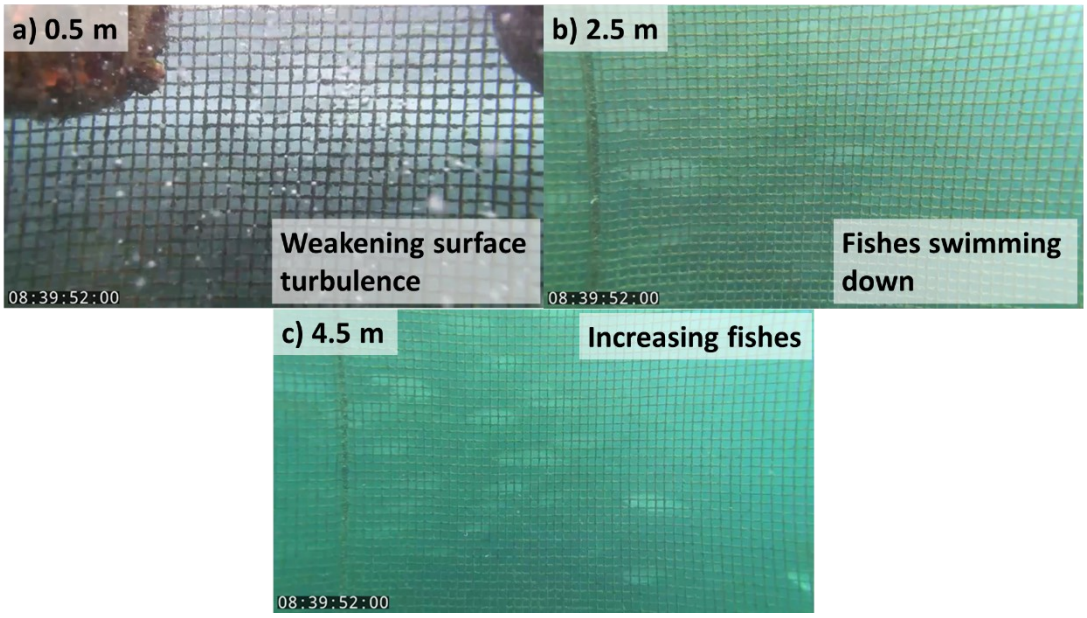

Figure 3-16 View from the three underwater cameras towards the end of feeding

Almost all measured flow speeds at 2.5 m before feeding started were at 0 cm/s, although fishes could be seen swimming at this depth. A possible reason for this could be the swimming speed not enough to induce outward flow, although this remains unclear. The first notable readings at 2.5 meters were observed briefly after continuous feeding started, peaking at around 8 cm/s. At that time, video showed that fishes that reached the surface first were going down while fishes at 4.5 m were going up. The number of fishes

at that depth must have reached a critical mass and reached a higher swimming speed to induce flow briefly. In the next three minutes, measurements were very small, most at 0 cm/s. Fishes could hardly be seen, suggesting few fishes swimming at this depth.

Flow speed then started to increase at 8:38 in the next three minutes, peaking at around 11-12 cm/s, and briefly dropping to 0 cm/s in between. More fishes started to become visible again, suggesting more of them going down from the surface after feeding (Figure 3-16b&c). Readings were at 0 cm/s when feeding was stopped. Fishes were still seen swimming down from the surface. Small amounts of flow, with speeds up to 3 cm/s, were detected in the next two minutes before dropping to 0 cm/s. At the end of the video, few fishes could be seen at 2.5 m, and they were swimming slower than even before feeding started.

Most flow speed readings 4.5 m were at 0 cm/s, whether many fishes were swimming there before feeding or very few could be seen during feeding. Rise of less than 4 cm/s at around 8:32 could be attributed to external current, although this could not be verified. At this point, the relationship between the fish activity and flow at the bottom of the fish cage could not yet be clarified.

All sensor modules from both sides of the third cage were able to collect data, as shown in Figure 3-17. Flow speed readings from all sensors at the beginning of measurement were at 0 cm/s. When the farmer started feeding gradually at 9:56, the fishes were seen accelerating towards the surface. However, flow speeds at 0.5 m from did not increase until around 90 seconds after. The number of fishes approaching the surface gradually increased, swimming fast. After then, surface readings on both sides rose drastically, with the rise at the north side lagging by around 10 seconds. Fishes started making large splashes at the surface. Flow speeds at the north and south sides were at around 18 cm/s

and 20 cm/s, respectively, when the farmer started giving feeds to the fishes continuously at 9:58.

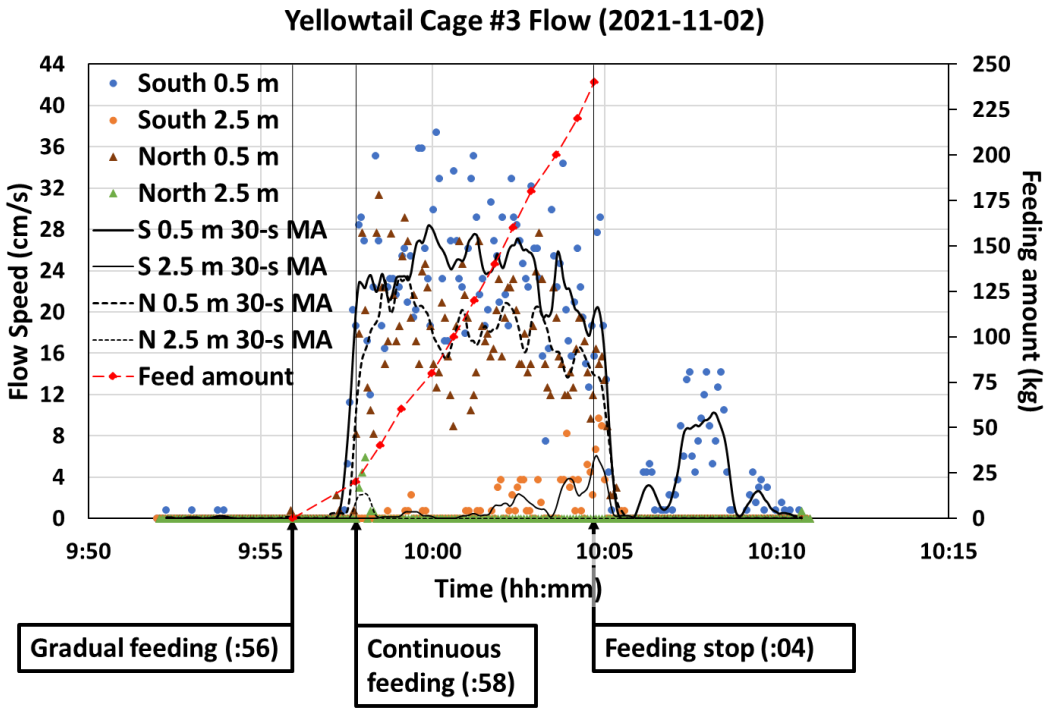

Figure 3-17 Flow speed results from the third cage, with the estimated feed amount

Flow speed at the north side quickly peaked at around 31 cm/s in the same minute continuous feeding started. On the other hand, flow at the south side remained steady at an average of 23 cm/s for around 1.5 minutes. It then reached the peak of around 37 cm/s at 10:00. After reaching their peaks, readings from both sides declined slowly. Like in the second cage, these would still reach a series of peaks, with each succeeding peak slightly smaller than the previous. Underwater camera observations showed most of the fishes at 0.5 m swimming close to the surface, with some reaching it to feed, as shown in Figure 3-18a&b. Most of them were seen from the camera at the south side, where feeds were being poured. Fish activity remained the same throughout the feeding. Flow speeds at the north and south sides when feeding ended were at 12 cm/s and 16 cm/s, respectively.

They dropped drastically to 0 cm/s right after. Fishes could be seen swimming down quickly.

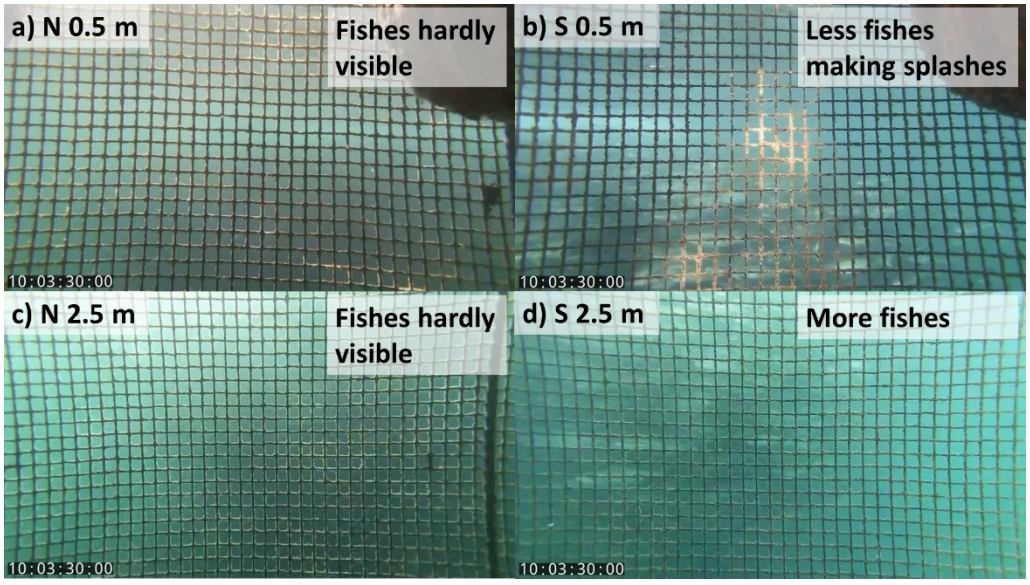

Figure 3-18 View from the underwater cameras at both depths and sides of the cage

For the whole feeding duration, surface flow speeds at both sides of the third cage exhibited a plateau-like trend. These were shown by the drastic rise and fall in speeds at the start and the end of feeding as well as by the slow decline from peak readings. The shape of the two trends almost looked similar. However, it could be observed the trend at the south side had a greater magnitude than the trend at the north side. The apparent movement of water surface outside the cage, as seen from the action camera video, seemed to indicate the presence of tidal currents moving southward. The offset between the trends could mean that the fish-induced flow heading north was reduced by the tidal current, resulting in smaller measurements by the north surface flow sensor. Results from this cage showed that measuring flow from opposite sides of the cage could cancel external currents from the measured flow induced by fishes.

Like in the second cage, there was also a brief rise in flow speed at 2.5 meters on the north side, although the rest of the readings from the sensor there were 0 cm/s. Fishes

could be seen swimming around at this depth when the farmer started feeding gradually, although their number was small that they were hardly visible at the video. Most were still at the bottom of the cage. At 9:57, more fishes were thus becoming more visible as more started swimming at this depth and towards the surface. Many fishes could be briefly seen at the north side when continuous feeding started, more than at the south. They were more concentrated at the north side before they started swimming towards the surface at the south side, where the farmer was pouring the feeds, as shown in Figure 3-19.

Figure 3-19 Fish farmer pouring bags of feed on the south side of the cage

Although fishes could be seen at 2.5 m at the south side, most were still swimming close to the surface. What was seen at this point was the bottom of the fish school. This could explain why flow speed readings were mostly 0 cm/s at this point at the first half of the feeding. Flow speed started increasing at 10:01 towards the end of feeding. Readings were less than 1 cm/s in the first minute. Flow increased to around 4 cm/s in the next minute before briefly dropping to 0 cm/s for 30 seconds. It then started increasing consistently in the next two minutes. Ten seconds after the farmer finished the last bag of feeds, flow continued to reach its peak at almost 10 cm/s before quickly dropping to 0 cm/s. Throughout this second half of the feeding, the number of fishes seen by the south

camera at 2.5 m gradually increased. Many fishes were seen swimming down to the bottom of the cage at the time flow peaked. In the next few minutes, many were still swimming at this depth although they were not as densely as during the feeding.

3.4. Long-term observation capability experiment

3.4.1. Setup

To demonstrate the sensor network's capability to operate for long-term observations, a three-day experiment was performed in July 2022 at a field station of the Fisheries Research and Education Agency located in Gotō City, Nagasaki Prefecture. Among the fish cages of the facility located in Nunoura Bay, we decided to deploy the sensor network in the two fish cages marked 4C and 4D. These cages, each with an area of 5 m x 5m and a depth 5 m, are adjacent to each as they share some parts of the frame structure – floaters, cage frames and walking platforms. They are surrounded by five pairs of fish cages at all but one side, which is the main docking side for the boat. Each cage contained around 200 two-and-a-half-year-old yellowtails, each with an average weight of 3 to 3.5 kg. Details of these cages are summarized in Table. 3.

Normally, fishes are fed once in two days. For this experiment however, the facility's coordinator decided to feed the fishes in both cages in all three days. The installation of sensor units and the power supply units was done in the morning of the first day, so we requested that the fishes be fed past 14:00, starting with cage 4C. For the next two days, feeding was done in the morning, although the exact time depended on arrival at the site to confirm data collection by the sensor network. Feeding was started at cage 4D at 9:21 on the second day, while it was started at 4C at 10:08 on the third day.

Throughout the experiments performed, the longest feeding duration observed was around 80 minutes and the earliest feeding was done at 8 AM. With these considerations, we decided to schedule the automatic data collection at 8 AM for three hours. The next scheduled operations for the day were at 2 PM and at 6 PM, collecting data for one hour

each. There were two three-hour gaps between the data collection periods. Figure 3-20 shows the sensor network's schedule of operation.

Fish cage no.	4C	4D
Location	Gotō City, Nagasaki Prefecture (長崎県五島市)	
Dimensions	5 m (length) x 5 m (width) x 5 m (depth)	
No. of sensor units	2 (1 per side)	2 (1 per side)
Sensor depths	0.9 and 2.9 m	0.9 and 2.9 m
Fish; average weight	Yellowtail/ブリ (*Seriola quinqueradiata*); 3-3.5 kg	
Population	219	201
Age	2 years, 6 months	

Table 3 Characteristics of fish population in the third experiment

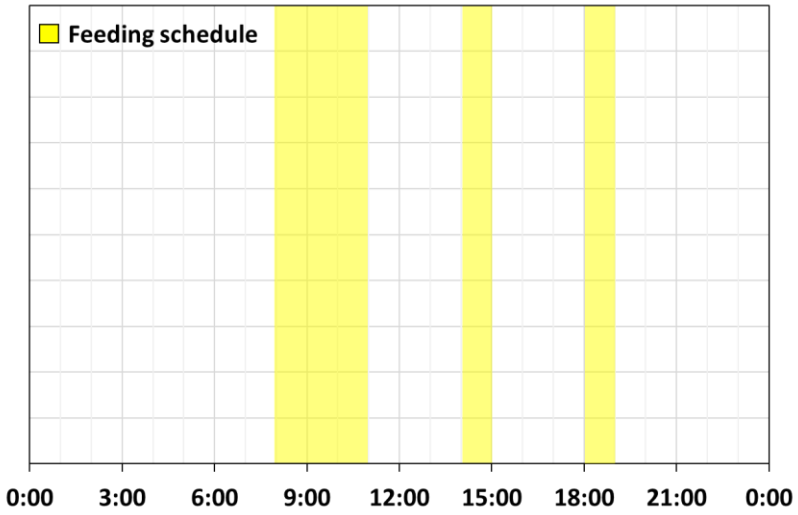

Figure 3-20 Automatic operation schedule of the sensor network

The feeder (a fish farmer in the first day; the coordinator in the second and third days) would bring two buckets, each containing 20 kg of EP feeds for each cage. He would scoop 10-20 pellets from the bucket every time and throw them to the fishes, as shown in Figure 3-21. He would pause to inspect how fishes were swimming in response to the feeds given. He would stop the feeding upon assessing that the fishes had been satiated. Total amount of feed given in each feeding for each cage was determined by measuring the amount of feed that remained after the feeder decided to stop and subtracting that amount from 20 kg. Feeding parameters are summarized in Table 4.

Figure 3-21 Fish farmer throwing feeds on the water using a scoop

Day	1 (Jul-13)		2 (Jul-14)		3 (Jul-15)	
Cage no.	4C	4D	4C	4D	4C	4D
Feed type	Extruded pellet (EP)					
Feeding start time	14:26	14:58	9:35	9:21	10:03	10:09
Feeding end time	14:48	15:29	9:51	9:31	10:08	10:15
Duration (min.)	22	31	16	10	5	6
Feed amount (kg)	17.79	15.29	9.15	8.35	~8-9	10
Feeding method	Manual (hand-thrown)					

Table 4. Feeding parameters in the third experiment

Like the setup in the third cage of the second experiment, we decided to install two sensor units with two sensor modules each on two opposing sides of both cages, as shown in Figure 3-22. Using the southwest and northeast sides of the cages meant that only one pair of sensor units could be used for each cage because there was no space for them on the side shared by the two cages. We therefore positioned each pair of sensor units to center of their northwest and southeast sides.

For designing the power management, we first obtain the system's daily energy requirement by estimating the power consumption of the sensor and top modules from the specifications of their components. Using Equation 3, the three sensor units have a P_U of around 24.3 W each. Because one sensor unit that contains the hub unit uses a more

powerful router, its estimated P_U is at around 26.3 W and the P_H of the hub unit computer is 10 W. We also add the power of the GPS time server, which is 2.2 W. From Equation 4, the P_{SN} therefore is at around 111.4 W. With an operation time of five hours per day, the calculated E_{SN} of the system using Equation 5 was at around 557 Wh/day or 2.01 x 10^6 J/day.

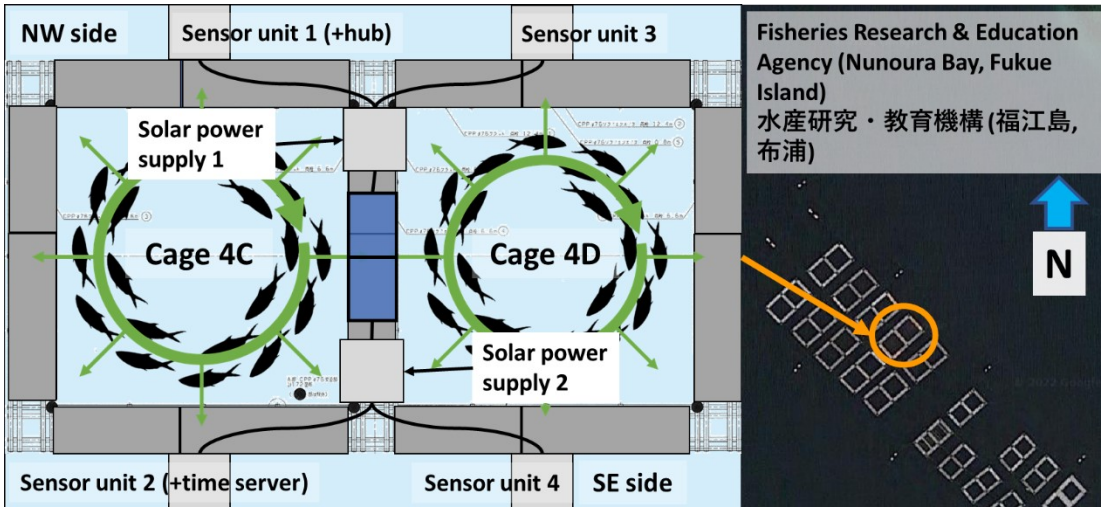

Figure 3-22 Top view of the third experiment setup

We decided to use the $\bar{t}_{Smin}$ at Nagasaki in December 2021 obtained from the Japan Meteorological Agency, with a value of 3.48 hours/day or 1.25 x 10^4 s/day [73]. Therefore, the P_{SP} calculated from Equation 6 was at around 159.88 W. Given the limited space in the fish cage, we decided to construct two power supply units, each powering two sensor units. The required battery energy capacity and panel output power for each pair of sensor units were around 1.00 x 10^6 J/day (278.5 Wh/day) and 80 W, respectively. We therefore decided to equip each power supply unit with a 1.56 x 10^6-J (432-Wh; 12 V 36 Ah) PV battery and a 100-W solar panel. The units' energy capacity is sufficient for the system's daily requirement to operation for five hours.

We mounted the power supply units and the solar panels on the middle platform, as shown in Figure 3-23. Each power supply unit provided power to the two sensor units of

each side of the cages. We placed the sensor/hub unit on the northwest side and the sensor unit with the GPS time server on the southeast side to balance the load distribution of the two power supply units.

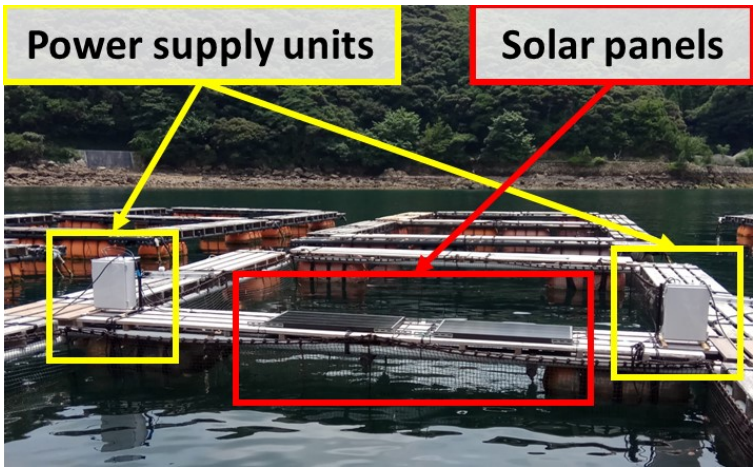

Figure 3-23 Two power supply units mounted on top of the fish cage platform

The procedure for assembling the sensor units was same as that in the previous experiment. We first inspected the sensor unit components for issues in power and network connections onshore. We then joined the module frames, connected the modules to each other, waterproofed the open connectors, and fixed the cables on the frames. Since the boats used by the facility are smaller than the feeding boats from the previous experiments and have no cranes, two sensor units were installed on the cages at a time, requiring 4-5 persons to carry each unit. The power supply units and the solar panels were then mounted on the middle platform before connecting their cables to the sensor units. Originally, we intended to position the sensor modules in each unit at the depths of 0.5 m and 2.5 m like in the previous experiment, so we did not adjust their positions in the modular frames. However, it turned out that the height of frame of these cages from the water surface is 0.4 m lower than that of the cages in the previous experiment. This

resulted to positioning the sensor modules at 0.9 m and 2.9 m below surface, as shown in Figure 3-24.

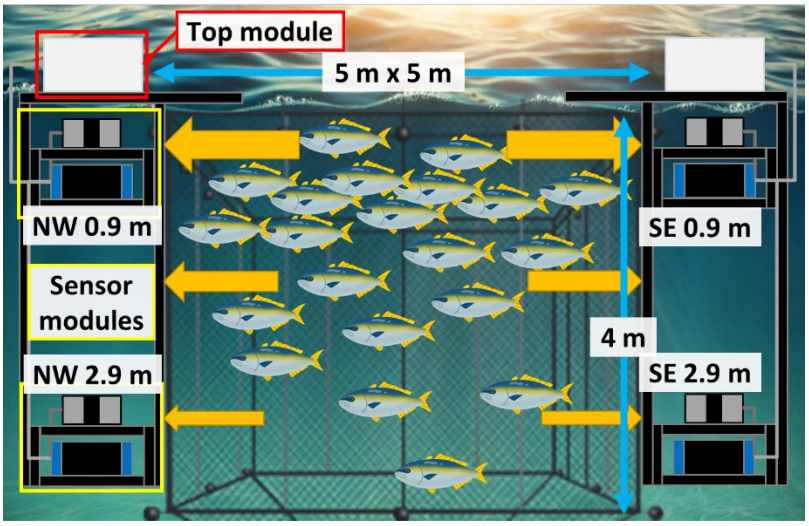

Figure 3-24 Side view of both cages the third experiment setup

At this point, the hub SBC has not yet been fully configured to automatically initialize its video management software to record videos to its own storage, whose size was also too small for 15 hours' worth of videos collected in three days. For this experiment, each network camera was configured to automatically record during the selected periods. Captured videos were then in each camera's own memory card (128 GB each).

Even though the sensor network was programmed to automatically start its data collection, we had to make sure that the hub unit computer was collecting data as scheduled. Because of the sensor network's limited Wi-Fi range, we had to go to the cages to remote access it. We decided to do this only during the 8:00 and the 14:00 schedules as staying in the facility in the evening would cause logistic problems. If the hub unit computer would not automatically synchronize its clock with the GPS time server, we would connect to it and manually force it to update its clock. Once the time had been adjusted, the programs for collecting data would start automatically.

Since the feeding on the first day started at 14:21 and lasted around an hour to finish the feeding in both cages, the sensor units would not have been able to collect measurements at its latter part had the sensors been let to switch off automatically at 15:00. We therefore overrode the switching schedule of the sensor network by manually setting the input of the power supply unit's relay to high and by manually running the terminal emulator software for logging the flow speed sensor data. We then reverted the system configuration back to collecting data automatically according to schedule.

3.4.2. Results

Among the eight sensor modules installed in the two cages, only the module positioned at 2.9 m of the southeast side of cage 4C was not able to collect any data throughout the experiment. We suspect a connection problem with the sensor module at 0.9 m, possibly due to loose contact between the connector pins or to excess application of waterproofing grease. Despite this, we were still able to observe flow speeds at 2.9 m through the sensor module from the opposite side of the cage.

As seen from the yellow gaps in Figure 3-25, there were parts within the operation intervals without collected flow data. This was attributed to the failure of the hub computer to automatically synchronize its clock with the time server after booting, although this was supposed to be fixed by increasing the frequency of updating the time. Therefore, it did not starting collect measurements at the actual times as scheduled. This was temporarily addressed by manually synchronizing the computer clock. Once the time was adjusted, the terminal emulator for collecting flow speed data automatically started recording data from all sensors. This could be addressed by creating a task to force synchronize the clock with the time server on startup. The network cameras, on the other

hand, have their own internal clocks running, allowing them to record videos independently throughout all scheduled times.

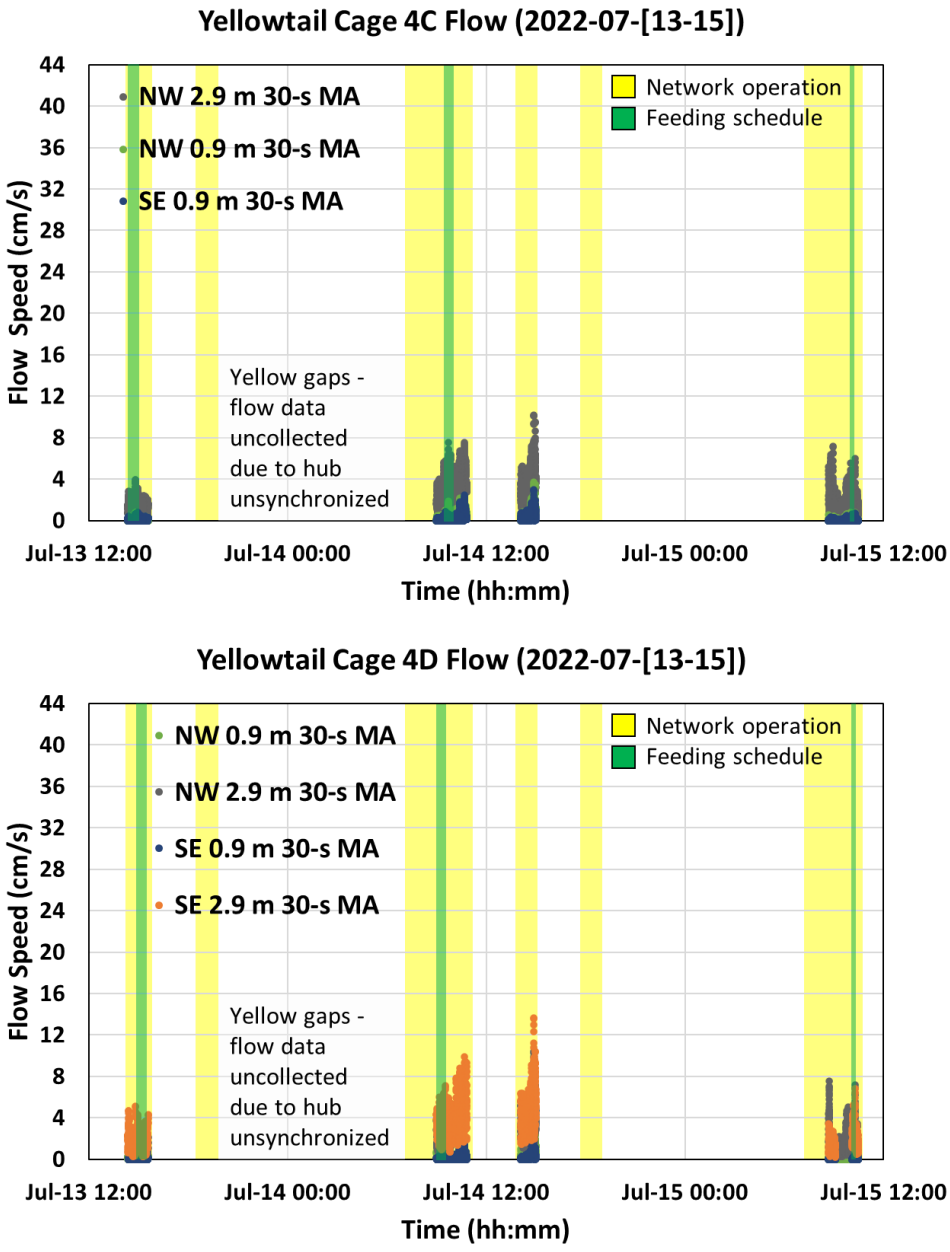

Figure 3-25 Flow measurement results from cages 4C and 4D in the third experiment

Throughout the entire experiment, flow speed measurements at 0.9 m in both cages were very low, most at 0 cm/s. On the other hand, flow speeds at 2.9 m were generally higher than those at the surface (Figures 3-26 to 29). Recorded videos also showed most

of the fishes swimming near the bottom of the cage and no fishes at 0.9 meters show most of the time. These results corresponded to the typical behavior of fishes while not feeding, as observed from the previous fish cage experiments.

On the first day of the experiment, the sensor network started its operation at 14:21 after manually synchronizing the hub computer clock (Figure 3-26). Before feeding started at cage 4C, many fishes could be seen swimming slowly at 2.9 m. Flow speed at that depth peaked at almost 8 cm/s. When it started at 14:26, fishes could be seen swimming to the surface to grab food. Flow speed measurements at 0.9 m remained at 0 cm/s throughout the feeding. Speeds at 2.9 m were at around 4 cm/s for around eight minutes before dropping to around 2 cm/s for around ten minutes. Fishes were less visible during those times compared to before feeding started. It increased again at 14:45 until the end of feeding at 14:50 and more fishes started to be seen at that depth. There was slight increase at 0.9 m after feeding ended to almost 4 cm/s, although there was no indication in fish activity at that depth.

Because of the delay in the sensor network operation, we decided to override the scheduling of the power supply unit to operate the sensor units. Rebooting the hub unit computer and the sensor units took around four minutes before becoming operational. We also overrode the recording schedule for the flow sensors. Feeding at cage 4D started at around 14:58. Throughout the feeding, flow speeds at 0.9 m were very small, although readings at the northwest side were slightly larger. There were also no noticeable patterns in flow speed at 2.9 m. However, readings at both sides showed similar trends, with readings at the southeast side slightly larger, which was opposite with the readings at 0.9 m. These offsets could still indicate cancellation of external currents.

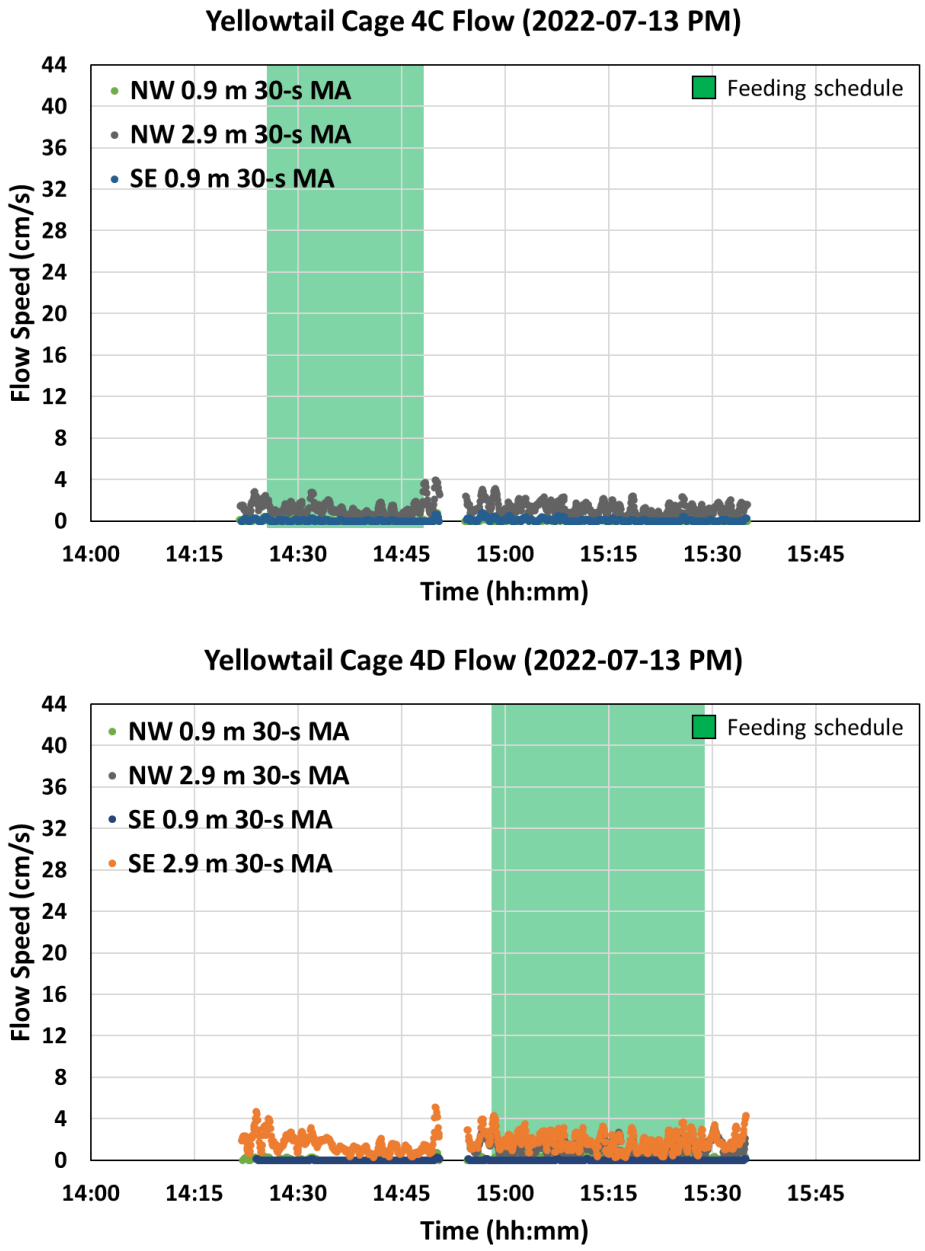

Figure 3-26 Flow speed moving averages from cages 4C and 4D on Day 1

Feeding at both cages on the second day were shorter compared to the first. It started at cage 4D at 9:21. Like in the previous day, flow speeds at 0.9 m were very small throughout the feeding, with those at the northwest side faster by 2 cm/s (Figure 3-27). Very few fishes could be seen grabbing food at the surface from the videos at this depth. Readings at 2.9 m were at 4-7 cm/s at the first half and increased to around 10 cm/s at the

second half. Video recordings showed few fishes visible at this depth, indicating most were at the bottom. More fishes began swimming at this depth at the start of feeding. Towards the end of feeding, they gradually went back at the bottom. Like the previous day's results, flow speeds at both depths exhibited similar patterns on both sides, with one side slightly faster.

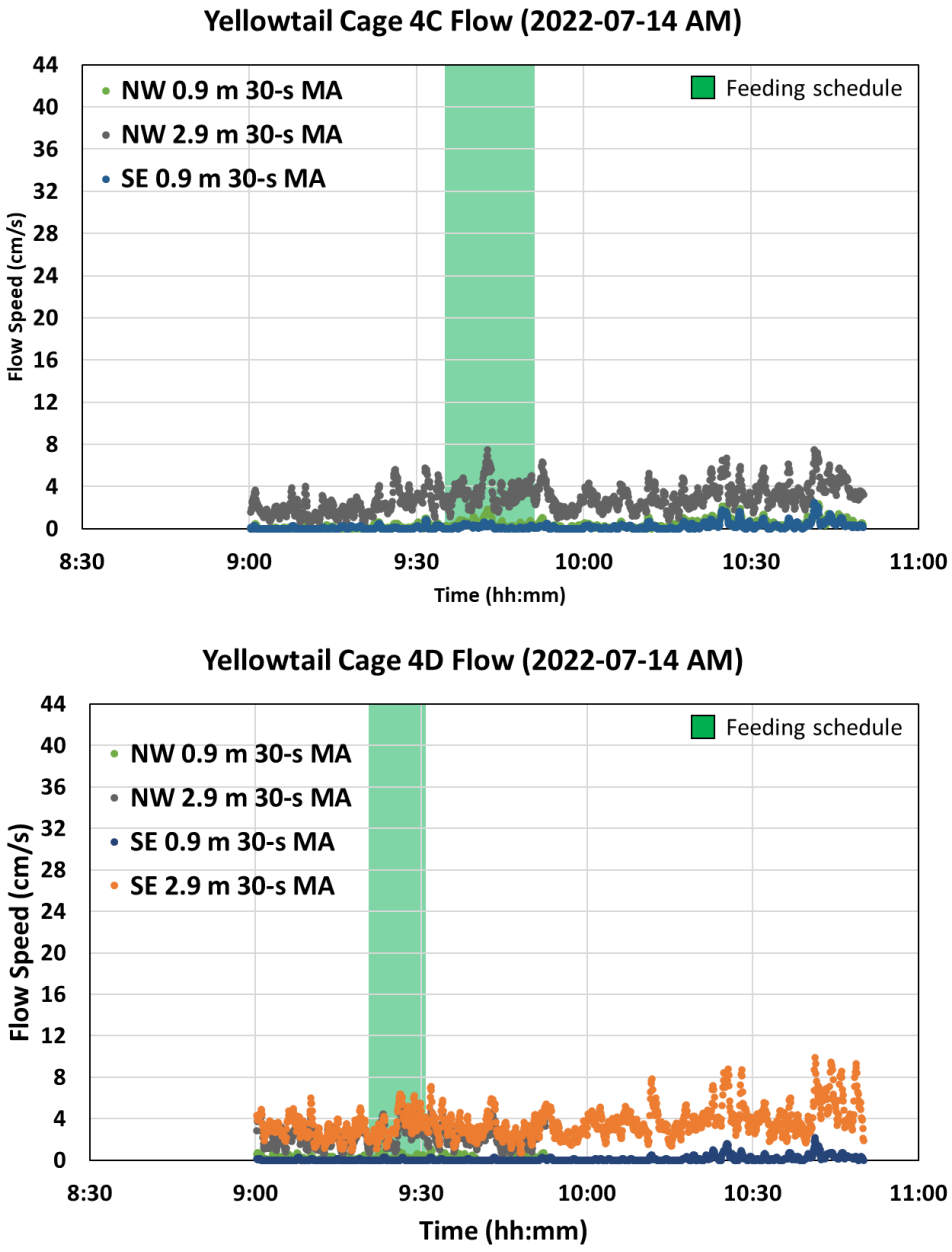

Figure 3-27 Flow speed moving averages from cages 4C and 4D on the morning of Day 2

Feeding started in cage 4C at 9:35 and ended at 9:51, six minutes longer than in 4D. Throughout the feeding, readings from 0.9 and 2.9 m were averaged at around 2 and 4 cm/s, respectively. At around 9:43, there was a spike in readings at both depths from the northeast side. At 0.9 m, fishes still exhibited the same feed grabbing behavior at that time. On the other hand, more fishes could be seen swimming from the bottom to 2.9 m. At this point, it is difficult to confirm whether this spike could be attributed to increase in fish activity or to external currents affecting the readings.

The sensor units also measured flow speeds in the cages for about an hour at around 14:05 of the same day (Figure 3-28). No feeding was made at this time, as these measurements were done to observe fish activity outside feeding schedules. A common trend in both cages was the gradual increase towards the end of data collection. Similar patterns were observed from both sides. No fishes were detected by the surface camera near the end of recording. On the other hand, few fishes could be seen at 2.9 m in the first few minutes of recording but gradually increased in number towards the end. Although the increase in readings could mainly be caused by the tidal currents, the fishes gradually swimming to 2.9 m from the bottom could also have contributed to this increase.

Feeding on the third day started at around 10 AM, starting with cage 4C. It only took 5-6 minutes at each cage, as shown in Figure 3-29. After synchronizing the hub computer clock, the sensor network started recording measurements at 8:41. However, the sensor unit at the southeast side of cage 4D stopped collecting data at 9:05, therefore losing one hour's worth of data. We suspected this to be caused by a malfunction in the Wi-Fi router and was fixed by resetting the unit's power.

The flow sensors in cage 4C did not measure any significant changes at 0.9 m. All their readings throughout the feeding were mostly at 0 cm/s even though recorded videos

showed fishes swimming quickly to the surface to grab feed. Flow speed at 2.9 m was low at the start of feeding, with an average of readings at around 1 cm/s. Many fishes, on the other hand, were seen at this depth. Flow speed eventually increased to an average of around 3 cm/s throughout the feeding, peaking at around 8 cm/s. Towards the end, fishes were seen gradually swimming up closer to the surface.

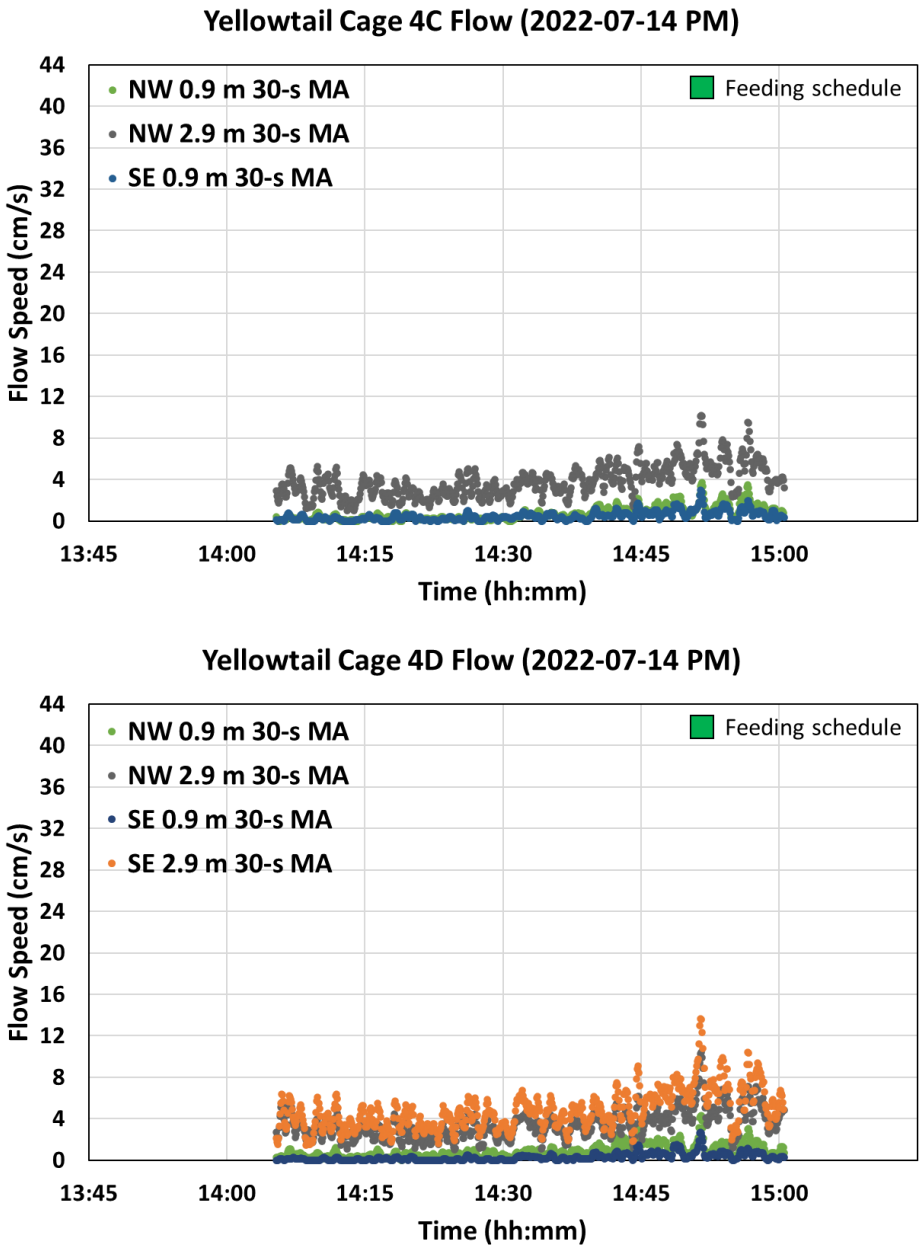

Figure 3-28 Flow speed moving averages from cages 4C and 4D on the afternoon of Day 2

Very small changes in surface flow speeds were also observed in cage 4D. Most readings measured from both sides were mostly at 0 cm/s, although a few moments were observed at the northwest side when flow speed briefly increased to 2-4 cm/s. Recorded fish activity was at the surface was like those in other video recordings. At 2.9 m, flow speed readings were at 2-4 cm/s when feeding started, although the flow sensors at both sides were already detecting flow speeds as high as 12 cm/s briefly. Average readings gradually declined to below 2 cm/s towards the end of feeding.

Throughout the experiment, no substantial changes in flow speeds could be observed during feeding times. Readings at 0.9 m remained smaller than the readings at 2.9 m, as seen from Figures 3-26, 27, and 29. Although fishes did swim up to the surface when feeds were thrown to the water, as shown in Figure 3-30, they did not form a massive group swimming in a circular pattern close to the surface, compared to the observations in previous cage experiments. Instead, they would grab feeds at the surface in small numbers and then swim in circles at around below one meter depth. This could be attributed to feeds thrown on the water in small amounts. As a result, they did not push enough water out of the fish cage to create flow detectable by the flow sensors.

Although it was difficult to establish a relationship between the flow speed readings and the recorded fish activities during feeding, we were able to partially demonstrate long-term observations of fish activity. The power supply units automatically switched on and provided power to the sensor units. Once we manually forced the hub unit to synchronize its clock on startup, the sensor units automatically started recording flow speed measurements and record videos of fish activity. The power supply unit was able to harvest solar energy to recharge the batteries that provided power to the sensor units, allowing them to collect hours' worth of data in three days.

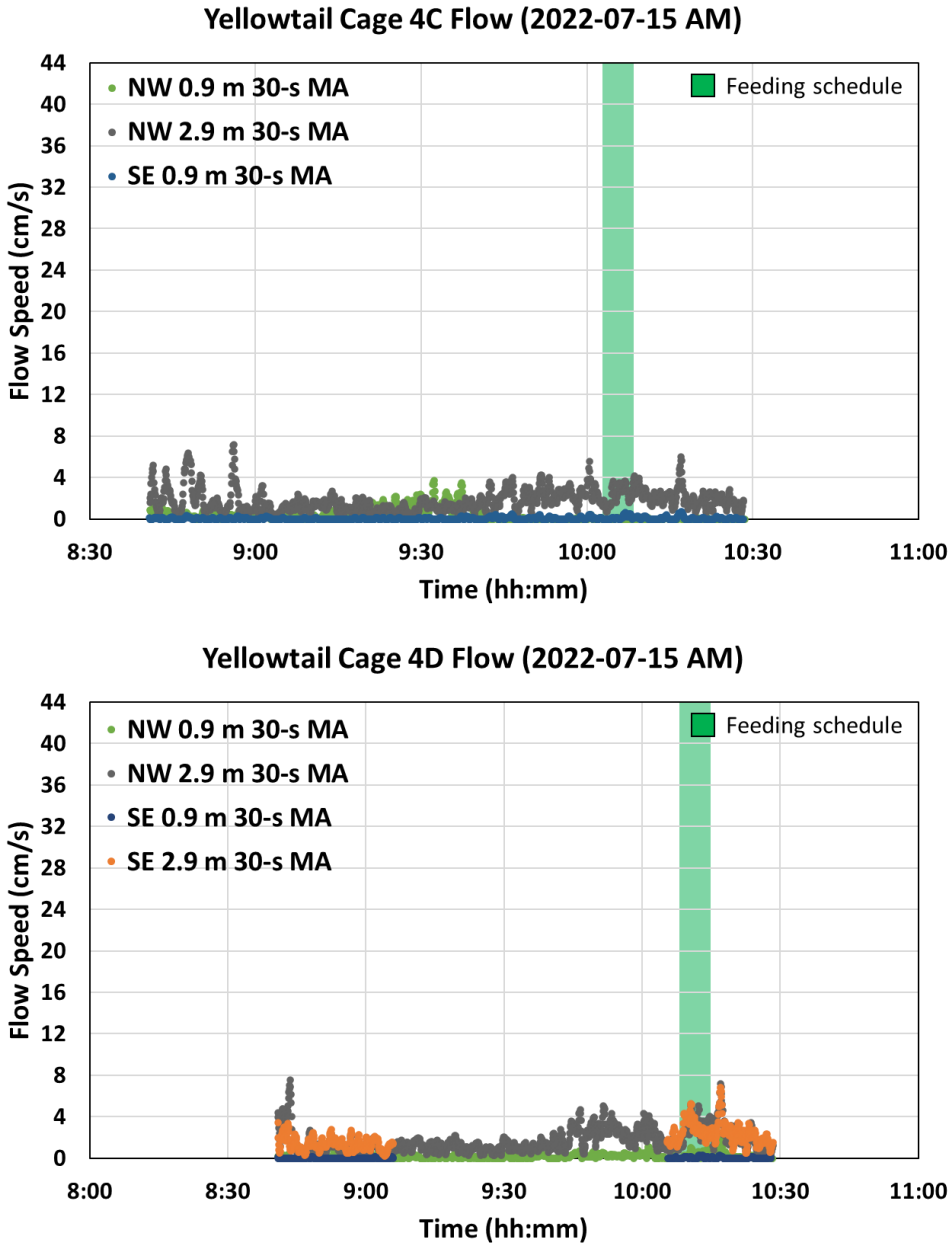

Figure 3-29 Flow speed moving averages from cage 4C and 4D on Day 3

Figure 3-30 Video record of fishes swimming to the surface to feed

3.5. Summary

As we developed the sensor network throughout the duration of the research, we gained insights on the properties of the fish activity during feeding and of its relationship with the fish-induced flow by performing three separate experiments in fish cages, measuring flow speeds at different depths at different sides of the cages especially during feeding. We also demonstrated the functionality of the components of the system we developed.

In the first experiment, we demonstrated the functionality of the flow sensors to measure the flow speeds induced by fishes underwater. We used two flow sensors as dataloggers that collected flow speeds at two depths. These dataloggers were deployed in two cages containing yellowtail amberjacks. We were able to use these sensors to clarify the difference in flow speeds at different depths, especially during feeding. We also observed the increase in fish activity at the surface i.e., more fishes swimming and splashing at the surface, corresponded to the increase in flow speeds and vice-versa.

In the second experiment, we demonstrated that the sensor network could collect flow speed measurements and underwater videos not only from different depths but also from different sides of a fish cage. We deployed the sensor network with eight sensor modules configured as multiple sensor units in three cages containing yellowtails. Shown in Figure 3-31 are the sensor units being brought to the fish cages to be installed. We observed in this experiment the drastic rise in flow speed as fishes went up to the surface rapidly and its gradual decline throughout the feeding, corresponding to the fishes gradually becoming satiated. We also found that increase in flow at lower depths could be useful indicator for the fishes returning to lower depths of the fish cage as a response to becoming satisfied with feeding.

In the third experiment, we were able to partially demonstrate long-term observations of fish activity by installing the sensor network in two cages containing yellowtails to collect flow speed data and videos for hours in three days. We found the lack of increase in flow speeds at the surface during feeding due to the fishes' behavior of grabbing feeds and swimming down quickly instead of forming a large school that could create substantial flow speeds.

Figure 3-31 Two sensor units loaded on the boat to be installed on the fish cages

Chapter 4
Discussion on feeding decision

Chapter 4. Discussion on feeding decision

4.1. Modelling of fish feeding activity

To be able to use flow speed measurements for assisting farmers in making feeding decisions, we first need to make a simplified model of the fish activity as a response to feeding, whose simulation output possesses some resemblance to the data we collected. We can then further develop it later and use the output of its simulation to predict the actual fish feeding behavior from the flow measurements from the sensor network. We can then use it later to optimize the feeding strategy for fishes in the cage.

Recalling the assumption made in the first chapter, as shown in Figure 4-1, it can be said that the primary sources of flow in the fish cage are the external currents and the circular movement of fishes. The speed of flow from the latter mainly depends on school's swimming speed and on its distribution throughout the depth of the cage. In turn, these parameters depend on the fishes' hunger or satiation and on the amount of feeds available in water. By simulating a simple model of the fish activity, we can establish some basic relationships of these parameters with each other. We then compare this model with the measurement data collected from the experiments.

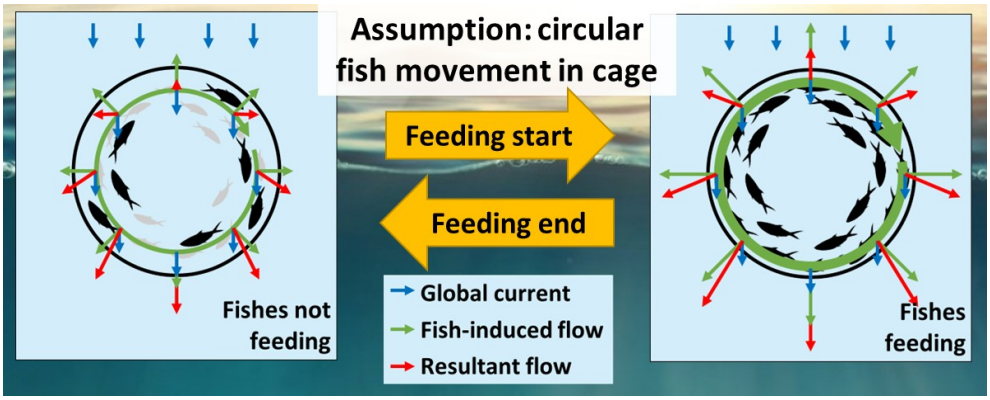

Figure 4-1 The assumptions on the fish activity and on the fish-induced flow revisited

We first make a state-space model of an individual fish's activity by identifying its state, input, and output variables, as shown in Figure 4-2. The model's state variables include the following: the fish's height from the bottom of the cage at time t, denoted by $h_f(t)$ in m; the circling speed at time t, denoted by $v_f(t)$ in m/s; and the satiation level of the fish, denoted by $S(t)$, having a value range of [0-1] with 0 and 1 to indicate hunger and satiation, respectively. For this model, we separate the circling speed along the horizontal plane, from the vertical speed or change in depth. The variables $h_f(t)$ and $v_f(t)$ also serve as the output of this model since these comprise its feeding behavior.

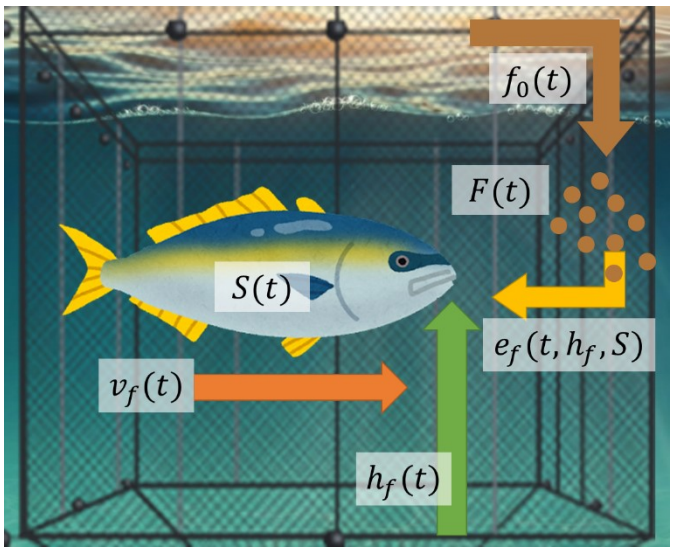

Figure 4-2 The input ($f_0(t)$, $F(t)$, and $e_f(t, h_f, S)$), state ($S(t)$, $h_f(t)$ and $v_f(t)$), and output variables ($h_f(t)$ and $v_f(t)$) of the fish feeding activity model

While there are several factors that affect the behavior of fishes in response to feeding, we simplify the input used in this model into one quantity: the instantaneous amount of feed eaten by the fish at time t as denoted by $e_f(t, h_f, S)$ in kg, which we shall also call the eating function. This is dependent on the amount of food in water, denoted by $F(t)$, as well as on the height of the fish $h_f(t)$. The variable $F(t)$, in turn, changes upon the amount dispensed on water at time t, as denoted by $f_0(t)$ in kg/s.

Not only the interaction of the fishes' feeding behavior with the environment is complex but also its interaction between the feeds in the water. To simplify the model, we establish several assumptions on the fish activity, on the fish cage environment, and on the feeding:

1. The induced flow speed at the average depth of the fishes is linearly proportional to their swimming speed.
2. For all fishes, $v_f(t)$ is constant throughout the feeding activity. In this simplified model, we establish that the $h_f(t)$ determines the depth where most flow is induced.
3. There is enough space for all fishes to swim around at a given depth without colliding with other fishes.
4. Water quality parameters such as the dissolved oxygen concentration and temperature are within ranges optimal for fish feeding.
5. Feeds exit the cage, due to dispersion by currents or to sinking, at a constant rate and is given by the constant coefficient k_1.
6. The fish either eats a constant amount of feed at time t, as denoted by c_f, or it does not.

Given the fifth assumption, we can establish a differential equation for $F(t)$ as

$$\dot{F}(t) = f_0(t) - k_1 \left(\sum_{i=0}^{n} \left(\frac{1 - S_i(t)}{n} \right) \right) F(t) \tag{8}$$

In this equation, the decrease in $F(t)$ is caused by the dispersion of feeds, as represented by k_1, and by the average hunger of n fishes in the cage, representing the amount consumed. The variable $f_0(t)$, on the other hand, contributes to the increase in $F(t)$ since feeds are supplied to the cage. Given the sixth assumption, we shall establish the eating function to have a binary output. Aside from its hunger level, a fish eats depending on its

height as well as on the amount of food in water. Supposing a fish at a certain $h_f(t)$ is hungry, it gets to eat when $F(t)$ is sufficient (more food sinking downwards with greater $F(t)$) and does not otherwise. We can illustrate this condition as a boundary line, as shown in Figure 4-3. The slope of this line at a given $S(t)$ is the coefficient for the fish's eagerness to eat, which we denote here as k_2. The value h_C is the cage depth (in meters) and represents the water surface in the $h_f(t)$ axis. When a given $h_f(t), F(t)$ is above a line of a given k_2, the fish eats and does not when is below the said line.

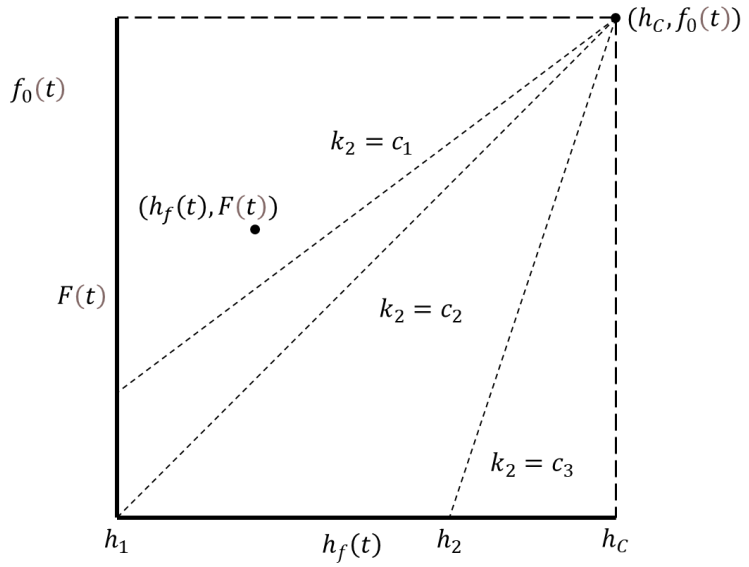

Figure 4-3 Illustration of the condition boundary line determining the value of $e_f(t, h_f, S)$ with 3 different values for k_2, and showing a given $\left(h_f(t), F(t)\right)$ resulting to eating

Therefore, the eating function of a single fish $e_f(t, h_f, S)$, is defined as

$$e_f(t, h_f, S) = \begin{cases} c_f, \ F(t) \geq k_2 \left(\sum_{i=0}^{n} \left(\frac{1-S_i(t)}{n}\right)\right)\left(h_f(t) - h_C\right) + f_0(t) \\ 0, \ F(t) < k_2 \left(\sum_{i=0}^{n} \left(\frac{1-S_i(t)}{n}\right)\right)\left(h_f(t) - h_C\right) + f_0(t) \end{cases} \quad (9)$$

We then represent our model for an individual fish activity as the following state-space equations:

$$\dot{\boldsymbol{x}} = A\boldsymbol{x} + B\boldsymbol{u}, \text{ where } \boldsymbol{x} = \begin{bmatrix} x_1 \\ x_2 \end{bmatrix} = \begin{bmatrix} S(t) \\ h_f(t) \end{bmatrix} \text{ and } \boldsymbol{u} = \begin{bmatrix} u_1 \\ u_2 \end{bmatrix} = \begin{bmatrix} F(t) \\ e_f(t, h_f, S) \end{bmatrix} \quad (10)$$

$$\boldsymbol{y} = C\boldsymbol{x} + D\boldsymbol{u}, \text{ where } C = \begin{bmatrix} 0 & 0 \\ 0 & 1 \end{bmatrix} \text{ and } D = \begin{bmatrix} 0 & 0 \\ 0 & 0 \end{bmatrix} \tag{11}$$

To determine matrices A and B, we need to explore how the states are affected by each other and by the input. Satiation of a fish naturally decreases over time and increases when it eats. However, the rate of increase slows down as satiation level approaches 1, following the law of diminishing returns. At the same time, the rate of decline in $S(t)$ decreases as it approaches 0. This can be written as the differential equation,

$$\tau_1 \frac{dS(t)}{dt} = -S(t) + \frac{1}{c_f} e_f(t, h_f, S) \tag{12}$$

where c_f is the constant amount of feed that a fish would consume at time t, which is used to normalize e_f, and τ_1 is the time constant for the change in the fish's satiation.

Without any food in water, a fish naturally tends to swim close to the bottom of the cage, regardless of hunger level. However, it tends to swim toward the surface when it is not full, and food is present in water. Then as it reaches satiation by eating, it swims back to the lower part of the cage. We therefore represent the change in $h_f(t)$ by the differential equation,

$$\tau_2 \frac{dh_f(t)}{dt} = \big(1 - S(t)\big)\Big(-a\frac{h_f(t)}{h_C} + b\frac{F(t)}{F_{max}}\Big), \text{ where } a + b = 1 \tag{13}$$

where F_{max} is the maximum amount of feed in water, whose value usually is the maximum $f_0(t)$, τ_2 is the time constant for the change in the fish's height, a is the coefficient for its aversion to swim to the surface, and b is the coefficient for its attraction to feeds dispensed on surface. The values of a and b may vary for each fish school in a cage depending on their species as well as on their rearing among other factors, but they always must add up to 1. Given the differential equations (12) and (13), the value of matrices A and B are therefore written as

$$A = \begin{bmatrix} \frac{1}{\tau_1} & 0 \\ 0 & \frac{-a}{h_C \tau_2}(1 - S(t)) \end{bmatrix} \text{ and } B = \begin{bmatrix} 0 & \frac{1}{c_f \tau_1} \\ \frac{-b}{F_{max} \tau_2}(1 - S(t) & 0 \end{bmatrix} \quad (11)$$

This model is best simulated using numerical analysis. We can setup the duration of simulation to be around the same with those of the conducted fish cage experiments. We can also setup the values of $f_0(t)$ across the decided duration to resemble the pattern of feeding made by the fish farmers during the experiments. Parameters such as n and h_C can also be approximated from the data provided by the farmers. As for the other parameters, we can adjust their values such that the output $h_f(t)$ corresponds to the flow measurements. We can get the averages of $h_f(t)$, e_f, and $S(t)$ for the n fishes as well as, $F(t)$ and check whether the observed changes correspond to observations in the fish cages. For this model to become useable in actual fish farms, this model needs to be further developed by considering the changes in $v_f(t)$ throughout the feeding activity as well as the changes in other parameters that have a significant impact on the fish feeding behavior.

4.2. Potential of flow measurement in feeding

Many patterns in flow could be observed from the results of the fish cage experiments. These could have been caused by various factors, such as the surrounding environment, the characteristics of the stocked fishes, and the nature of feeding among others. Going back to the hunger and food availability, the method the feeds were given could have affected the response of the fishes. However, there were notable points common in some of the cages, particularly towards the end of feeding. Surface flow in most of the cages increased to a certain speed and gradually declined as feeding progressed, as observed in the first two fish cage experiments.

There were also the observations of brief increase in flow below the surface at the start of and towards the end of feeding. These could suggest that fishes started swimming up and gathering at the surface to feed, as well as swimming back to the lower end of the cage, as observed in the second cage experiment. Flow values at the time feeding stopped in one cage can be different from the other. The advantage of installing two sensor units at two opposing sides of the cage was being able to detect these changes from at least one side of the cage. As was the case of the third cage, the rise of flow when feeding started was only detected at the north side while rise close to the end of feeding was only detected at the south side. These observed flow patterns could be used for deciding on when to stop feeding.

We can compare the flow measurements from the sensor units to the developed fish feeding activity model and observe the patterns in flow that correspond to the output of the model simulation. As we obtain model parameters that characterize the fishes, the cage environment, and the feeding as accurately as possible, we can formulate a feeding strategy that maximizes the satisfaction of the fishes while minimizing the amount of uneaten food in water. With that said, the model needs to be developed further to take more parameters into account for more accurate comparison with the flow measurements.

Since it is assumed that the fishes circle around and induce flow out of the cage, measurement of flow as to visualize fish behavior would be very much useful cages with fishes belonging to the carangiform and thunniform locomotion group, such as yellowtails and tunas. Such fish groups move mostly their rear body and tail fin to propel themselves and are fast swimmers and would therefore tend to circle around the cage. Feasibility of this system for fishes of other swimming groups still needs to be explored.

There was also a problem with near-zero flow speed readings at some depths of installation despite the substantial number of fishes swimming there. This could be attributed to the very small volume of water going through the flow sensor's small cross section area. This could have resulted to insufficient momentum from the water flow to rotate the propeller, resulting to very small readings. For the experiments in the nearer future, this could be addressed by attaching a funnel to the inlet of the sensor. By doing so, more water flowing at the same speed would enter the funnel and go through the sensor pipe with more speed to conserve mass, giving it more momentum to rotate the propeller. This makes the sensor more sensitive to smaller changes in flow. The speed at the mouth of the funnel would then be calculated from the speed at the sensor pipe through the ratio between cross-section areas of the two places.

Developing this system as a DX application on aquaculture remains in the process of using expert knowledge to assist farmers' feeding decisions as this system still needs to be further developed, in terms of hardware, fish activity estimation and relationship of flow with feeding (Figure 4-4).

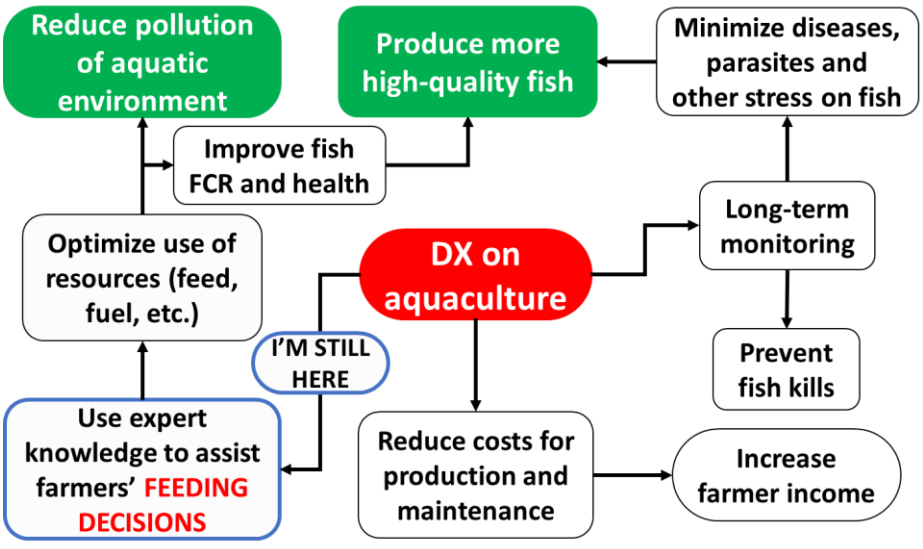

Figure 4-4 Current state of the system as DX application for aquaculture

4.3. Future fish farm sensor system

To set the direction of this research, given all the insights discussed, we envision a DX system for a fish farm with multiple cages. It is imagined collecting various sensor measurements aside from flow speeds not only to assist fish farmers with their feeding practices but also to gather various information on the fishes and the environment that could help them improve their overall culturing method. A network of sensor nodes (sensor units) would be installed around each fish cage of different shapes and sizes, containing various kinds of cultured fishes, as shown in Figure 4-5.

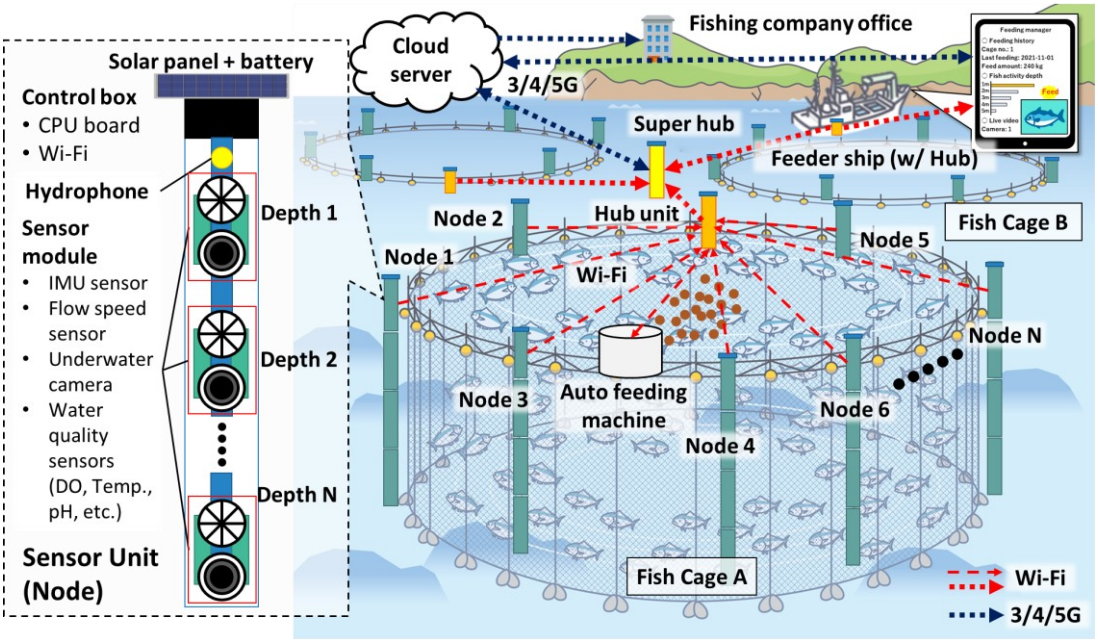

Figure 4-5 Envisioned DX system applied to a fish farm with multiple cages

Each node would consist of multiple flow speed sensors measuring flow velocities for every depth of choice, probably every meter below the surface to get a more detailed distribution of the fish school's activity. The DX system will have to feature more robust sensors that can maintain accurate measurements for extended periods of time. Due to their moving parts, the developed propeller flow speed sensors are vulnerable to mechanical failure caused by long-term exposure to the likes of seawater corrosion and

biofouling. As a result, the sensor network would not be able to collect accurate flow measurements in the fish cages. These could be replaced by sensors with no moving parts, which could be more sensitive to changes in flow.

A potential sensor that could be used include an underwater pitot-static-tube flow sensor similar to the one developed by Kishimoto et al. for tracking marine animals, as shown in Figure 4-6 [74]. It measures the flow speed using Bernoulli's principle, calculating the difference between the ambient pressure and the ram pressure from the flowing water. Another sensor that could be used would be a modified version of a tilt-current meter (TCM) that measures current speeds from the readings of an IMU tilted by the current [75]. Such sensor could measure flow velocity from different directions although it needs to be modified such that the TCM could transmit data to the sensor network in real-time.

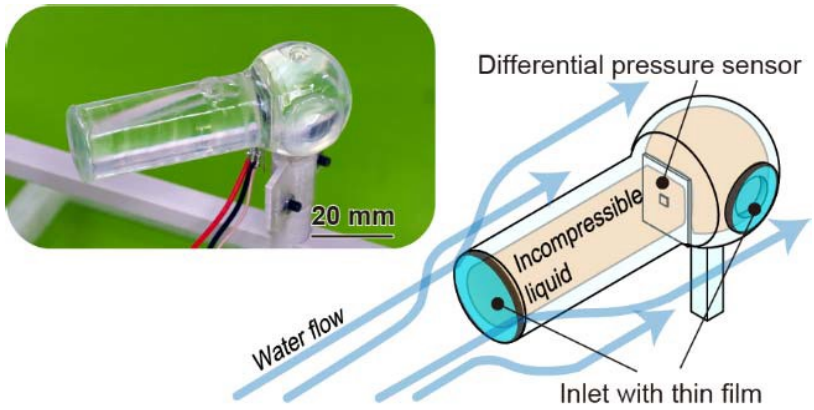

Figure 4-6 A pitot-static-tube-based flow speed sensor for monitoring marine animals [74]

In addition to measuring flow, each node also has various water quality sensors at multiple depths. Interrelated parameters such as dissolved oxygen concentration, temperature, pH, salinity among others are essential factors must be within optimum levels to maximize the fishes' overall welfare – metabolism, appetite, resistance against

diseases and parasites, and growth among others [76]. Measuring these parameters can help farmers monitor their health and growth to produce high quality meat.

The sensor unit would have at least one underwater camera to observe the fish activity and their distribution at different depths, especially during feeding. In addition, these cameras could also be used to detect uneaten feeds that would either float on the surface or sink to the benthic zones and inform the farmers how much feeds are wasted. Hydrophones would also be featured in the nodes for recording sounds made by the fishes at the surface to estimate their feeding activities during feeding [60]. While this kind of sensing is most useful in environments with minimal noise, the sensor system could be trained to detect noise from various sources such as feed-ejecting machines, which could be cancelled out from the sounds collected during feeding. IMUs in sensor units could also be used to characterize the movement not only of the sensor nodes in the water but also of the cage they would be attached to, which could be caused by strong waves.

As discussed in the previous chapters, the sensor network must have a power supply system with a capacity for energy-harvesting – solar, wind, tidal, or other sources – so that it could operate continuously off-grid and perform long-term observations of fish activity and water environment in fish cages. Although we presented a system with power supply units separate from the sensor units, installation of energy harvesting and storage components in each sensor unit could be an alternative design for the system. Design decisions on this would depend on the capacity of each component as well as on the limitations in the fish cage such as the amount of space for installation and how much energy could be harvested from the environment per day and on the required amount of energy set by daily operation schedule of the network.

Each sensor node could be designed to have its own computer above surface to perform simple corresponding calculations on the sensor readings to obtain the measurements before timestamping them. This computer could also possibly be used to automatically recalibrate the sensors whose readings would drift over time. In each cage, sensor nodes would communicate in a star Wi-Fi network, where one node would be designated as the hub unit which would collect sensor data from the rest of the nodes. Alternatively, a single hub unit could also be used to collect data from all nodes in the whole fish farm, given sufficient wireless range and available storage capacity. A hub unit could also be attached to a feeding boat and collect data from its own sensors or from other nodes in each fish cage upon arriving at the farm to perform feeding tasks. In whatever configuration, data gathered by the hub unit would be transmitted either directly to the onsite farmer's device or to a super hub with a larger capacity, which could send the data to a cloud server through a 4G or 5G network. Alternatively, the hub unit of the feeding boat could also perform a store-and-forward transmission, uploading data to the cloud once it connects to the internet onshore.

In addition to collecting sensor data, the cloud server could also collect various data from the farm – fish information, feeding history, among others, which could be accessed or be updated by the farmer onsite. Using all the data gathered, it could be trained to calculate the optimum timing and amount of feeding in each cage and remotely operate an automatic feeding machine in one of the cages that would also be connected to the hub unit or inform the farmer onsite of the target feeding parameters. This is where the fish activity model would play an important role for optimizing the feeding in each cage. It would also be able to get this machine's status so the farmer could perform maintenance on it, such as refilling the feeds among. Ultimately, the fishing company office would

have access to all the data from the farm through its connection to the cloud server and can grant specific data access to the farmers and to other employees and stakeholders in the farm.

4.4. Summary

To use flow speed measurements for assisting farmers in making feeding decisions, we developed a simplified model of the fish activity as a response to feeding. We established several assumptions to address the complex interaction of the fish with the environment and with the feeding and decided the height of the fish as the model's primary output. We established the model input to be the instantaneous amount of feed eaten, which would depend on the amount of feed in water as well as on the amount dispensed at the surface. This model will have to be further developed by considering the changes in other outputs and other parameters that have a significant impact on the fish feeding behavior. We can then use it later to optimize the feeding strategy for fishes in the cage.

While various patterns in measured flow were observed from the experiment, there were notable observations in flow at different depths that indicate the circling speed and depth distribution of the fishes throughout the feeding, such as drastic increase of surface at the start of feeding and its gradual decline as feeding progressed as well as the brief increase in flow at the lower depths. These could indicate the behavior of fishes when becoming satiated and be used to determine when to stop feeding. We can compare the flow measurements from the sensor units with the simulation of developed fish feeding activity model and determine an optimal feeding strategy. Developing this system as a DX application on aquaculture remains in the process of using expert knowledge to assist farmers' feeding decisions as this system still needs to be further developed.

We envisioned a DX system for a fish farm with multiple cages to map out the direction of this research in the future. Each cage would have multiple sensor nodes installed at the different sides of the cage, collecting various measurements at multiple

depths using improved flow speed sensors for estimating the fish activity throughout the cage and arrays of water quality sensors for monitoring the health of the fishes. The sensor network would have a power supply system with a capacity for harvesting and store energy to meet the requirements of the sensor units to operate throughout the duration of the daily schedule set by the user farmers. We proposed different configurations for the sensor network for collecting data from the sensor nodes, having one hub unit for each cage or for the whole farm which would upload data to the cloud server wirelessly. We also envisioned the cloud server's various capabilities, remotely operating an automated feeding machine or informing the farmers of optimal parameters for fish feeding by training from collected sensor data. This thesis focused on the development of the sensor network up to data collection at the hub unit.

Chapter 5
Conclusion

Chapter 5. Conclusion

5.1. Summary

Application of DX has become a need in aquaculture not only for producing more high-quality farmed fishes but also for improving the culture environment by reducing the pollutants it generates, making the industry more sustainable. This very much needed to optimize fish feeding in which appetite estimation has conventionally relied on the subjective experience of expert fish farmers, resulting in differences in the quality of harvests and in the inefficiency in feeding by novice farmers. This dissertation presented a system that estimates the fish activity through flow measurements for assisting in making feeding decisions in cage aquaculture.

In this research, we developed a modular sensor network that measures fish-induced flow and observes underwater activity from multiple depths and from more than one side of a fish cage. We implemented this by constructing sensor modules, each with a customized flow speed sensor and a network camera. We designed them to be connectable to each other at different depths to form sensor units whose sensor data are relayed by top modules that connect to a hub unit onsite.

To be able to make long-term observations of fish activity, we developed an offshore sensor system for the sensor network by programming the sensor and the hub units to automatically operate and gather data during certain periods throughout the day as desired the user. This supplies off-grid power to the sensor units through solar energy harvesting with a sufficient capacity to meet the daily energy demand of the sensor units. We designed the power supply to switch power according to the set daily schedule.

To visualize the relationship of flow speeds to the fish activity, especially during feeding, we performed three fish cage experiments, deploying the sensor network in fish cages and collected flow speeds and fish activity videos for days. For every experiment we performed, we demonstrated the functionality an added or upgraded system component, starting from the developed sensors to the modular sensor network performing long-term observations. We compared the flow measurements with the video recordings of the fish activity during feeding and observed patterns of increase and decrease of flow at different depths, which indicated changes in swimming speed and depths of fishes throughout the feeding tasks and would suggest satiation of the fishes.

In addition, we developed a simplified fish feeding activity model that we can simulate to determine the height of the fishes in response to feeds dispensed on water. With further improvements, we can compare the output of this model with the flow measurements and optimize the feeding strategy by determining the fish-induced flow that would indicate satiation of the fishes. To map out the direction of this research in the future, we also envisioned a DX system for a fish farm with multiple cages and designed the flow of information on the fish feeding activity from the cage to the stakeholders of the farm.

In the end, this research contributes to the development of DX application in cage aquaculture by introducing a flexible self-correcting system that could help farmers visualize underwater fish activity and help them improve their feeding decisions and achieve feeding optimization.

5.2. Future work

There are several tasks for developing this system further to observe the fish feeding behavior more reliably. This includes development of improved sensors resilient to mechanical faults. Further development of the fish feeding activity model to characterize

the activity of fishes as response to their feeding remains important for better visualization of flow they induce. This includes considering the changes circling speed in response to feeding as well as adding more inputs to the model to further resemble the actual fish behavior and their cage environment. This means adding more sensors to the developed sensor network. In addition, more data needs to be collected and analyzed in relation to the feeding decisions, so that we can further understand how to establish the model's various parameters.

Acknowledgements

All the credit is due to God, who has been the source of strength to complete this dissertation, which I dedicate to Him. Without His grace, I would not have been able to complete this doctoral program or even be here in Japan to study. From Him, I received all the help that I needed and received through everyone mentioned below.

I am most grateful to Professor Kazuo Ishii for accepting me into his laboratory and for supervising me not only in completing this dissertation but also in carrying out my research during the whole time of my study. I learned so much from him on how to think like a researcher and an engineer as well as on the realities and the best practices of the research fields I am involved in, that is, underwater field robotics. I would also like to thank him for his patience with me throughout all the consultations.

Professor Yuya Nishida had been next in command in the supervision of my research, having guided me in the minute details of the research activities such as sensor unit design and development, parts procurement, and paper writing. As with Prof. Ishii, I also learned from him the best practices of underwater robotics.

I would also like to thank to Professors Hiroaki Wagatsuma, Hiroyuki Miyamoto, and Keisuke Watanabe. As members of the Examination Committee, they have provided me much needed feedback for completing my thesis and for preparation of my public presentation.

There are so many people in Ishii Laboratory who I want to thank. Firstly, Daigo Katayama (my Japanese tutor during the first few months), Yoshiki Tanaka and Moeko Tominaga were my first Japanese friends in the laboratory who helped me with many things related to the laboratory, such as handling equipment as well as activities inside and outside the campus grounds. They also helped my comply with civil requirements in

the country (insurance, registration, etc.) as well as with adjusting to the Japanese lifestyle (bills payment, places, apartment matters, translations, etc.). Enrico di Maria and Raji Alahmad were the two international students in the laboratory who supported me so much on towards completion of my dissertation. They gave me different sorts of advice, whether on the research topic that I had to defend or on the procedures for completing it. Ms. Kanako Shirahashi and Ms. Yufuko Takahara, the respective secretaries of Profs. Ishii and Nishida, helped me accomplish the various paperwork related to the research project I engaged in. I learned from Binghe Li (or Hyoga Yamamoto) how to properly use the CNC machine for fabricating various parts for my sensor units. Kota Mishima, a student of Prof. Nishida, helped me with the construction of the sensor units as well as with the conduction of the fish cage experiments. Thanks also to everyone else in the laboratory who helped with many things, especially in preparation for the experiments.

I would also like to thank everyone in the Academic and Student Sections of Kyutech Wakamatsu Campus for all the support they provided in completing and for their patience regarding the submission of this dissertation. I would also like to thank Professor Tomohiro Shibata for accepting me to the Global Advanced Assistive Robotics program. I would also like to credit the Ministry of Education, Culture, Sports, Science and Technology (MEXT) for the Monbukagakusho scholarship, without which my study here in Japan would be impossible.

I would like to acknowledge Belltechne Co. Ltd., our partner company in this research collaboration, for constructing the mounting frames of the sensor unit, for providing the access to the fish cages for the experiment, and for their inputs and support for proper execution of the experiment. Special thanks to Mr. Tokuo Suetsugu and Mr. Yoshinori

Yatsunami for their onsite assistance in conducting the fish cage experiments, and to the rest of everyone in the company who joined.

Ms. Yoko Yoshioka, Mrs. Masako Ōnomi, and Mrs. Minako Nishiyama, provided me so many things I needed for living in Japan, particularly food, clothes, and cookware. Together with Pastor Eriya Izumi and the rest of Shimonoseki Baptist Church, they showed me a glimpse of the supportiveness of the Japanese community.

Rollyn Labuguen and Noel Victorino, my Filipino friends in Kyutech, and helped me adjust in living in Japan, especially during the first few weeks. Harold Bolingot, after his graduation from Kyutech, handed over to me most of his household belongings, which have helped me minimize my expenses for everyday living.

Thanks to Mike King Li and the rest of the Chewsday Growth Group, and my friends in Overcomers Support Group – Rey Ramos, Ben Young, Barney Alba, and Ronne Legaspi for all their encouragement and spiritual guidance throughout the entire time of living alone here in Japan.

Last but not the least, I would like to thank my family – Mom, Dad, Kuya, and Red, and my relatives from both sides, for their encouragement and support even from afar, for keeping in touch with me and keeping me updated on all what has been happening back home. Special mention to my aunt Dulce Solpico-Parel and her husband Allen Parel for sending me snacks and clothes during my stay in Japan.

SOLI DEO HONOR ET GLORIA!

References

[1] Food and Agriculture Org., "The State of World Fisheries and Aquaculture 2022. Towards Blue Transformation," Food and Agriculture Org., Rome, Italy, 2022.

[2] Bur. of Fisheries and Aquatic Resour., Philippines, "Philippine Fisheries Profile 2020," Bur. of Fisheries and Aquatic Resour., Philippines, Quezon City, Philippines, 2021.

[3] R. Cruz, V. Kumar and J. Ragaza, "Some Current Trends and Challenges in Philippine Aquaculture, with an Emphasis on Synergies with Biodiversity Initiatives," *World Aquaculture,* vol. 50, no. 2, pp. 35-42, 2019.

[4] M. L. San Diego-McGlone, R. V. Azanza, C. L. Villanoy and G. S. Jacinto, "Eutrophic waters, algal bloom and fish kill in fish farming areas in Bolinao, Pangasinan, Philippines," *Marine Pollution Bulletin,* vol. 57, no. 6-12, pp. 295-301, 2008.

[5] Aquac. Dept., Southeast Asian Fisheries Develop. Center, "SEAFDEC/AQD highlights 2015," Aquac. Dept., Southeast Asian Fisheries Develop. Center, Tigbauan, Philippines, 2016.

[6] Japan Fisheries Agency, "FY2019 Trends in Fisheries & FY2020 Fisheries Policy Summary," Japan Fisheries Agency, Tokyo, Japan, 2019.

[7] Statistics Bur., Japan, "Fisheries," in *Statistical Handbook of Japan 2020*, Tokyo, Statistics Bur., Japan, 2020, pp. 60-62.

[8] Org. for Econ. Co-operation and Develop., "Fisheries and Aquaculture in Japan," Org. for Econ. Co-operation and Develop., 2021.

[9] I. Takeda, "The Measures for Sustainable Marine Aquaculture in Japan," *Bulletin of Fisheries Research Agency,* no. 29, pp. 135-141, February 2010.

[10] Y. Sawada, T. Okada, S. Miyashita, O. Murata and H. Kumai, "Completion of the Pacific bluefin tuna Thunnus orientalis (Temminck et Schlegel) life cycle," *Aquaculture Research,* vol. 36, no. 5, pp. 413-421, 2005.

[11] K. Okuzawa, T. Takebe, N. Hirai and K. Ikuta, "Status of resource enhancement and sustainable aquaculture practices in Japan," in *Proceedings of the International Workshop on Resource Enhancement and Sustainable Aquaculture Practices in Southeast Asia 2014 (RESA)*, M. R. R. Romana-Eguia, F. D. Parado-Estepa, N. D. Salayo and M. J. H. Lebata-Ramos, Eds., Tigbauan, Philippines, Aquaculture Dept., Southeast Asian Fisheries Development, 2015, pp. 41-52.

[12] Statistics Bur., Japan, "Declining Birth Rate and Aging Population," in *Statistical Handbook of Japan 2020*, Tokyo, Japan, Statistics Bur., Japan, 2020, pp. 13-15.

[13] M. Fujise and T. Kanmuri, "The Issues Surrounding Aquaculture Feeds and the Current Measures Associated with Them in Japan," *Bulletin of Fisheries Research Agency,* no. 31, pp. 1-7, October 2010.

[14] M. Martinez-Porchas and L. R. Martinez-Cordova, "World Aquaculture: Environmental Impacts and Troubleshooting Alternatives," *The Scientific World Journal,* vol. 2012, 2012.

[15] R. L. Naylor, R. J. Goldburg, J. H. Primavera, N. Kautsky, M. C. M. Beveridge, J. Clay, C. Folke, J. Lubchenco, H. Mooney and M. Troell, "Effect of aquaculture on world fish supplies," *Nature,* vol. 405, p. 1017–1024, 2000.

[16] A. Ahmad, S. R. S. Abdullah, H. A. Hasan, A. R. Othman and N. ‘. Ismail, "Aquaculture industry: Supply and demand, best practices, effluent and its current issues and treatment technology," *Journal of Environmental Management,* vol. 287, 2021.

[17] R. S. S. Wu, "The environmental impact of marine fish culture: towards a sustainable future," *Marine Pollution Bulletin,* vol. 31, no. 4-12, pp. 159-166, 1995.

[18] M. Krkošek, J. S. Ford, A. Morton, S. Lele, R. A. Myers and M. A. Lewis, "Declining Wild Salmon Populations in Relation to Parasites from Farm Salmon," *Science,* vol. 318, no. 5857, pp. 1772-1775, 2007.

[19] A. R. Brown, M. Lilley, J. Shutler, C. Lowe, Y. Artioli, R. Torres, E. Berdalet and C. R. Tyler, "Assessing risks and mitigating impacts of harmful algal blooms on mariculture and marine fisheries," *Reviews in Aquaculture,* vol. 12, no. 3, pp. 1663-1688, 2020.

[20] R. A. Quiñones, M. Fuentes, R. M. Montes, D. Soto and J. León-Muñoz, "Environmental issues in Chilean salmon farming: a review," *Reviews in Aquaculture,* vol. 11, no. 2, pp. 375-402, 2019.

[21] T. Maes, R. Thompson, G. Hanke, A. Budziak, T. Vlachogianni, J. v. Franeker, E. Priestland, P. Nilsson, S. Werner, J. Veiga, L. Oosterbaan, F. Galgani and M. Matiddi, "Harm caused by marine litter : MSFD GES TG marine litter : thematic report," Publications Office, European Union, Luxembourg, 2016.

[22] H. Sun, J. Li, L. Tang and Z. Yang, "Responses of crucian carp Carassius auratus to long-term exposure to nitrite and low dissolved oxygen levels," *Biochemical Systematics and Ecology,* vol. 44, no. 1, pp. 224-232, 2012.

[23] M. Sun, S. G. Hassan and D. Li, "Models for estimating feed intake in aquaculture: A review," *Computers and Electronics in Agriculture,* vol. 127, pp. 425-438, 2016.

[24] Y. Wei, Q. Wei and D. An, "Intelligent monitoring and control technologies of open sea cage culture: A review," *Computers and Electronics in Agriculture,* vol. 169, 2020.

[25] P. Klebert, P. Lader, L. Gansel and F. Oppedal, "Hydrodynamic interactions on net panel and aquaculture fish cages: A review," *Ocean Engineering,* vol. 58, no. 15, pp. 260-274, 2013.

[26] C. Ebert and C. H. C. Duarte, "Digital Transformation," *IEEE Software,* vol. 35, no. 4, pp. 16-21, 2018.

[27] T. Mäkitie, M. Steen, T. M. Thune, H. B. Lund, A. Kenzhegaliyeva, E. F. Ullern, P. F. Kamsvåg, A. D. Andersen and K. M. Hydle, "Greener and smarter? Transformations in five Norwegian industrial sectors," SINTEF, Trondheim, 2020.

[28] M. G. Zhabitskii, Y. A. Andryenko, V. N. Malyshev, S. V. Chuykova and A. A. Zhosanov, "Digital transformation model based on the digital twin concept for intensive aquaculture production using closed water circulation technology," *IOP Conference Series: Earth and Environmental Science,* vol. 723, 2021.

[29] W. R. Rola and M. R. Hasan, "Economics of aquaculture feeding practices: a synthesis of case studies undertaken in six Asian countries," in *Economics of aquaculture feeding practices in selected Asian countries*, M. R. Hasan, Ed., Rome, Food and Agri. Org., 2007, pp. 1-31.

[30] T. Bandara, "Alternative feed ingredients in aquaculture: Opportunities and challenges," *Journal of Entomology and Zoology Studies,* vol. 6, no. 2, pp. 3087-394, 2018.

[31] R. L. Olsen and M. R. Hasan, "A limited supply of fishmeal: Impact on future increases in global aquaculture production," *Trends in Food Science & Technology,* vol. 27, no. 2, pp. 120-128, 2012.

[32] A. Ido, M.-F.-Z. Ali, T. Takahashi, C. Miura and T. Miura, "Growth of Yellowtail (Seriola quinqueradiata) Fed on a Diet Including Partially or Completely Defatted Black Soldier Fly (Hermetia illucens) Larvae Meal," *Insects,* vol. 12, no. 8, 2021.

[33] C. Zhou, D. Xu, K. Lin, C. Sun and X. Yang, "Intelligent feeding control methods in aquaculture with an emphasis on fish: a review," *Reviews in Aquaculture,* vol. 10, no. 4, pp. 975-993, 2018.

[34] T.-H. Wu, Y.-I. Huang and C.-J. Ming, "Development of an adaptive neural-based fuzzy inference system for feeding decision-making assessment in silver perch (Bidyanus bidyanus) culture," *Aquaculture Engineering,* vol. 66, pp. 41-51, 2015.

[35] M. V. Goulão, C. A. P. Andrade, N. M. A. Gouveia, J. R. J. Gomes, V. M. F. A. Timóteo and F. Soares, "Evaluación de pérdidas de piensos en una piscifactoría en mar abierto y su uso en modelos del crecimiento de peces de cultivo y de la ración diaria," *AquaTIC,* no. 13, 2001.

[36] Z. Wang and K. M. Y. Leung, "Effects of unionised ammonia on tropical freshwater organisms: Implications on temperate-to-tropic extrapolation and water quality guidelines," *Environmental Pollution,* vol. 205, pp. 240-249, 2015.

[37] C. F. Hurtado, B. Cancino-Madariaga, C. Torrejón and P. P. Villegas, "Separation of nitrite and nitrate from water in aquaculture by nanofiltration membrane," *Desalination and Water Treatment,* vol. 57, no. 54, pp. 26050-26062, 2016.

[38] G. A. Santos, J. W. Scharma, R. E. P. Mamauag, J. H. W. M. Rombout and J. A. J. Verreth, "Chronic stress impairs performance, energy metabolism and welfare indicators in European seabass (Dicentrarchus labrax): The combined effects of fish crowding and water quality deterioration," *Aquaculture,* vol. 299, no. 1-4, pp. 73-80, 2010.

[39] K. P. Ang and R. J. Petrell, "Pellet wastage, and subsurface and surface feeding behaviours associated with different feeding systems in sea cage farming of salmonids," *Aquacultural Engineering,* vol. 18, no. 2, pp. 95-115, 1998.

[40] F. Gerlotto, M. Soria and P. Fréon, "From two dimensions to three: the use of multibeam sonar for a new approach in fisheries acoustics," *Canadian Journal of Fisheries and Aquatic Sciences,* vol. 56, no. 1, pp. 6-12, 1999.

[41] M. Garcia, S. Sendra, G. Lloret and J. Lloret, "Monitoring and control sensor system for fish feeding in marine fish farms," *IET Communications,* vol. 5, no. 12, pp. 1682-1690, 2011.

[42] M. Føre, J. A. Alfredsen and A. Gronningsater, "Development of two telemetry-based systems for monitoring the feeding behaviour of Atlantic salmon (Salmo salar L.) in aquaculture sea-cages," *Computers and Electronics in Agriculture,* vol. 76, no. 2, pp. 240-251, 2011.

[43] M. Føre, K. Frank, T. Dempster, J. A. Alfredsen and E. Høy, "Biomonitoring using tagged sentinel fish and acoustic telemetry in commercial salmon aquaculture: A feasibility study," *Aquacultural Engineering,* vol. 78B, pp. 163-172, 2017.

[44] K. R. Skøien, M. O. Alver, A. P. Zolich and J. A. Alfredsen, "Feed spreaders in sea cage aquaculture – Motion characterization and measurement of spatial pellet distribution using an unmanned aerial vehicle," *Computers and Electronics in Agriculture,* vol. 129, pp. 27-36, 2016.

[45] D. Karimanzira, M. Jacobi, T. Pfuetzenreuter, T. Rauschenbach, M. Eichhorn, R. Taubert and C. Ament, "First testing of an AUV mission planning and guidance system for water quality monitoring and fish behavior observation in net cage fish farming," *Information Processing in Agriculture,* vol. 1, no. 2, pp. 131-140, 2014.

[46] M. Eichhorn, C. Ament, M. Jacobi, T. Pfuetzenreuter, D. Karimanzira, K. Bley, M. Boer and H. Wehde, "Modular AUV System with Integrated Real-Time Water Quality Analysis," *Sensors,* vol. 18, no. 6, 2018.

[47] T. H. Kim, K. U. Yang, K. S. Hwang, D. J. Jang and J. G. Hur, "Automatic submerging and surfacing performances of model submersible fish cage system operated by air control," *Aquacultural Engineering,* vol. 45, no. 2, pp. 74-86, 2011.

[48] D. Li, Z. Wang, S. Wu, Z. Miao, L. Du and Y. Duan, "Automatic recognition methods of fish feeding behavior in aquaculture: A review," *Aquaculture,* vol. 528, 2020.

[49] C. Zhou, K. Lin, D. Xu, L. Chen, Q. Guo, C. Sun and X. Yang, "Near infrared computer vision and neuro-fuzzy model-based feeding decision system for fish in aquaculture," *Computers and Electronics in Agriculture,* vol. 146, pp. 114-124, 2018.

[50] C. Zhou, D. Xu, L. Chen, S. Zhang, C. Sun, X. Yang and Y. Wang, "Evaluation of fish feeding intensity in aquaculture using a convolutional neural network and machine vision," *Aquaculture,* vol. 507, pp. 457-465, 2019.

[51] M. Saberioon, A. Gholizadeh, P. Cisar, A. Pautsina and J. Urban, "Application of machine vision systems in aquaculture with emphasis on fish: state-of-the-art and key issues," *Reviews in Aquaculture,* vol. 9, no. 4, pp. 369-387, 2017.

[52] J. Zhao, W. J. Bao, F. D. Zhang, Z. Y. Ye, Y. Liu, M. W. Shen and S. M. Zhu, "Assessing appetite of the swimming fish based on spontaneous collective behaviors in a recirculating aquaculture system," *Aquacultural Engineering,* vol. 78B, pp. 196-204, 2017.

[53] A. Pautsina, P. Císař, D. Štys, B. F. Terjesen and Å. M. O. Espmark, "Infrared reflection system for indoor 3D tracking of fish," *Aquacultural Engineering,* vol. 69, pp. 7-17, 2015.

[54] M. M. Saberioon and P. Cisar, "Automated multiple fish tracking in three-Dimension using a Structured Light Sensor," *Computers and Electronics in Agriculture,* vol. 121, pp. 215-221, 2016.

[55] D. An, J. Hao, Y. Wei, Y. Wang and X. Yu, "Application of computer vision in fish intelligent feeding system—A review," *Aquaculture Research,* vol. 52, no. 2, pp. 423-437, 2021.

[56] J. Tao, Y. Gao, Y. Qiao, H. Zheng, X. Wang, L. Wan and J. Chang, "Hydroacoustic observation of fish spatial patterns and behavior in the ship lock and adjacent areas of Gezhouba Dam, Yangtze River," *Acta Ecologica Sinica,* vol. 30, no. 4, pp. 233-239, 2010.

[57] G. Rakowitz, M. Tušer, M. Říha, T. Jůza, H. Balk and J. Kubečka, "Use of high-frequency imaging sonar (DIDSON) to observe fish behaviour towards a surface trawl," *Fisheries Research,* Vols. 123-124, pp. 37-48, 2012.

[58] H. Zhang, Q. Wei and M. Kang, "Measurement of swimming pattern and body length of cultured Chinese sturgeon by use of imaging sonar," *Aquaculture,* vol. 434, pp. 184-187, 2014.

[59] R. Mallekh, J. P. Lagardère, J. P. Eneau and C. Cloutour, "An acoustic detector of turbot feeding activity," *Aquaculture,* vol. 221, no. 1-4, pp. 481-489, 2003.

[60] R. Mallekh, J. P. Lagardère and A. Mariani, "Acoustic characteristics of two feeding modes used by brown trout (Salmo trutta), rainbow trout (Oncorhynchus mykiss) and turbot (Scophthalmus maximus)," *Aquaculture,* vol. 240, no. 1-4, pp. 607-616, 2004.

[61] C. Polonschii, D. Bratu and E. Gheorghiu, "Appraisal of fish behaviour based on time series of fish positions issued by a 3D array of ultrasound transducers," *Aquacultural Engineering,* vol. 55, pp. 37-45, 2013.

[62] T. Noda, Y. Kawabata, N. Arai, H. Mitamura and S. Watanabe, "Animal-mounted gyroscope/accelerometer/magnetometer: In situ measurement of the movement performance of fast-start behaviour in fish," *Journal of Experimental Marine Biology and Ecology,* vol. 451, pp. 55-68, 2014.

[63] K. F. Cubitt, H. T. Williams, D. Rowsell, W. J. McFarlane, R. G. Gosine, K. G. Butterworth and R. S. McKinley, "Development of an intelligent reasoning system to distinguish hunger states in Rainbow trout (Oncorhynchus mykiss)," *Computers and Electronics in Agriculture,* vol. 62, no. 1, pp. 29-34, 2008.

[64] G. M. Soto-Zarazúa, E. Rico-García, R. Ocampo, R. G. Guevara-González and H.-R. G, "Fuzzy-logic-based feeder system for intensive tilapia production (Oreochromis niloticus)," *Aquaculture International,* vol. 18, p. 379–391, 2010.

[65] S. Zhao, W. Ding, S. Zhao and J. Gu, "Adaptive neural fuzzy inference system for feeding decision-making of grass carp (Ctenopharyngodon idellus) in outdoor intensive culturing ponds," *Aquaculture,* vol. 498, pp. 28-36, 2019.

[66] Chang, C. M, W. Fang, R. C. Jao, C. Z. Shyu and I. C. Liao, "Development of an intelligent feeding controller for indoor intensive culturing of eel," *Aquacultural Engineering,* vol. 32, no. 2, pp. 343-353, 2005.

[67] P. Klebert, P. Lader, L. Gansel and F. Oppedal, "Hydrodynamic interactions on net panel and aquaculture fish cages: A review," *Ocean Engineering,* vol. 58, pp. 260-274, 2013.

[68] A. Chacon-Torres, L. G. Ross and M. C. M. Beveridge, "The effects of fish behaviour on dye dispersion and water exchange in small net cages," *Aquaculture,* vol. 73, no. 1-4, pp. 283-293, 1988.

[69] L. C. Gansel, S. Rackebrandt, F. Oppedal and T. A. McClimans, "Flow Fields Inside Stocked Fish Cages and the Near Environment," *Journal of Offshore Mechanics and Arctic Engineering,* vol. 136, no. 3, 2011.

[70] M.-F. Tang, T.-J. Xu, G.-H. Dong, Y.-P. Zhao and W.-J. Guo, "Numerical simulation of the effects of fish behavior on flow dynamics around net cage," *Applied Ocean Research,* vol. 64, pp. 258-280, 2017.

[71] C. I. M. Martins, L. Galhardo, C. Noble, B. Damsgård, M. T. Spedicato, W. Zupa, M. Beauchaud, E. Kulczykowska, J.-C. Massabuau, T. Carter, S. R. Planellas and T. Kristiansen, "Behavioural indicators of welfare in farmed fish," *Fish Physiology and Biochemistry,* vol. 38, no. 1, p. 17–41, 2012.

[72] World Meteorological Organization, "Measurements of Sunshine Duration," in *Guide to Instruments and Methods: Volume I – Measurement of Meteorological Variables*, Geneva, Switzerland, World Meteorological Organization, 2018, pp. 299-313.

[73] Japan Meteorological Agency, "Monthly total of sunshine duration (h): Nagasaki," 2022. [Online]. Available: https://www.data.jma.go.jp/obd/stats/etrn/view/monthly_s3_en.php?block_no=47817&view=12.

[74] T. Kishimoto, R. Saito, H. Tanaka and H. Takahashi, "Pitot-Static-Tube-Based Waterflow Sensor for Marine Biologging via Inside Sealing of an Incompressible Liquid," *IEEE Sensors Journal,* vol. 21, no. 18, pp. 19806-19814, 2021.

[75] N. S. Lowell, D. R. Walsh and J. W. Pohlman, "A comparison of tilt current meters and an acoustic doppler current meter in vineyard sound, Massachusetts," in *2015 IEEE/OES Eleveth Current, Waves and Turbulence Measurement (CWTM)*, St. Petersburg, FL, USA, 2015.